

Volume 22, Number 2

February, 1967

SOVIET ATOMIC ENERGY

АТОМНАЯ ЭНЕРГИЯ
(ATOMNAYA ENERGIYA)

TRANSLATED FROM RUSSIAN



CONSULTANTS BUREAU

SOVIET ATOMIC ENERGY

Soviet Atomic Energy is a cover-to-cover translation of *Atomnaya Energiya*, a publication of the Academy of Sciences of the USSR.

An arrangement with Mezhdunarodnaya Kniga, the Soviet book export agency, makes available both advance copies of the Russian journal and original glossy photographs and artwork. This serves to decrease the necessary time lag between publication of the original and publication of the translation and helps to improve the quality of the latter. The translation began with the first issue of the Russian journal.

Editorial Board of *Atomnaya Energiya*:

Editor: M. D. Millionshchikov

Deputy Director, Institute of Atomic Energy
imeni I. V. Kurchatov
Academy of Sciences of the USSR
Moscow, USSR

Associate Editors: N. A. Kolokol'tsov
N. A. Vlasov

A. I. Alikhanov

A. A. Bochvar

N. A. Dollezhal'

V. S. Fursov

I. N. Golovin

V. F. Kalinin

A. K. Krasin

A. I. Leipunskii

V. V. Matveev

M. G. Meshcheryakov

P. N. Palei

V. B. Sherchenko

D. L. Simonenko

V. I. Smirnov

A. P. Vinogradov

A. P. Zefirov

Copyright © 1967 Consultants Bureau, a division of Plenum Publishing Corporation, 227 West 17th Street, New York, N. Y. 10011. All rights reserved. No article contained herein may be reproduced for any purpose whatsoever without permission of the publishers.

Subscription
(12 Issues): \$95

Single Issue: \$30
Single Article: \$15

Order from:



CONSULTANTS BUREAU

227 West 17th Street, New York, New York 10011

SOVIET ATOMIC ENERGY

A translation of *Atomnaya Énergiya*

Volume 22, Number 2

February, 1967

CONTENTS

ARTICLES

	Engl./Russ.	
Potential of the Uranium Atom and Calculation of the Ionization Energy—L. P. Kudrin and M. Ya. Mazeev	85	83
Calculation of the Dissociation Energy of Calcium and Uranium Monofluorides—L. P. Kudrin and M. Ya. Mazeev	90	85
Synthesis of Isotopes of Element 102 with Mass Numbers 254, 253, and 252—V. L. Mikheev, V. I. Ilyushchenko, M. B. Miller, S. M. Polikanov, G. N. Flerov, and Yu. P. Kharitonov	93	90
Calculation of the Passage of Fast Neutrons through Graphite—L. M. Shirkin	101	97
Analytical Solution of the Problem of Neutron Thermalization in a Heavy Moderator—M. V. Kazarnovskii	104	100
Calculating the Spatial and Energy Distribution of Thermal Neutrons in a Heterogeneous Reactor—M. V. Fedulov	112	108
Determination of the Effective Multiplication (Breeding) Factor of Neutrons from the Measured Differential Reactivity—T. S. Dideikin and B. P. Shishin	119	113

ABSTRACTS

Slowing Down of Neutrons in a Hydrogenous Medium—Yu. A. Platovskikh	123	118
Diffraction of Slow Neutrons by Stratified Systems—V. F. Turchin	124	119
Shielding Properties of Stone Concrete—V. B. Dubrovski, M. Ya. Kulakovski, P. A. Lavdanski, V. I. Savitski, V. N. Solov'ev, and A. F. Mirenkov	125	119
Shielding Properties of Borated Heat-Resistant Chromite Concretes—D. L. Broder, V. B. Dubrovski, M. Ya. Kulakovski, P. A. Lavdanski, V. I. Savitski, V. N. Solov'ev, and A. F. Mirenkov	126	121
Heat Release in Borated Concrete Shields—V. B. Dubrovski, M. Ya. Kulakovski, P. A. Lavdanski, V. I. Savitskii, and V. N. Solov'ev	127	121
Differential Albedo of a Narrow Beam of Fast Neutrons from a Semiinfinite Water Scatterer—L. Ya. Gudkova, V. G. Zolotukhin, V. P. Mashkovich, and A. I. Mis'kevich	128	122
Use of Albedo Boundary Conditions to Reduce the Region of Iteration—V. S. Shulepin	130	123
Variable-Thickness, Premoderating, High-Sensitivity Neutron Detector—Yu. A. Vakarin, L. N. Veselovskii, B. S. Gribov, A. V. Kolotkov, V. G. Kuznetsov, and V. A. Sakovich	130	124
Thermal Column Converter for Shielding Studies—V. P. Mashkovich, A. N. Nikolaev, B. I. Sinitsyn, V. K. Sakharov, and S. G. Tsypin	132	125

LETTERS TO THE EDITOR

Stopping Power of Nickel for Protons and He ₄ ⁺ Ions in the Energy Range 20 to 95 keV—G. F. Bogdanov, V. P. Kabaev, F. V. Lebedev, and G. M. Novikov	133	126
--	-----	-----

CONTENTS

(continued)

	Engl./Russ.	
Nuclear Properties of the Isotopes of Element 102 with Mass Numbers 255 and 256 -V. A. Druin, G. N. Akap'ev, A. G. Demin, Yu. V. Lobanov, B. V. Fefilov, G. N. Flerov, and L. P. Chelnokov	135	127
Beam of Helium Ions with a Current of 200 mA and an Energy of 70 keV -N. V. Pleshivtsev, V. I. Martynov, G. G. Tomashev, Yu. F. Grigorovich, and B. K. Shembel'	137	128
Pulse Method for Measuring how Neutron Spectra of Finite-Sized Water Samples Deviate from the Equilibrium Maxwell Spectra-S. B. Stepanov	140	131
Dose Rate of γ -Radiation due to Capture in Water-V. M. Mordashev	143	133
Measurement of Reactor Absorption Cross Sections of Gd ¹⁵⁴ and Gd ¹⁵⁶ -E. I. Grishanin, G. M. Kukavadze, V. I. Lependin, L. Ya. Memelova, I. G. Morozov, V. V. Orlov, and D. T. Pilipets	144	133
Turbulent Thermal Diffusivity in a Current of Liquid with High Thermal Conductivity -V. M. Borishanskii and T. V. Zablotskaya	147	135
Calculation of the Stored Energy in Irradiated Graphite, from X-ray Data -M. S. Koval'chenko and V. V. Ogorodnikov	150	138
Radon Emanation from Uraniferous Ores and Minerals Immersed in Liquid -M. I. Prutkina and V. L. Shashkin	153	140
 NEWS OF SCIENCE AND TECHNOLOGY		
VI International Conference on Nuclear Photography-N. A. Perfilov	155	142
Engineering Cost Factors and Outlook for the Use of Field Radiometric Moisture Gages and Soil Density Gages in Crop Land Improvement-V. A. Emel'yanov and V. I. Sinitsyn	158	144
Train of Glove Boxes for Handling γ -Active Materials-G. I. Lukishov, K. D. Radionov, and G. U. Shcherbenok	161	146
Chemical Uses of Nuclear Reactors and Particle Accelerators in the USA -B. G. Dzantiev, and A. K. Pikaev	163	147
Delegation of Soviet Medical Scientists Visits USA-E. I. Vorob'ev	166	149
IAEA Discussion of Radioactive Wastes Disposal-G. Apollonov	169	151
 BOOKS REVIEWS.	 170	 152
ERRATA	192	141

The Russian press data (podpisano k pechati) of this issue was 2/2/1967.
Publication therefore did not occur prior to this date, but must be assumed
to have taken place reasonably soon thereafter.

POTENTIAL OF THE URANIUM ATOM AND CALCULATION
OF THE IONIZATION ENERGY

L. P. Kudrin and M. Ya. Mazeev

UDC 537.561

The potential of the uranium atom and ions are calculated on the statistical model, allowing for exchange interaction and electron correlation. It is demonstrated that due allowance for electron correlation is essential in calculating the integral atomic characteristics. The ionization energies I_1, I_2, I_3 are calculated from the curves obtained for the atomic and ionic potentials. Theoretical results are compared with experiment.

The simplest description of the heavy atom or ion is the statistical Thomas-Fermi model (TF) [1]. The introduction of exchange interaction [2] considerably improves this model. Allowing for electron correlation in the atom was first proposed by Gombash [3] on the basis of an expression for the correlation energy of a rarefied electron gas obtained by Wigner [4]. Later this correction to the statistical model was introduced by D. Kirzhnits [5]. Strict account of correlation for the inner region of the atom on the basis of the Hell-Man-Brakner approximation for an electron gas of high density was carried out in [6]. The remaining quantum corrections to the statistical TF model were also considered up to an accuracy of \hbar^2 terms in [6]. A reasonable interpolation for any density of the electron gas was proposed by Erma [7]. Despite the fundamental difficulties associated with the limited applicability of the model itself near the boundary of the atom (or ion), the calculation of the integral characteristics of heavy atoms, such as the ionization potentials of the atoms (and especially ions), the polarizability, and so forth may well prove fruitful [7] within the framework of the statistical model, allowing for the corrections indicated.

In this paper we calculate the ionization potentials of the uranium atom (the first three, I_1, I_2, I_3) on the basis of the statistical model for the atomic core (the atom minus the valence electrons under consideration) and also for the actual uranium atom.

The expression for the ionization potentials in the Gombash notation has the form

$$I_n = e^2 \int_{N_1-n}^{N_1-n+1} \frac{Z-N}{r_0} dN + \frac{\kappa'_a{}^3}{4\kappa_h} + f_0, \quad (1)$$

TABLE 1. Values of the Dimensionless Boundaries of the Uranium and Calcium Atoms

U (Z = 92)		Ca (Z = 20)		U (Z = 92)		Ca (Z = 20)	
q	x_0	q	x_0	q	x_0	q	x_0
0.0	22.838	0.0	12.262	1.6	16.883	—	—
0.1	22.216	0.1	11.797	1.7	16.658	—	—
0.2	21.656	0.2	11.384	1.8	16.441	—	—
0.3	21.147	0.3	11.011	1.9	16.233	—	—
0.4	20.679	0.4	10.672	2.0	16.032	—	—
0.5	20.247	0.5	10.361	2.1	15.839	—	—
0.6	19.845	0.6	10.073	2.2	15.652	—	—
0.7	19.469	0.7	9.8052	2.3	15.471	—	—
0.8	19.116	0.8	9.5553	2.4	15.296	—	—
0.9	18.784	0.9	9.3209	2.5	15.127	—	—
1.0	18.470	1.0	9.1003	2.6	14.963	—	—
1.1	18.173	—	—	2.7	14.804	—	—
1.2	17.890	—	—	2.8	14.650	—	—
1.3	17.621	—	—	2.9	14.500	—	—
1.4	17.364	—	—	3.0	14.355	—	—
1.5	17.118	—	—	—	—	—	—

where Z is the charge on the nucleus, N_1 is the number of electrons in the atom or ion, n is the number of missing electrons, $\kappa_k = 2.871 e^2 a_0$; $\kappa'_a = 0.8349 e^2$; $f_0 = 0.01674 e^2/a_0$; a_0 is the Bohr radius, and r_0 is the boundary of the atom or ion. The second and third terms on the right-hand side of

TABLE 2. Ionization Potentials of the Uranium and Calcium Atoms

Ionization potential, eV	U	Ca
I_1	5.65	6.22
I_2	14.36	—
I_3	25.13	—

Translated from *Atomnaya Énergiya*, Vol. 22, No. 2, pp. 83-85, February, 1967. Original article submitted August 9, 1966.

TABLE 3. Statistical Potential $\Psi(x)$ and Derivative $\Psi'(x)$ for Uranium (Atom and Ions)

x	U			U ⁺			U ⁺⁺		
	$\Psi(x)$	$\Psi'(x)$	x	$\Psi(x)$	$\Psi'(x)$	x	$\Psi(x)$	$\Psi'(x)$	x
0.10000 (-16)	0.10000 (+01)	—	0.10000 (-15)	0.10000 (-101)	-0.160745 (+01)	0.0000	0.10000 (+01)	—	—
0.29245 (-09)	0.10000 (+01)	-0.16061 (+01)	0.20560 (00)	0.78549 (00)	-0.79852 (00)	0.27382 (-08)	0.10000 (+01)	-0.16060 (+01)	-0.16060 (+01)
0.40811 (-05)	0.99997 (00)	-0.16040 (+01)	0.30122 (00)	0.71552 (00)	-0.67186 (00)	0.11198 (-06)	0.10000 (+01)	-0.16054 (+01)	-0.16054 (+01)
0.41781 (-04)	0.99998 (00)	-0.15992 (+01)	0.39685 (00)	0.65598 (00)	-0.57739 (00)	0.10265 (-04)	0.99998 (00)	-0.15997 (+01)	-0.15997 (+01)
0.10127 (-03)	0.99984 (00)	-0.15860 (+01)	0.49247 (00)	0.60444 (00)	-0.50340 (00)	0.10210 (-02)	0.97840 (00)	-0.15422 (+01)	-0.15422 (+01)
0.97286 (-03)	0.99848 (00)	-0.15437 (+01)	0.58810 (00)	0.55926 (00)	-0.44364 (00)	0.10268 (00)	0.87713 (00)	-0.10036 (+01)	-0.10036 (+01)
0.47705 (-02)	0.99278 (00)	-0.14683 (+01)	0.71560 (00)	0.50693 (00)	-0.37970 (00)	0.19831 (00)	0.79135 (00)	-0.81008 (00)	-0.81008 (00)
0.10249 (-01)	0.98492 (00)	-0.14048 (+01)	0.81122 (00)	0.47255 (00)	-0.34050 (00)	0.30190 (00)	0.71506 (00)	-0.67109 (00)	-0.67109 (00)
0.20210 (-01)	0.97134 (00)	-0.13253 (+01)	0.90685 (00)	0.44163 (00)	-0.30705 (00)	0.39753 (00)	0.65559 (00)	-0.57680 (00)	-0.57680 (00)
0.39136 (-01)	0.94732 (00)	-0.12199 (+01)	0.10025 (01)	0.41368 (00)	-0.27821 (00)	0.50900 (00)	0.59617 (00)	-0.49213 (00)	-0.49213 (00)
0.59058 (-01)	0.92387 (00)	-0.11374 (+01)	0.15125 (01)	0.30106 (00)	-0.17475 (00)	0.60472 (00)	0.55196 (00)	-0.43440 (00)	-0.43440 (00)
0.82964 (-01)	0.89766 (00)	-0.10584 (+01)	0.20225 (01)	0.22772 (00)	-0.11793 (00)	0.70034 (00)	0.51278 (00)	-0.38658 (00)	-0.38658 (00)
0.10289 (-01)	0.87713 (00)	-0.10031 (+01)	0.25325 (01)	0.17702 (00)	-0.83526 (-01)	0.79597 (00)	0.47779 (00)	-0.34634 (00)	-0.34634 (00)
0.20648 (-01)	0.78479 (00)	-0.79715 (+01)	0.30425 (01)	0.14048 (00)	-0.61295 (-01)	0.89159 (00)	0.44635 (00)	-0.31206 (00)	-0.31206 (00)
0.39773 (-01)	0.65548 (00)	-0.57663 (+01)	0.35525 (01)	0.11330 (00)	-0.46235 (-01)	0.10191 (01)	0.40909 (00)	-0.27561 (00)	-0.27561 (00)
0.60492 (-01)	0.55188 (00)	-0.43429 (+01)	0.41900 (01)	0.88158 (-01)	-0.33509 (-01)	0.14972 (01)	0.30374 (00)	-0.17699 (00)	-0.17699 (00)
0.79617 (-01)	0.47772 (00)	-0.34626 (+01)	0.44450 (01)	0.80111 (-01)	-0.29696 (-01)	0.20072 (01)	0.22952 (00)	-0.11924 (00)	-0.11924 (00)
0.40193 (00)	0.40904 (00)	-0.27355 (+01)	0.49550 (01)	0.66599 (-01)	-0.23593 (-01)	0.25172 (01)	0.17830 (00)	-0.84351 (-04)	-0.84351 (-04)
0.12105 (00)	0.36131 (00)	-0.22762 (+01)	0.54650 (01)	0.55791 (-01)	-0.18999 (-01)	0.29953 (01)	0.14340 (00)	-0.63002 (-01)	-0.63002 (-01)
0.14018 (00)	0.32133 (00)	-0.19191 (+01)	0.59750 (01)	0.47039 (-01)	-0.15478 (-01)	0.35053 (01)	0.11549 (00)	-0.47418 (-01)	-0.47418 (-01)
0.15930 (00)	0.28743 (00)	-0.16357 (+01)	0.64850 (01)	0.39872 (-01)	-0.12737 (-01)	0.40153 (01)	0.94244 (-01)	-0.36502 (-01)	-0.36502 (-01)
0.18162 (+01)	0.25398 (00)	-0.13733 (00)	0.69950 (01)	0.33948 (-01)	-0.10575 (-01)	0.50034 (01)	0.65431 (-01)	-0.23118 (-01)	-0.23118 (-01)
0.20074 (+01)	0.22951 (00)	-0.11922 (00)	0.75050 (01)	0.29012 (-01)	-0.88476 (-02)	0.59916 (01)	0.46724 (-01)	-0.15405 (-01)	-0.15405 (-01)
0.25174 (+01)	0.17829 (00)	-0.84333 (00)	0.80150 (01)	0.24867 (-01)	-0.74537 (-02)	0.70116 (01)	0.33681 (-01)	-0.10551 (-01)	-0.10551 (-01)
0.30274 (+01)	0.14141 (00)	-0.61829 (00)	0.85250 (01)	0.21365 (-01)	-0.63178 (-02)	0.79997 (+01)	0.24843 (-01)	-0.75451 (-02)	-0.75451 (-02)
0.34737 (+01)	0.11702 (00)	-0.48216 (00)	0.90350 (01)	0.18389 (-01)	-0.53844 (-02)	0.90197 (+01)	0.18269 (-01)	-0.54831 (-02)	-0.54831 (-02)
0.39996 (+01)	0.94846 (-01)	-0.36772 (00)	0.95450 (01)	0.15846 (-01)	-0.46114 (-02)	0.10008 (+02)	0.13566 (-01)	-0.41195 (-02)	-0.41195 (-02)
0.45096 (+01)	0.78227 (-01)	-0.28815 (00)	0.10055 (02)	0.13663 (-01)	-0.39669 (-02)	0.10896 (+02)	0.99944 (-02)	-0.31641 (-02)	-0.31641 (-02)
0.49877 (+01)	0.65840 (-01)	-0.23254 (00)	0.10565 (02)	0.11782 (-01)	-0.34262 (-02)	0.11984 (+02)	0.72209 (-02)	-0.24881 (-02)	-0.24881 (-02)
0.54977 (+01)	0.55184 (-01)	-0.18739 (00)	0.11075 (02)	0.10154 (-01)	-0.29700 (-02)	0.13004 (+02)	0.49482 (-02)	-0.20881 (-02)	-0.20881 (-02)
0.60077 (+01)	0.46548 (-01)	-0.15275 (00)	0.11585 (02)	0.87410 (-02)	-0.25832 (-02)	0.13992 (+02)	0.31453 (-02)	-0.16723 (-02)	-0.16723 (-02)
0.64859 (+01)	0.39877 (-01)	-0.12726 (00)	0.12095 (02)	0.75098 (-02)	-0.22538 (-02)	0.15012 (+02)	0.15591 (-02)	-0.14565 (-02)	-0.14565 (-02)

0.69959 (+01)	0.33960 (-01)	-0.10563 (-04)	0.12605 (02)	0.64339 (-02)	-0.19723 (-02)	0.16032 (+02)	0.13827 (-02)	-0.13473 (-02)
0.75059 (+01)	0.29029 (-01)	-0.88347 (-04)	0.13115 (02)	0.54912 (-02)	-0.17309 (-02)			
0.80159 (+01)	0.24892 (-01)	-0.74394 (-04)	0.13625 (02)	0.46627 (-02)	-0.15234 (-02)			
0.84940 (+01)	0.21589 (-01)	-0.63666 (-04)	0.14135 (02)	0.39324 (-02)	-0.13448 (-02)			
0.90040 (+01)	0.18601 (-01)	-0.54198 (-04)	0.14645 (02)	0.32888 (-02)	-0.11910 (-02)			
0.95140 (+01)	0.16043 (-01)	-0.46355 (-04)	0.14900 (02)	0.29919 (-02)	-0.11223 (-02)			
0.10024 (+01)	0.13851 (-01)	-0.39810 (-04)	0.15665 (02)	0.22038 (-02)	-0.94489 (-03)			
0.10502 (+01)	0.12075 (-01)	-0.34629 (-04)	0.15920 (02)	0.19694 (-02)	-0.89435 (-03)			
0.11012 (+01)	0.10432 (-01)	-0.29933 (-04)	0.16430 (02)	0.15368 (-02)	-0.80476 (-03)			
0.11490 (+01)	0.90929 (-02)	-0.26175 (-04)	0.16940 (02)	0.11461 (-02)	-0.72926 (-03)			
0.12000 (+01)	0.78479 (-02)	-0.22735 (-04)	0.17450 (02)	0.79071 (-03)	-0.66682 (-03)			
0.12988 (+01)	0.58783 (-02)	-0.17378 (-04)	0.17960 (02)	0.46389 (-03)	-0.61689 (-03)			
0.13498 (+01)	0.50496 (-02)	-0.15165 (-04)	0.18470 (02)	0.15929 (-03)	-0.57990 (-03)			
0.14008 (+02)	0.43265 (-02)	-0.13234 (-02)						
0.14518 (+02)	0.36955 (-02)	-0.11550 (-02)						
0.14996 (+02)	0.31771 (-02)	-0.10162 (-02)						
0.15985 (+02)	0.22959 (-02)	-0.77723 (-02)						
0.16495 (+02)	0.19262 (-02)	-0.67465 (-02)						
0.17993 (+02)	0.11054 (-02)	-0.43455 (-02)						
0.18503 (+02)	0.90078 (-03)	-0.36919 (-02)						
0.19013 (+02)	0.72776 (-03)	-0.31033 (-02)						
0.19491 (+02)	0.59154 (-03)	-0.26023 (-02)						
0.20001 (+02)	0.47146 (-03)	-0.21141 (-02)						
0.20511 (+02)	0.37521 (-03)	-0.16662 (-02)						
0.20798 (+02)	0.33084 (-03)	-0.14290 (-02)						
0.21021 (+02)	0.30095 (-03)	-0.12508 (-02)						
0.21212 (+02)	0.27846 (-03)	-0.11019 (-03)						
0.21403 (+02)	0.25878 (-03)	-0.95607 (-03)						
0.21595 (+02)	0.24187 (-03)	-0.81288 (-03)						
0.21818 (+02)	0.22557 (-03)	-0.64856 (-03)						
0.22009 (+02)	0.21450 (-03)	-0.50953 (-03)						
0.22200 (+02)	0.20608 (-03)	-0.37166 (-03)						
0.22423 (+02)	0.19957 (-03)	-0.21159 (-04)						
0.22615 (+02)	0.19683 (-03)	-0.74443 (-05)						
0.22710 (+02)	0.19645 (-03)	-0.57130 (-06)						
0.22742 (+02)	0.19647 (-03)	+0.17237 (-06)						
0.22838 (+02)	0.19696 (-03)	+0.86245 (-05)						

Note: Numbers in brackets indicate decimal order, i.e., 0.1000(16-) means 10⁻¹⁷.

formula (1) do not depend on Z , and their sum equals about 2.109 eV. Hence on the Gombash model the problem of calculating the ionization energy of the atoms and ions reduces to the determination of r_0 and the density distribution of the atomic electrons, or the corresponding atomic and ionic electrostatic potentials. For this purpose we must solve the Thomas-Fermi-Dirac (TFD) equation with a correction for electron correlation. The nonlinear differential equation for the dimensionless atomic (ionic) potential Ψ has the form

$$\Psi'' = x \left[\left(\frac{\Psi}{x} \right)^{1/2} + \beta'_0 \right]^3, \quad (2)$$

where $\beta'_0 = 0.2394/Z^{2/3}$; $x = r/\mu$ is a dimensionless coordinate, and $\mu = 0.88534a_0/Z^{1/3}$. In the present problem equation (2) is supplemented by the boundary conditions

$$\Psi(0) = 1; \quad \Psi(x_0) = \frac{\beta'^2}{16} x_0; \quad x_0 \Psi'(x_0) - \Psi(x_0) = -q, \quad (3)$$

where $x_0 = r_0/\mu$; $q = (Z - N_1/Z)$. Thus the three boundary conditions for the second-order equation determine both the boundary x_0 (depending on the degree of ionization q) and the potential Ψ . We note that formulas (1) to (3) also describe the affinity of the electron toward the atom.

Equation (2) can only be solved numerically.* The integration of Eq. (3) was carried out by the Runge-Kutta method [3] on an electronic computer. Thus, using approximate value of x_0 , the initial data for the $\Psi(x)$ curve at x_0 were calculated, i. e., $\Psi(x_0)$ and $\Psi'(x_0)$, after which integration proceeded on the basis of a variable step corresponding to a given accuracy of determining x_0 . The calculation was repeated for each value of q . The function Ψ in the neighborhood of the point $x=0$ may be represented as a series

$$\Psi(x) = 1 + \frac{4}{3}x + \frac{3}{2}\beta'_0 x^{3/2} + \dots \quad (4)$$

Here $\Psi(0) = \Psi(10^{-16})$ to an accuracy of the 16th decimal place and $\Psi'(0) = \Psi'(10^{-16})$ to an accuracy of the 8th. The approximate value of x_0 was found from an approximate formula corresponding to the asymptotic behavior of the solution of equation (2) at $x_0 \gg 1$:

$$x_0 = 12^{2/3} \left(\frac{7.772Z}{n} \right)^{1/3} \left[1 - \left(\frac{n}{Z} \right)^{1/4} \right].$$

Table 1 gives values of x_0 obtained by solving equation (2) as a function of charge q (in electron-charge units) for the uranium and calcium atoms. We note that, in the present investigation, analogous calculations were carried out in parallel for the uranium and calcium atoms in order to check the accuracy of the actual statistical model in calculating the ionization energy. On the basis of these data, formula (1) was used to calculate the three first ionization potentials of the uranium atom and the first ionization potential of the calcium atom (Table 2).

The parallel calculations of the uranium and calcium atoms were carried out because both contained two weakly-bound S electrons (for uranium these were the 7S electrons). Of course, this analogy is rather remote, but unfortunately neither theoretical nor experimental data relating to the ionization potentials of the actinides (to which uranium is most akin as regards the structure of the outer electron shells) are available. We may assert a priori that the uranium atom is better described by the statistical model than the calcium atom, since the former is the heavier. The importance of the correction to the TF model is evident from the fact that the corresponding values for the ionization potential of U in the TF model are a long way from the true ones (thus $I_1 = 1.78$ eV, $I_2 = 7.98$ eV, $I_3 = 16.79$ eV). Sometimes, the values presented for I_2 and I_3 are used in practical calculations for the ionization equilibrium of uranium plasma, while I_1 is taken as 4 eV [8], which is also too small.

A fairly correct measurement of the I_1 of uranium was carried out in [9] by the method of surface ionization ($I_1 = 6.08 \pm 0.08$ eV). No experimental determinations of I_2 and I_3 have been made. The theoretical and experimental results agree closely (to within 5%). Considering that the statistical model gives more reliable values of I_n as the value of n increases, the values given in Table 2 for I_2 and I_3 are fairly reliable. The experimental value of I_1 for calcium is 6.11 eV, i. e., the accuracy of the calculation is better than 8%.

* As far as we know [3], Gombash-type equations have only been integrated numerically for the atoms of noble gases (argon, krypton, and xenon).

We may also consider certain additional corrections to the values obtained for I_1 . In the case of uranium, it would be really more correct to consider the problem of the motion of the hexavalent electrons in the statistical field of the core (radon, $Z=86$). However, even in the approximation of the Hartree-Fock self-consistent field, this problem requires the solution of six integral-differential equations, which involves great computing difficulties. A simplified version of the problem would consider the role of the valence electrons simply as a deformation of the core, which could be treated as a perturbation. The deformation of the core leads to a change in the motion of the orbital electrons themselves. Thus the corresponding correction to the ionization potential is a correction of the second order of smallness with respect to the perturbation and (as may easily be seen) tends to increase I_1 . However, even when considering the effects of the two 7S electrons in the potential field of the core, this problem is not simple, and is analogous to the problem of the isotopic shift of levels considered in nuclear physics [10]. This kind of adiabatic problem with a small parameter ($v_{\text{val}}/v_{\text{core}} \ll 1$) may in principle be solved, but there would be little point in solving it simply to make the accuracy better than 5%, especially as the potential of the core would again have to be treated on the statistical model, and the correction is one of the second order with respect to the perturbation, i. e., it is very small.

The calculation of the statistical potential Ψ is not only of importance in connection with the problem considered here. The function $\Psi(x)$ is also used in estimating such atomic characteristics as the polarizability, the diamagnetic susceptibility, etc., and also in other problems, for example, in calculating electron scattering at heavy atoms. In view of this, we consider it desirable to present the values of $\Psi(x)$ and $\Psi'(x)$ for U, U^+ , and U^{++} in Table 3 (see pp. 3-4).

LITERATURE CITED

1. L. Thomas, Proc. Cambr. Phys. Soc., 23, 542 (1927); E. Fermi, Z. Phys., 48, 73 (1928).
2. P. Dirac, Proc. Cambr. Phys. Soc., 26, 376 (1930).
3. P. Gombash, Statistical Theory of the Atom and Its Application [Russian translation], Moscow, IL (1951).
4. E. Wigner, Trans. Farad. Soc., 34, 678 (1938).
5. D. Kirzhnits, "Trudy FIAN", XVI, 1 (1961).
6. G. Baraff, Phys. Rev., 123, 2087 (1961).
7. V. Erma, Phys. Rev., 132, 2100 (1963).
8. J. Katz and E. Rabinowicz, Chemistry of Uranium [Russian translation], Moscow, IL (1948).
9. I. Bakulina and I. Ionov, ZhÉTF, 36, 1001 (1959).
10. I. Gol'dman, ZhÉTF, 24, 177 (1953).

CALCULATION OF THE DISSOCIATION ENERGY OF
CALCIUM AND URANIUM MONOFLUORIDES

L. P. Kudrin and M. Ya. Mazeev

UDC 539.196.6

The dissociation energies of the CaF and UF molecules were calculated by a variational method. The electron density distribution in Ca^+ was calculated for this purpose from the statistical model of the atom and on the Hartree-Fock approximation; the electron density in U^+ was also calculated from the statistical model, on the basis of the author's earlier paper [1]. The electron density in the F^- ion was calculated on the Hartree-Fock principle. Both methods gave dissociation energies agreeing closely with experiment for the CaF. For UF there were no experimental data.

The calculation of the dissociation energy of diatomic molecules on the statistical model is, generally speaking, a very coarse approximation, since the chemical bond is determined by the electrons in the highest shells. The statistical theory gives an especially poor description of the peripheral parts of the atom; hence it is almost impossible to obtain any reliable result for the bond energy. For homopolar molecules, in fact, such estimates only give very coarse and approximate values of dissociation energy [2]. However, in considering typical heteropolar molecules (ionic bond), (the alkali halide molecules in particular belong to this class) it is reasonable to suppose that the molecules consist of ions with closed electron shells, for which the statistical description is more accurate. For example, the KF molecule may be considered as a system of interacting K^+ and F^- ions, the electron-shell structures of which are respectively similar to those of Ar and Ne. The results of specific calculations carried out in the 1930's by Jensen and Gombash [2] for the RhBr and LiBr molecules agree very well with experimental data, both in the value of the dissociation energy D and in the equilibrium distance between the nuclei δ . It should be noted that these calculations were based on coarse assumptions. Thus the statistical electron density in Jensen's calculation used the Lenz-Jensen distribution (rather arbitrary at large distances from the nucleus), the exchange interaction energy, etc., being omitted. However, the successful application of the statistical model to the alkali halide molecules (even under coarse assumptions) suggests that this model may give quite accurate results in calculating the D of other heteropolar molecules, if the model itself is somewhat refined.

The problem may be presented as follows. The total energy of a system of two ions is written down on the assumption that the potential of the electron cloud in this system is made up of the potentials of the electron clouds of the free ions:

$$V_e = V_{e1} + V_{e2}.$$

Then the energy of the two separated ions is subtracted from this. The interaction energy thus obtained is minimized with respect to the distance between the nuclei of the ions. The energy minimum gives the desired dissociation energy of the molecule, and δ_0 corresponds to the value of the equilibrium distance between the nuclei.

Let the electron-density distributions ρ_1 and ρ_2 in the ions X^+ and Y^- making up the molecule XY be known and let the ions lie at a distance of δ from each other. Then the interaction energy of these ions may be put in the form [2]

$$U = U_c + U_n + U_e + U_h + U_a + U_w, \quad (1)$$

where (in atomic units)

$$U_c = (Z_1 - N_1)(Z_2 - N_2) \frac{1}{\delta};$$

$$U_n = Z_2 \gamma_1(\delta) + Z_1 \gamma_2(\delta);$$

Translated from *Atomnaya Énergiya*, Vol. 22, No. 2, pp. 85, 88-89, February, 1967. Original article submitted August 9, 1966.

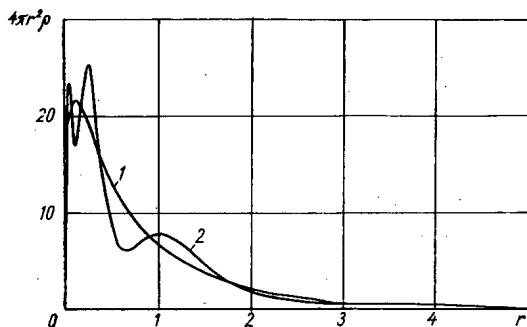


Fig. 1. Radial electron-density distribution for the calcium atom: 1) Statistical model; 2) self-consistent field.

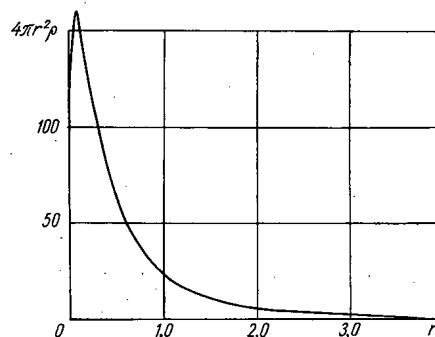


Fig. 2. Radial electron-density distribution for the uranium atom (statistical model).

$$U_e = -\frac{1}{2} \left[N_2 \gamma_1(\delta) + N_1 \gamma_2(\delta) + \int \gamma_1 \rho_2 dv + \int \gamma_2 \rho_1 dv \right];$$

$$U_k = \kappa_k \int [(\rho_1 + \rho_2)^{5/3} - \rho_1^{5/3} - \rho_2^{5/3}] dv;$$

$$U_a = -\kappa_a \int [(\rho_1 + \rho_2)^{4/3} - \rho_1^{4/3} - \rho_2^{4/3}] dv \quad (\kappa_k = 2.871, \kappa_a = 0.7386);$$

$$U_w = \int [W_D(\rho_1 + \rho_2) - W_D(\rho_1) - W_D(\rho_2)] dv;$$

$W_D = -\frac{0.05647 \rho^{4/3}}{0.1216 + \rho^{1/3}}$; Z_1, Z_2 are the charges on the nuclei of the ions X^+ and Y^- , and N_1 and N_2 are the numbers of electrons belonging to these ions.

The physical meaning of the various components of U may be interpreted as follows. The electrostatic interaction energy of the ionic point charges is described by U_c . The origin of the remaining terms lies in the spatial extent of the electron clouds, which overlap as the ions come together. Thus the nucleus of one of the ions lies under the influence of the non-Coulomb field of the effective charge of the nucleus $V_{e2}(r_2) r_2 + Z_2$. The term accounting for this screening is written as U_n . The energy U_e represents the reduction in the electrostatic repulsion of the electron clouds resulting from their partial overlapping, U_k describes the variation in the kinetic energy of the electron clouds of the ions, while U_a and U_w describe the variation in the exchange and correlation energy respectively. The potential of each electron cloud with respect to ions has the form

$$V_{ei}(r_i) = -\frac{N_i}{r_i} + \gamma_i(r_i), \quad i = 1, 2, \quad (2)$$

where $\gamma_i(r_i)$ r_i is the effective charge of the i -th nucleus, reduced by the charge of the ion at a distance of r_i ($\gamma > 0$).

The expression for the correlation energy corresponds to the Wigner approximation, which is valid for small electron densities. This description of the interaction energy differs from that of Jensen by its incorporation of terms U_a and U_w , which are important at the periphery of the ion.

The electron-density distribution for the ions Ca^+ and U^+ was found by means of the dimensionless potentials Ψ of these ions obtained in [1]. The functions Ψ were calculated by solving the Thomas-Fermi-Dirac equation with the Wigner correction for correlation interaction.

The electron density ρ is expressed in terms of Ψ as follows

$$\rho(r) = \frac{Z}{4\pi\mu^3} \left[\left(\frac{\Psi(x)}{x} \right)^{1/2} + \beta_0' \right]^3 \quad (3)$$

where $x = \frac{r}{\mu}$; $\mu = \frac{0.8853}{Z^{1/3}}$, $\beta_0 = \frac{0.2394}{Z^{2/3}}$. In calculating ρ for the F^- ion there is no need to employ the statistical model; it is sufficient to use the well-known wave functions in the Hartree-Fock approximation [3]. Then radial charge density $P(r) = 4\pi r^2 \rho(r)$ is calculated in terms of known radial electron functions $R(nl, r)$:

$$P(r) = \sum_{nl} 2(2l+1) R^2(nl, r). \quad (4)$$

Knowing $P(r)$, we may use Poisson's equation to calculate the effective potential of the ion. It is convenient to write this equation so that the unknown function is no longer the potential V_e but the quantity

$$\lambda(r) = \gamma(r)r = [Z + V_e(r)r] - (Z - N),$$

i.e., $\frac{d^2\lambda(r)}{dr^2} = \frac{P(r)}{r}$ (5)

The boundary conditions have the form

$$\lambda(r)|_{r=0} = N; \quad \lim_{r \rightarrow \infty} \lambda(r) = 0,$$

and in the case of a statistical distribution of density the second of these may be written

$$\lambda(r)|_{r=r_0} = 0,$$

where r_0 is the boundary of the ion.

In order to verify the accuracy of the statistical distribution, a calculation of this kind was also carried out for Ca^+ , for which the wave functions in the Hartree-Fock approximation are already known [4, 5]. For comparison, Fig. 1 and 2 give the radial densities, $P(r)$, for Ca^+ and U^+ .

The following results were obtained from these calculations:

a) In the first form of the calculation, in which the statistical distribution was used for Ca^+

$$D_{CaF} = 5.89 \text{ eV}; \quad \delta_0 = 3.99a_0;$$

b) in the case of the quantum-mechanical density distributions (Hartree-Fock approximation)

$$D_{CaF} = 5.99 \text{ eV}; \quad \delta_0 = 4.00a_0;$$

c) the statistical distribution for U^+ gave

$$D_{UF} = 5.09 \text{ eV}; \quad \delta_0 = 4.70a_0.$$

The value obtained in [6] (in which the dissociation energy of metal halides was determined by studying the equilibrium of reactions in flames) was

$$D_{CaF} = 135 \pm 7 \text{ kcal/mole} = (5.88 \pm 0.29) \text{ eV}.$$

The agreement between the results obtained for the dissociation energy in the two calculations for CaF clearly indicates the importance of the corrections for exchange and correlation interaction introduced into the statistical model. The good agreement between theory and experiment for CaF suggests that the method may also be regarded as reliable in calculating the value of D_{UF} .

LITERATURE CITED

1. L. P. Kudrin and M. Ya. Mazeev, *Atomnaya Énergiya*, 22, 83 (1966).
2. P. Gombash, *Statistical Theory of the Atom* [Russian translation], Moscow, IL (1951).
3. Froese, *Proc. Cambridge Phys. Soc.*, 53, 206 (1957).
4. D. Hartree and W. Hartree, *Proc. Roy. Soc.*, 164, 167 (1938).
5. D. Hartree, *Calculations of Atomic Structures* [Russian translation], Moscow, IL (1960).
6. L. V. Gurvich and V. G. Ryabova, *Teplofizika Vysok. Temp.*, 2, 401 (1964).

SYNTHESIS OF ISOTOPES OF ELEMENT 102 WITH
MASS NUMBERS 254, 253, AND 252

V. L. Mikheev, V. I. Ilyushchenko, M. B. Miller,
S. M. Polikanov, G. N. Flerov, and Yu. P. Kharitonov

UDC 546.799.92

In experiments on the irradiation of Pu^{242} and Pu^{239} with O^{16} and O^{18} ions in the extracted beam of the 310-cm cyclotron of the Joint Institute for Nuclear Research, isotopes of 102^{254} , 102^{253} and 102^{252} have been synthesized. Their properties are given below:

Isotope	$T_{1/2}$, sec	E_{α} , meV
102^{254}	75 ± 15	8.11 ± 0.03
102^{253}	95 ± 10	8.01 ± 0.03
102^{252}	4.5 ± 1.5	8.41 ± 0.03

In order to identify the isotopes, the excitation functions are measured in crossover reactions and the α decay of the daughter nuclei is recorded.

The synthesis and systematic investigation of the properties of the various isotopes of element 102 is of considerable interest. On the basis of the study of these properties, extrapolation in the region of the far transuranic elements of the existing systematics for α decay, as well as for spontaneous fission, can be verified experimentally. In particular, the effect of the neutron subshell $N=152$ on the decay characteristics of the isotopes of element 102 is interesting, together with the probability of their formation in reactions with heavy ions.

The first experiments for synthesizing isotopes of element 102, carried out in 1957-1958 [1-4], were undertaken under very difficult conditions. The only available method for synthesizing element 102 until now has been the bombardment of heavy targets with accelerated heavy ions. Because of the high tendency to fission of the recipient nuclei, the transverse cross section of the reactions which result in the formation of isotopes of element 102 is only 10^{-32} - 10^{-31} cm^2 . The intensities of the heavy ion beams used in the first experiments were ~ 0.1 μA . Together with the small cross section, this led to the observed effects being small and only poorly reproducible.

The photoemulsions and ionization chambers used for recording the decays of the nuclei obtained had insufficient energy resolution and a low functional reliability. Experience in working with short-lived nuclei and information about the mechanisms of heavy-ion nuclear reactions were extremely small. All this involves verification and refining of the results of the first experiments on element 102, since these results—obtained in various laboratories—are in poor agreement among themselves.

The first experiment to synthesize an isotope of element 102 with mass number 251-253 was carried out in 1957 by a joint team of Swedish, American, and English researchers on the cyclotron in Stockholm [1]. It was reported that in experiments involving the irradiation of Cm^{244} targets containing 4% Cm^{246} by C^{13} ions, an isotope of element 102, which was found to undergo α decay, was separated by a chemical method. The half-life of the isotope was 10 min and the α -particle energy was 8.5 ± 0.1 MeV.

This experiment, under considerably better experimental conditions, was repeated in the University of California [2], but the results of the first experiment were not reproduced successfully.

In 1957, in Moscow, experiments were undertaken in the internal beam of the cyclotron in the Institute of Nuclear Energy for synthesizing element 102 by irradiating Pu^{241} with O^{16} ions. Photoemulsions were used to record the α decay. As a result of the experiments [3, 5], an isotope with $2 < T_{1/2} < 40$ sec was obtained, which emitted α -particles with energy 8.9 ± 0.4 MeV.

Translated from *Atomnaya Énergiya*, Vol. 22, No. 2, pp. 90-97, February, 1967. Original article submitted August 20, 1966.

Based on the assumption that the most probable reaction giving isotopes of element 102 is the emission from the excited nucleus of four neutrons, the conclusion was drawn that the observed effect is evidently associated with the decay of the isotope 102^{253} .

In 1958, an experiment was carried out [4] in which synthesis of isotope 102^{254} was reported on the heavy-ion linear accelerator at Berkeley (USA). Identification was accomplished by observing the daughter product Fm^{250} , formed through decay of the isotope 102^{254} . It was found that the half-life of 102^{254} was 3 sec. In further experiments [6], α -particles with energy 8.3 MeV were recorded, which are related to the isotope 102^{254} . However, experiments carried out in the Joint Institute of Nuclear Research in 1965 [7, 8] showed that the half-life of 102^{254} is about 50 sec and the α -particle energy is 8-10 MeV.

The present experiment is devoted to the confirmation of the properties of the isotope 102^{254} started in [7, 8] and also to the synthesis and investigation of the properties of the isotopes 102^{253} and 102^{252} .

EXPERIMENTAL PROCEDURE

The experiments were carried out in the extracted beam of the 310-cm heavy-ion cyclotron in the Joint Institute of Nuclear Research. The experimental equipment, basically, was the same as that used in the synthesis of 102^{254} in the extracted beam of the 150-cm heavy-ion cyclotron [8, 9].

The procedure, similar to that developed in Dr. Ghiorso's laboratory [10], is based on a method for absorbing recoil atoms from a gas jet which issues from a small orifice in the gas-filled space where the recoil atoms are decelerated. After a specified cycle of accumulation of the recoil atoms on a plane metallic catcher, it is suddenly swivelled during 0.1 sec at an angle of 90° and enters below a silicon surface-barrier detector that records the α -particles from decay of the nuclei produced. Through the use of an electronic system, amplitude-time analysis of the pulses could be carried out simultaneously with two detectors. In all, there were four catchers for recoil atoms in the chamber, arranged at an angle of 90° to one another. The catchers are fixed to the ends of a four-bladed "maltese-cross" mechanism. The activity on one catcher was measured simultaneously with the buildup of recoil atoms on another catcher. During pulsing of the ion beam bombarding the target, the electronic circuit was locked.

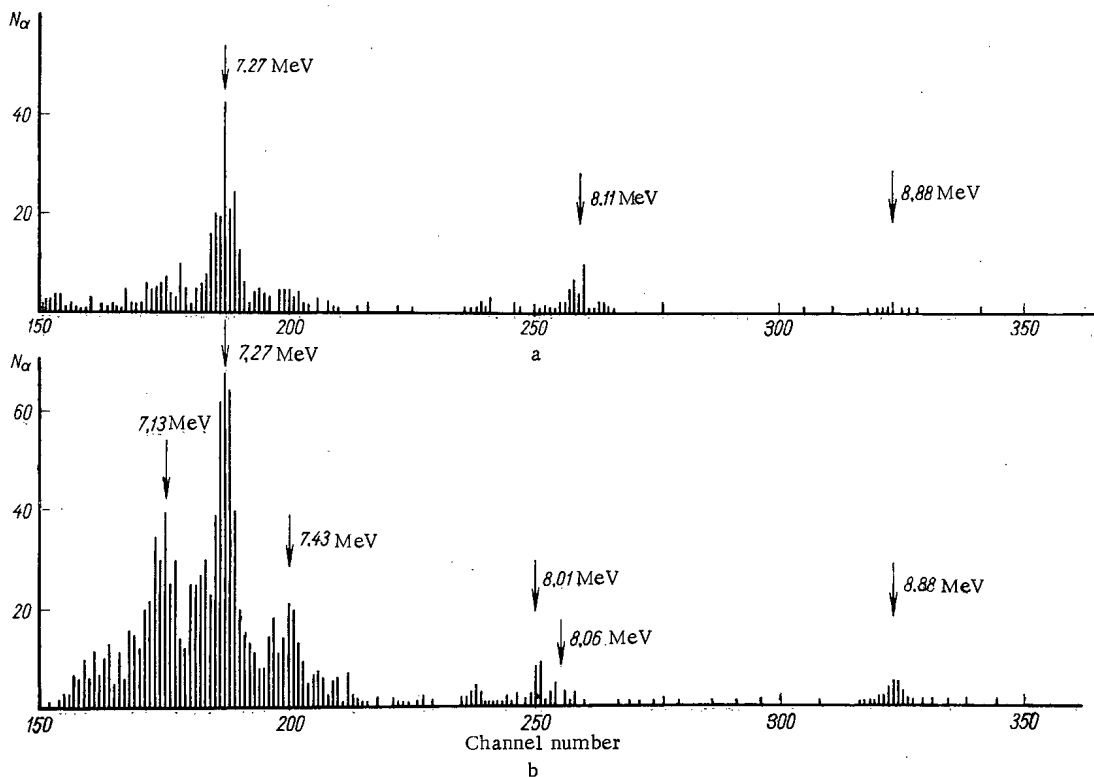


Fig. 1. Spectra of α -particles accompanying the decay of nuclei formed as a result of bombarding Pu^{242} targets with O^{16} ions with energies of 88 MeV (a) and 102 MeV (b).

The stabilization circuit for the entire measurement loop by pulses from a stable-amplitude generator used in the electronic equipment, and which was supplied continuously to the input of the pre-accelerator, allowed the stability of position of the groups of α -particles in the energy spectra obtained to be maintained to an accuracy of 10–15 keV at a level of 8 MeV during three days of continuous operation.

For stabilizing the collection factor of the recoil atoms, a fresh layer of silicone vacuum paste was deposited on the collector every time it passed below the gas jet, by means of the simplest device. As already mentioned in [9], the use of vacuum paste permits the requirement on the purity of the working gas to be reduced sharply. No variations of the collection factor were observed in this case, which fell outside the limits of statistical error of the number of pulses recorded during a time which exceeded three days of continuous operation and without changing the gas. The absolute value of the collection factor, equal to 50%, was determined by the Tb^{149}g produced in the reaction $\text{Pr}^{141}(\text{C}^{13}, 4n)\text{Tb}^{149}\text{g}$.

The energy of the ion beam was varied by means of aluminum-foil absorbers. The energy of the bombarding ions was measured by a semiconductor detector method similar to that described in [11].

The α -spectra and the half-life of the nuclear reaction products were recorded in the experiments. Identification of the isotopes obtained in the experiments was carried out by the excitation functions in the crossover reactions, and by observation of the decay of the daughter products. The results are given below for the individual isotopes.

ISOTOPE 102^{254}

Isotope 102^{254} was synthesized by the irradiation of a Pu^{242} target containing 5% Pu^{240} with O^{16} ions. Figure 1a shows one of the α -particle spectra obtained with an ion energy of 88 MeV (laboratory system of coordinates). The buildup cycle of activity on the collector τ , equal to the measurement cycle of the semiconductor (solid state) detector, was 200 sec. A sharp group of α -particles with an energy of 8.11 ± 0.03 MeV can be seen. This value coincides with value of 8.10 ± 0.05 MeV, obtained for the isotope 102^{254} synthesized in the reaction $\text{Am}^{243}(\text{N}^{15}, 4n)102^{254}$ [8]. The decay curves of the nuclei emitting α -particles with energy 8.11 ± 0.03 MeV in independent and separate series of measurements with $\tau = 200$ sec and $\tau = 100$ sec are plotted in Fig. 2. The weighted mean value of $T_{1/2} = 75 \pm 15$ sec is in good agreement with that given in [7, 8].

The activity yield curve with $E_{\alpha} = 8.11 \pm 0.03$ MeV is shown in Fig. 3. Its shape and position agree well with the calculated data for reactions involving the boil-off of four neutrons.

The formation cross section of isotope 102^{254} at the maximum of the excitation function of the reaction $\text{Pu}^{242}(\text{O}^{16}, 4n)102^{254}$ is 3.4×10^{-32} cm².

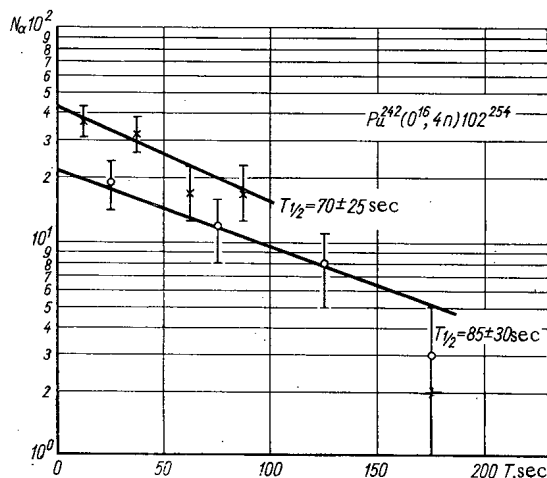


Fig. 2. Decay curves of nuclei emitting α -particles with energy 8.11 ± 0.03 MeV ($\tau = 100$ sec, upper curve; $\tau = 200$ sec, lower curve).

ISOTOPE 102^{253}

Figure 1b shows a typical spectrum of the α -particles obtained by the irradiation of a Pu^{242} target with O^{16} ions having an energy of 102 MeV and $\tau = 200$ sec. A group of α -particles with energy 8.01 ± 0.03 MeV can be seen in the spectrum. The decay curves of the nuclei emitting α -particles with energy 8.01 ± 0.03 MeV, obtained in independent measurements with $\tau = 100$ sec and $\tau = 200$ sec are shown in Fig. 4. Processing of these curves by the least squares method gives a mean value for the half-life of $T_{1/2} = 95 \pm 10$ sec. The activity yield curve with $E_{\alpha} = 8.01 \pm 0.03$ MeV is plotted in Fig. 3. Its form and position relative to the curve for the $\text{Pu}^{242}(\text{O}^{16}, 4n)102^{254}$ reaction agrees well with the calculated values for the reaction $\text{Pu}^{242}(\text{O}^{16}, 5n)102^{253}$. The cross section at the maximum is 4.4×10^{-32} cm².

In order to confirm that the decay of isotope 102^{253} is recorded in the experiments on irradiation of Pu^{242} by

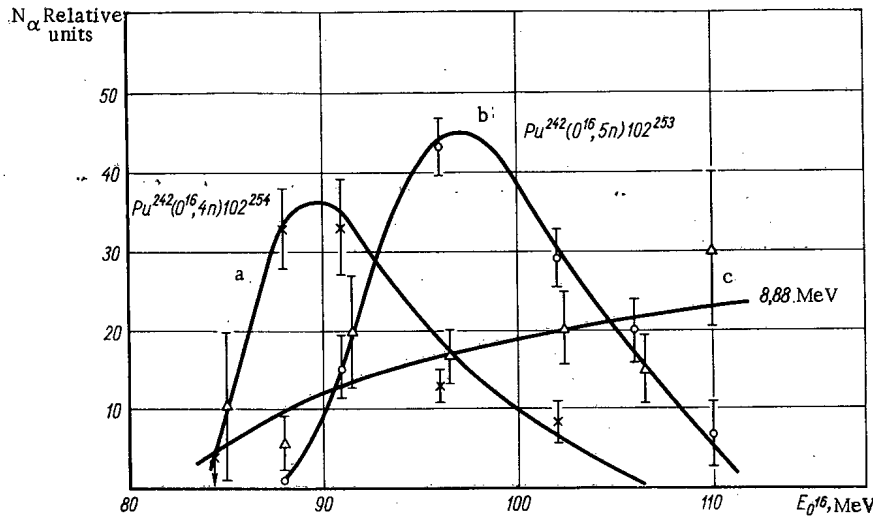


Fig. 3. Activity yield curves with $E_{\alpha} = 8.11 \pm 0.03$ MeV (a), $E_{\alpha} = 8.01 \pm 0.03$ MeV (b) and $E_{\alpha} = 8.88$ MeV (c).

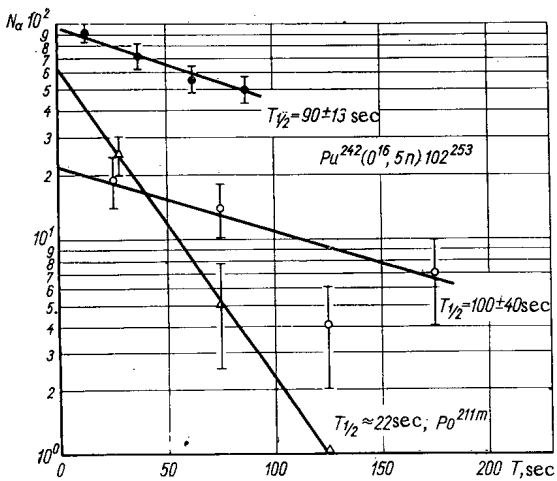


Fig. 4. Decay curves of nuclei emitting α -particles with energy 8.01 ± 0.03 ($\tau = 100$ sec, upper curve; $\tau = 200$ sec, center curve; the lower curve corresponds to the decay of Po^{211m}

O^{16} ions, an experiment was run to observe the α decay of the daughter nuclei Fm^{249} , formed by α decay of isotope 102^{253} . The essence of the experiment consists in the following. The cross, with the four recoil-atom collectors is set into oscillatory motion so that below each of the two solid-state detectors set at an angle of 90° to the axis of the ion beam, the collector on which the recoil atoms have accumulated from the gas jet and the perfectly clean collector which does not pass below the gas jet, pass in turn.

Thus, each detector registers the decay for one-half of the time of both the primary nuclei and secondary nuclei, and for the other half of the time only the secondary nuclei are recorded which are incident on the surface of the detector as a result of recoil from the preceding α decay.

There, as in the experiments for recording secondary products [8], the sensitive surface of the solid-state detector itself was used as the collector for the daughter nuclei. The electronic circuit enabled us to record which one of the collectors was under the detector at the instant of recording one or other pulse;

this made it possible to easily distinguish between the decay of primary products contaminated insignificantly with secondary products, and secondary products only.

The half-life of Fm^{249} of about 2.5 min [12, 13] and E_{α} according to data from [13], of 7.52 ± 0.03 MeV, agrees well with the results of our experiments on the synthesis of the isotope Fm^{249} in the reaction $Pu^{242}(C^{12}, 5n)Fm^{249}$. The experiments for observing the daughter products were carried out with an O^{16} ion energy of 96 MeV and $\tau = 100$ sec.

In these experiments, a total of 113 pulses with energy 8.01 MeV and 29 pulses with energy 8.11 MeV were recorded by the two detectors. In the secondary products, five pulses with energy 7.10 ± 0.03 MeV, 7 pulses with energy 7.40 ± 0.03 MeV and three pulses with energy 7.52 ± 0.03 MeV were recorded.

Although, in the system used for recording the secondary products, their half-lives are not determined and the presence only of the groups of pulses mentioned above (pulses were recorded

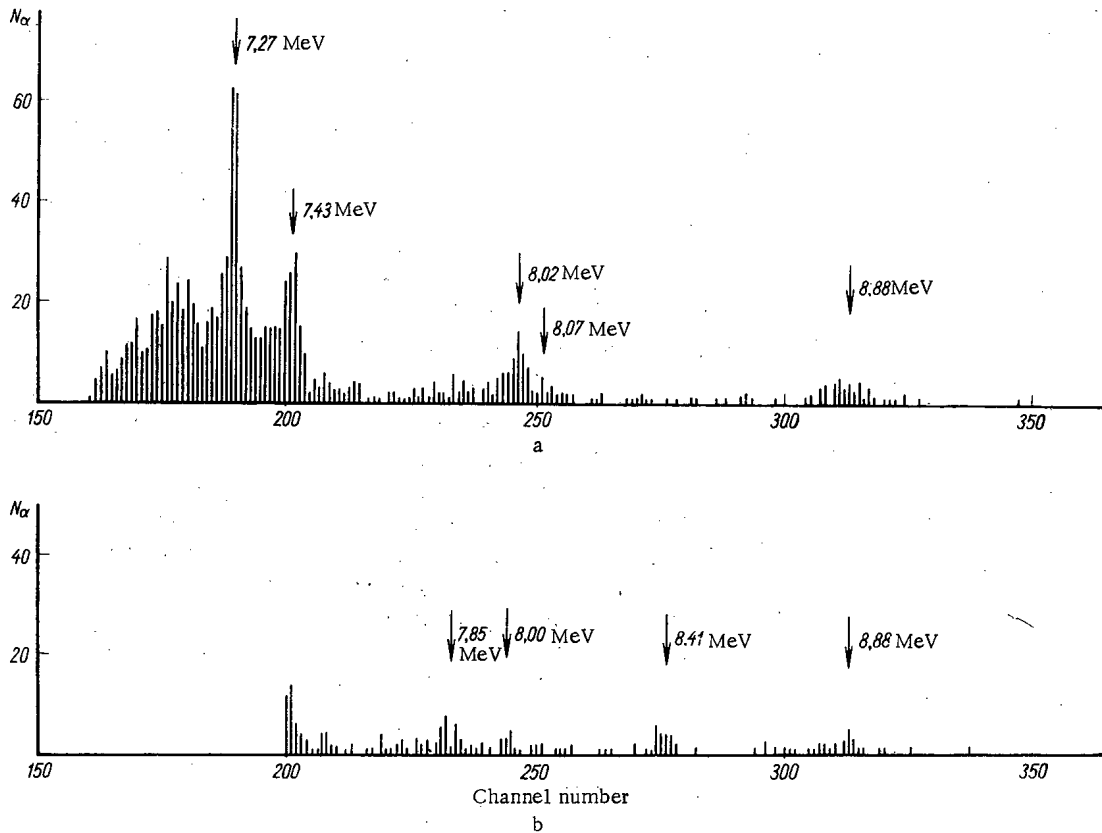


Fig. 5. Total spectrum of α -particles accompanying decay of the nuclei formed by bombardment of a Pu^{239} target with O^{18} atoms at energies of 90 and 196 MeV; a) $\tau = 200$ sec, and the spectrum of the α -particles corresponding to the bombardment of the same target by O^{18} ions with energy 96 MeV; b) $\tau = 12$ sec.

corresponding to $E_{\alpha} > 6.8$ MeV) allows us to relate them to Cf^{245} , Fm^{250} and Fm^{249} respectively. The recording efficiency for the secondary products only, is one-quarter relative to the recording efficiency for the primary products.

Thus, the observation of 29 decay events with the emission of α -particles, having an energy of 8.11 ± 0.03 MeV in the primary products, and seven decay events with $E_{\alpha} = 7.40 \pm 0.03$ MeV in the secondary products, serves as additional confirmation of the identification of the activity with $E_{\alpha} = 8.11 \pm 0.03$ MeV as relating to the isotope 102^{254} .

Taking account of the fact that Fm^{249} , according to data from [13], only undergoes α decay in $\sim 40\%$ of cases, we should have recorded ~ 10 Fm^{249} disintegrations in the 113 pulses corresponding to the isotopes 102^{253} .

The values of 3 obtained may be due statistically, but not exclusively, to the fact that Fm^{249} undergoes α -disintegration in a smaller fraction of cases than is indicated in [13]. Although, of course, the number of daughter nuclei disintegrations recorded is small, taking into account that in the primary products there were more than 1000 pulses in the range 6.8–7.5 MeV and in the secondary products there were only groups with energies 7.10; 7.40 and 7.52 MeV, the data obtained can be considered as additional confirmation of synthesis of the isotopes 102^{254} and 102^{253} .

The groups of α -particles noted in the spectra of Figs. 1a and 1b, with energies 8.88 and 7.27 MeV, obviously, are due to the decay of the Po^{211m} isomer, which is formed by lead impurities in the target.

The half-life for the 8.8 MeV line is ~ 22 sec (see Fig. 4), which agrees well with the value of 25 sec obtained in [14]. The form of the excitation function of the conversion reaction leading to Po^{211m} , which

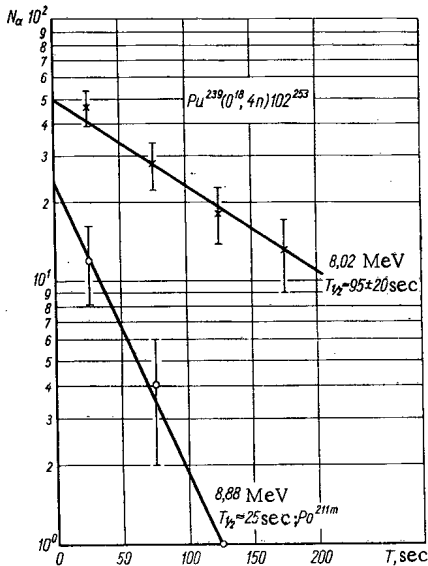


Fig. 6. Decay curves of the nuclei emitting α -particles with energies of 8.02 ± 0.03 and 8.88 MeV.

follows from Fig. 3, differs sharply from the form of the excitation function of the reaction with neutron boil-off from the compound nucleus.

The background in the region of the α -group with energy 8.01 MeV from $\text{Po}^{211\text{m}}$, as analysis shows, does not exceed 10% of the effect due to the isotope 102^{253} , at an energy of 96 MeV for the O^{16} ions.

For additional confirmation that the activity with $E_\alpha = 8.01 \pm 0.03$ MeV and $T_{1/2} = 95$ sec is related to the isotope 102^{253} , experiments were carried out to produce this isotope in the reaction $\text{Pu}^{239}(\text{O}^{18}, 4n)102^{253}$.

The total spectrum of the α -particles obtained for O^{18} ion energies of 90 and 96 MeV is shown in Fig. 5a, for a value of $\tau = 200$ sec. A sharply defined group of α -particles with energy 8.02 ± 0.03 MeV can be seen. The decay curve is plotted in Fig. 6. The half-life, $T_{1/2} = 95 \pm 20$ sec, agrees well with the value of 95 ± 10 sec obtained in the experiments on the irradiation of Pu^{242} by O^{16} ions. The excitation function of the activity with $E_\alpha = 8.02$ MeV's is shown in Fig. 7. Its shape and position are in good agreement with the calculated values for the reaction $\text{Pu}^{239}(\text{O}^{18}, 4n)102^{253}$. The cross section at the maximum is 5.1×10^{-32} cm².

The groups of α -particles with energies of 8.88 and 7.27 MeV, noted in the spectrum in Fig. 5a, with a half-life of about 25 sec (see Fig. 6) and with a monotonic excitation function (see Fig. 7), are obviously due to the decay of the $\text{Po}^{211\text{m}}$ isomer, as in the case with O^{16} ions.

Thus, all the experimental data obtained confirm that the half-life of the isotope 102^{253} is 95 ± 10 sec and that the energy of the most intense group of the α -particles is 8.01 ± 0.03 MeV. This group obviously, is due to the decay at the excited level of Fm^{249} , because according to classification [15], isotope 102^{253} must have a larger α decay energy than the isotope 102^{254} .

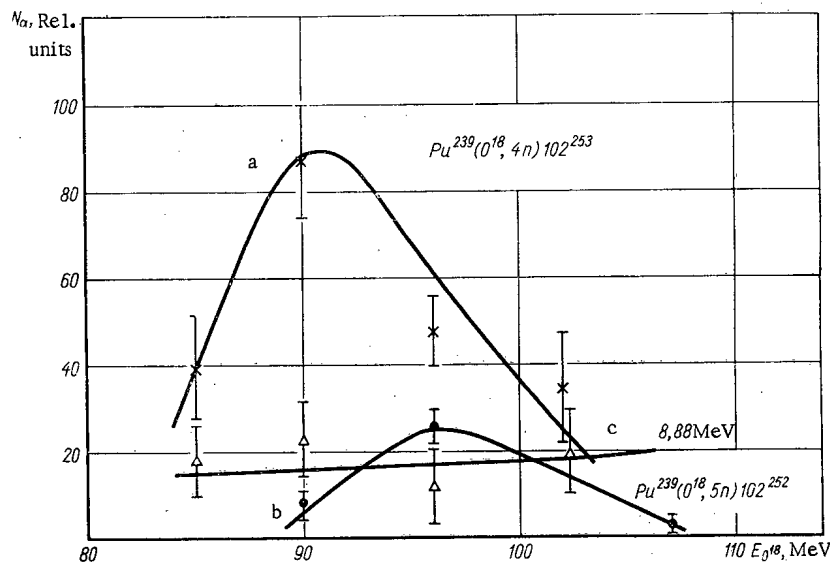


Fig. 7. Activity yield curves with a) $E_\alpha = 8.02 \pm 0.03$ MeV; b) $E_\alpha = 8.41 \pm 0.03$ MeV; and c) $E_\alpha = 8.88$ MeV.

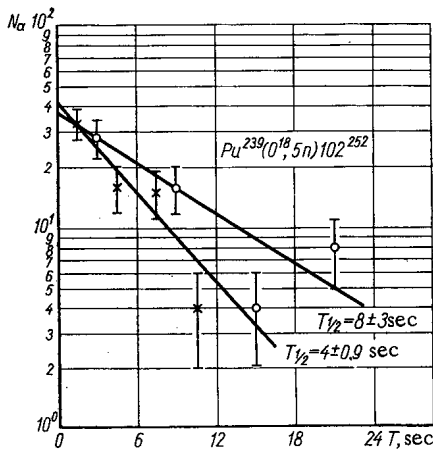


Fig. 8. Decay curves of nuclei emitting α -particles with energy 8.41 ± 0.03 MeV ($\tau = 12$ sec, lower curve; $\tau = 24$ sec, upper curve).

It can be seen from the spectra of Figs. 1b and 5a, that we cannot exclude that in 20–30% of cases of decay of isotope 102^{253} , α -particles are emitted with energy 8.06 ± 0.03 MeV. However, the inadequacy of the statistics does not permit reliable conclusions to be drawn concerning this. Decay with the emission of α -particles having $E_\alpha > 8.10$ MeV, even if recorded occurs in no more than 10% of cases.

ISOTOPE 102^{252}

Isotope 102^{252} was synthesized by irradiating a Pu^{239} target with O^{18} ions. The spectrum of the α -particles obtained at an ion energy of 96 MeV and with $\tau = 12$ sec is shown in Fig. 5b. The decay curves of the activity with $E_\alpha = 8.41 \pm 0.03$ MeV, obtained in independent measurements with $\tau = 12$ sec and $\tau = 24$ sec, are shown in Fig. 8. The weighted mean value for the half-life is 4.5 ± 1.5 sec. The activity yield curve with $E_\alpha = 8.41 \pm 0.03$ MeV is shown in Fig. 7. Its shape and position relative to the yield curve of the reaction $\text{Pu}^{239}(\text{O}^{18}, 4n)102^{253}$ agrees well with the calculated values for the reaction $\text{Pu}^{239}(\text{O}^{18}, 5n)102^{252}$. The cross section at the maximum is 1.6×10^{-32} cm². For additional verification that in the given case decay of the isotope 102^{252}

occurs, an experiment was carried out for observing the daughter product Fm^{248} , which emits α -particles with energy 7.85 MeV [8, 13]. The experiment is set up similar to the experiment for observing decay of the daughter products of isotopes 102^{254} and 102^{253} . Thirty α -particles, with energy 8.40 ± 0.03 MeV, were recorded in the primary products and three pulses were obtained with energy 7.85 ± 0.03 MeV in the recordings of the daughter products. The expected number of pulses was 7–8. The deviation does not fall outside the statistical limit. However, in the systematics of α decay [15], the point corresponding to the isotope Fm^{248} on the curve of log half-life versus α decay energy for isotopes of Fm is displaced somewhat downwards. It cannot be excluded that Fm^{248} undergoes electron capture in approximately 50% of cases. It should be borne in mind generally that by choosing suitable statistics for recording the α decay of the primary and daughter nuclei by the proposed scheme, we can determine very easily the ratio of the probabilities of α decay and electron capture for the daughter nuclei.

The experimental data obtained confirm the synthesis of the isotope 102^{252} in the reaction $\text{Pu}^{239}(\text{O}^{18}, 5n)102^{252}$, with $T_{1/2} = 4.5 \pm 1.5$ sec and $E_\alpha = 8.41 \pm 0.03$ MeV.

DISCUSSION OF RESULTS

The results of the investigation of isotope 102^{254} , described in this paper, are in good agreement with the earlier investigations of the properties of isotope 102^{254} carried out in the nuclear reaction laboratory of the Joint Institute of Nuclear Research [7, 8]. According to these results, the isotope 102^{254} is considerably more stable than was indicated from [4].

The properties of isotope 102^{253} , determined in this present paper, also differs from those stated in [3, 5]. However, it had been noted already in [3] that the observed effect might be associated with decay of the isotope 102^{252} . The values for the half-life and α -particle energy ($2 < T_{1/2} < 40$ sec; $E_\alpha = 8.9 \pm 0.4$ MeV) within the limits of measurement error coincide with the data of this paper for the isotope 102^{252} ($T_{1/2} = 4.5 \pm 1.5$ sec; $E_\alpha = 8.41 \pm 0.03$ MeV). The overestimate of the value for the α -particle energy might be caused by the procedure for preliminary processing of the photoemulsions for use inside the cyclotron chamber in a vacuum of $\sim 10^{-5}$ ion. In connection with this, it should be noted that in the 310-cm cyclotron of the Joint Institute of Nuclear Research, the properties of the isotope Fm^{249} were investigated in detail [13]; work on the synthesis of Fm^{249} was undertaken in Moscow simultaneously with the work on synthesizing element 102, in which photoemulsions were also used [12].

The value of $T_{1/2} = 160$ sec, obtained in [13]; agrees well with value of $T_{1/2} = 150$ sec obtained in [12]. However, measurements of the energy of the emitted α -particles indicated that it was not 7.9 ± 0.3 MeV but 7.52 ± 0.03 MeV. It cannot be excluded that there was a systematic error in determining the α -particle energy in the studies of element 102 and Fm^{249} , associated with the determination of the stopping power of the photoemulsion.

The question of the possible fraction of electron capture in the decay of the isotopes 102^{252} , 102^{253} , and 102^{254} requires a special investigation. If it be assumed that the even energy isotopes 102^{252} and 102^{254} do not undergo electron capture to any appreciable extent, then the extrapolated value of the partial half-life for the isotope 102^{253} with $E_{\alpha} = 8.01 \pm 0.03$ MeV is ~ 3 min, without taking into account possible prohibition. Thus, the isotope 102^{253} evidently undergoes electron capture in approximately 50% of cases. More quantitative conclusions could be drawn only after carrying out experiments to observe the products of electron capture of the isotopes 102^{252} , 102^{253} , and 102^{254} .

In conclusion, the authors deem it their duty to thank the staff of the U-300 cyclotron under the direction of B. A. Zager and I. A. Shelaev for ensuring the smooth operation of the accelerator with the extracted ion beam. The authors thank K. A. Gavrilov and Yu. S. Korotkin for the preparation of the targets which remained stable under the high-intensity beams of ions, A. M. Sukhov and L. P. Chelnokov for developing the high-stability electronic equipment and A. G. Belov for assistance in setting up the equipment and carrying out the measurements.

LITERATURE CITED

1. P. Fields et al., Phys. Rev., 107, 1460 (1957).
2. A. Ghiorso et al., Phys. Rev. Lett., 1, No. 1, 17 (1958).
3. G. N. Flerov et al., "Dokl. AN SSSR." 120, 73 (1958).
4. A. Ghiorso et al., Phys. Rev. Lett., 1, No. 18 (1958); No. 1, 18 (1958).
5. G. N. Flerov et al., ZhÉTF, 38, 82 (1960).
6. A. Ghiorso, Atomnaya Énergiya, 7, 338 (1959).
7. E. D. Donets et al., Atomnaya Énergiya, 20, 223 (1966).
8. B. A. Zager et al., Atomnaya Énergiya, 20, 230 (1966).
9. V. L. Mikheev, "Pribory i tekhnika éksperimenta", No. 4, 27 (1963).
10. R. Macfarlane and R. Griffioen, Nucl. Instrum. Methods, 24, 461 (1963).
11. Kh. Kekk et al., "Pribory i tekhnika éksperimenta", No. 4, 27 (1963).
12. V. P. Perelygin et al., ZhÉTF, 37, 1558 (1959).
13. G. N. Akap'ev et al., Preprint P-2704, Joint Institute of Nuclear Research, Dubna (1966).
14. I. Perlman et al., Phys. Rev., 127, 917 (1962).
15. V. Viola and G. Seaborg, J. Inorg. Nucl. Chem., 28, 697 (1966).

CALCULATION OF THE PASSAGE OF FAST NEUTRONS THROUGH GRAPHITE

L. M. Shirkin

UDC 539.125.52

Using the Monte-Carlo method, the author calculates the results of passing neutrons from a plane unidirectional source, with $E_0 = 3.3$ or $E_0 = 8.0$ MeV, through graphite. The angle of incidence is taken as 0° . The graphite layer thicknesses considered are from 0.9 to 6 times the free-path length. The author calculates the dose, energy and numerical albedos of graphite and also the angular and energetic distributions of the reflected neutrons and the angular distribution of the energy of scattered neutrons. He plots the mean cosine of the angle of scattering vs. the albedo, and also vs. the value of the energy angular-distribution constant. The data obtained may be found useful in the design of shadow and labyrinth shielding.

Using the Monte-Carlo method, I have calculated the results of passing neutrons from a plane unidirectional source, with energies 3.3 and 8.0 MeV, through graphite. I studied the albedo and angular energy distribution of the scattered neutrons emerging from graphite layers of various thicknesses. The method used in the calculation was described in [1]. The neutrons were taken to be normally incident on the graphite surface. They were moderated to 0.1 MeV. Data on the cross sections and angular distributions of neutrons scattered by carbon were taken from [2]. In calculating the dose I used the function given in [3] for converting neutron fluxes to doses.

Albedo

When neutrons fall on the boundary of a medium, the albedo β is that fraction of the incident neutrons which suffer reflection [4]. For fast neutrons, in addition to β_N , the relative number of back-scattered neutrons, we consider also β_D , the dose albedo, and β_E , the energy albedo: these are the ratios of the dose and the energy of the reflected neutrons to the dose and energy of the incident neutrons, respectively. To find the albedo of graphite, I calculated the histories of 500 neutrons with $E_0 = 3.3$ MeV and 1000 neutrons with $E_0 = 8.0$ MeV. I thus plotted the albedo vs. the scatterer thickness, and found the angular and energy distributions of the reflected neutrons.

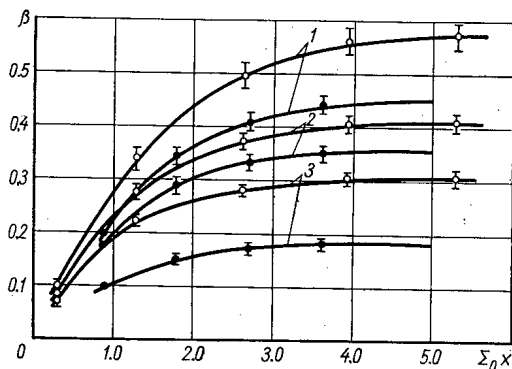


Fig. 1. Albedo of neutrons vs. thickness of graphite layer. \circ) $E_0 = 3.3$ MeV; \bullet) $E_0 = 8.0$ MeV. (1) β_N ; (2) β_D ; (3) β_E .

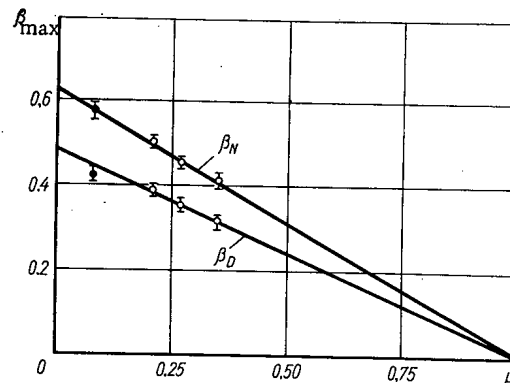


Fig. 2. Albedo for graphite vs. μ . \circ) $E_0 = 8.0$ MeV; \bullet) $E_0 = 3.3$ MeV.

Translated from *Atomnaya Énergiya*, Vol. 22, No. 2, pp. 97-100, February, 1967. Original article submitted May 12, 1966; revised October 21, 1966.

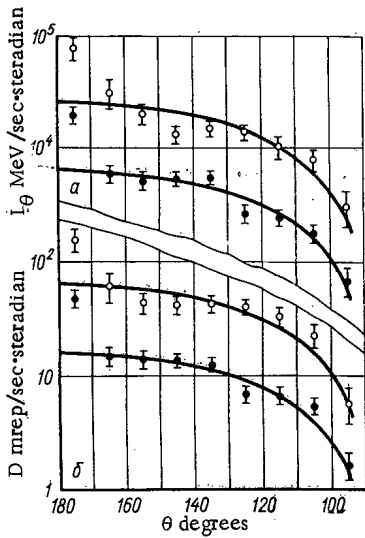


Fig. 3. Angular distributions of energy (a) and dose (b) of back-scattered neutrons. (○) $E_0 = 3.3$ MeV; (●) $E_0 = 8.0$ MeV. Each point corresponds to an energy flux or dose in a 10° range.

Figure 1 plots the albedo of the neutrons vs. the thickness of the graphite layer. This approximately follows the law

$$\beta = \beta_{\max}(1 - e^{-a\Sigma_0 x}),$$

where β_{\max} is the albedo of an infinitely thick reflector, a is a constant, and $\Sigma_0 x$ is the thickness of the graphite. For the energy and dose albedos $a \approx 0.8-0.9$. As we do not at present have the necessary data on the angular distribution of neutrons scattered by carbon, it is desirable to consider the influence of the mean cosine of the angle of scattering on the value of the albedo.

We can expect that, other things being equal, the number of reflected neutrons will be proportional to $(1-\mu)$, where μ is the mean cosine of the angle of total scattering (inelastic and elastic) of electrons incident on carbon. I also calculated the albedo of neutrons with $E_0 = 8.0$ MeV: here, in the energy range 6.5-8.0 MeV, instead of $\mu \approx 0.27$ [2] I took $\mu = 0.21$ and $\mu = 0.35$.

From these calculations I was able to plot the albedo vs. μ . The graph is shown in Fig. 2 (in drawing it I used the obvious fact that $\beta = 0$ when $\mu = 1$). Figure 3 shows the calculated angular distributions of the energy and dose of neutrons back-scattered from graphite. It will be seen that in both cases the calculated points (except between 180 and 170°) lie satisfactorily on cosine-law curves. The angle θ is reckoned from the direction of motion of the primary neutrons. The curves were calculated from the formula

$$I_\theta(D) = (\text{const}) \cdot \cos \theta.$$

Figure 4 shows the energy distribution of the back-scattered neutrons.

Angular Distribution of Energy of Scattered Neutrons.

I considered layers of graphite with thicknesses from 0.9 to 6 times the free-path length in barrier geometry. For the source with $E_0 = 3.3$ MeV the number of neutrons was 1000, while for that with $E_0 = 8.0$ MeV it was 2000.

Figure 5 shows the angular distribution of the energy flux of scattered neutrons at various distances from the source. The rms errors were calculated in the same way as in [5]. Each point corresponds to the energy flux in a 10° range. Examination of this figure enables us to draw the following conclusions.

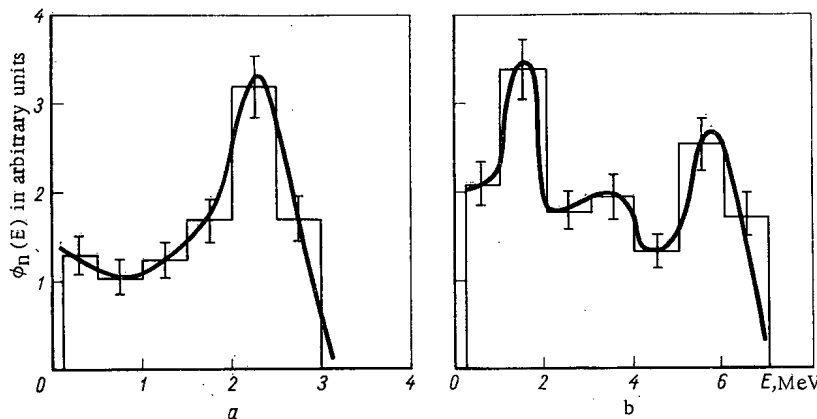


Fig. 4. Energy distribution of back-scattered neutrons. (a) $E_0 = 3.3$ MeV; (b) $E_0 = 8.0$ MeV.

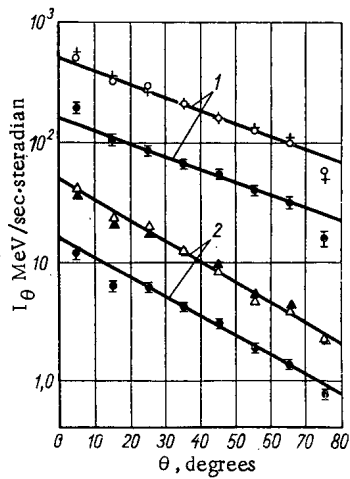


Fig. 5. Angular distribution of energy of scattered neutrons in graphite. (1) $E_0 = 3.3$ MeV; (2) $E_0 = 8.0$ MeV. \circ) $\Sigma_0x = 1.3$; $+$) $\Sigma_0x \approx 5.5$; \triangle) $\Sigma_0x = 0.9$; \blacktriangle) $\Sigma_0x = 5.0$; \bullet) averaged over whole barrier.

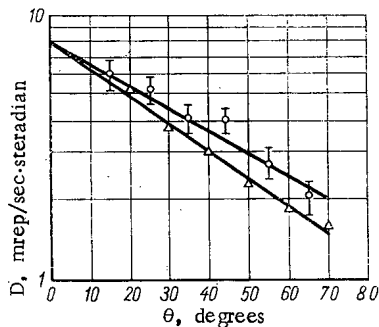


Fig. 7. Angular distribution of dose of scattered neutrons with $E_0 = 3.3$ MeV in graphite. \circ) $\Sigma_0x \approx 3$ (calculated for plane unidirectional source, dose of scattered neutrons in 10° interval); \triangle) $\Sigma_0x \approx 3.3$ (experimental [7], isotropic point source).

plane unidirectional source, the agreement between the theoretical and experimental data must be regarded as satisfactory.

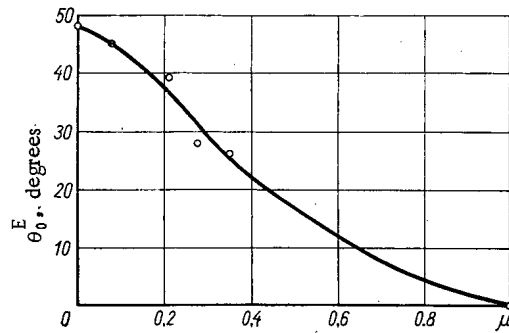


Fig. 6. Constant of angular energy distribution, θ_0^E , vs. μ . \bullet) $E_0 = 3.3$ MeV; \circ) $E_0 = 8.0$ MeV.

(i) The angular dependence of the energy flux per unit solid angle of fast neutrons scattered in graphite through an angle θ is given approximately by an exponential curve of the form

$$I(\theta) \sim e^{-\theta/\theta_0^E}$$

where θ_0^E is the constant of the angular energy distribution. (ii) θ_0^E is practically independent of the thickness of the shielding barrier. It is interesting to observe that this law is not obeyed for neutrons scattered in water or hydrogen (for which θ_0^E decreases markedly as the barrier thickness increases). (iii) The constant θ_0^E depends on the initial energy of the neutrons. Thus for neutrons with $E_0 = 8.0$ MeV, $\theta_0^E = 28^\circ$, while for neutrons with $E_0 = 3.3$ MeV, $\theta_0^E = 45^\circ$ which is nearly 1.6 times greater.

As in the case of the albedo, I also studied how the mean cosine of the angle of total scattering of the incident neutrons affects the value of θ_0^E . This is plotted in Fig. 6. It enables us to find approximately the value of θ_0^E for neutrons of any energy in graphite.

Figure 7 compares the theoretical and experimental [7] distributions of the dose of scattered neutrons in graphite. For $E_0 = 3.4$ MeV and $\Sigma_0x = 3.3$, the experimental value of the constant of the angular dose distribution θ_0^D , in graphite is equal to 41° (converted to the value per unit solid angle), while the calculated value is $\theta_0^D = 50^\circ$ (for $\Sigma_0x \approx 3$). Considering that the experiments were carried out with an isotropic point source, whereas the calculations refer to a

LITERATURE CITED

1. L. M. Shirkin. *Atomnaya Énergiya*, 17, 509 (1964).
2. L. P. Abagyan et al., *Group Constants for Design of Nuclear Reactors*. Moscow, Atomizdat (1964).
3. R. Aaronson et al., *Shielding of Means of Transportation Fitted with Nuclear Motors*. Moscow, Izd. Inostr. Lit., [Russian translation] p. 40 (1961).
4. B. Price et al., *Ibid.*, p. 431.
5. L. M. Shirkin, *Atomnaya Énergiya*, 20, 162 (1966).
6. L. M. Shirkin, *Atomnaya Énergiya*, 19, 288 (1965).
7. V. A. Dulin et al., *Atomnaya Énergiya*, 17, 486 (1964).

ANALYTICAL SOLUTION OF THE PROBLEM OF NEUTRON THERMALIZATION IN A HEAVY MODERATOR

M. V. Kazarnovskii

UDC 621.039.512.4

A model of a kernel for neutron scattering in a heavy moderator is presented. The kernel has the correct asymptotic behavior at high energies and leads to a scattering operator which yields zero when applied to the Maxwell distribution. The model includes three arbitrary functions of neutron velocity which may be chosen so as to give the best approximation of true scattering kernels. Within the framework of the diffusion approximation, the neutron distribution function is found for this model in integral form for the general case of an arbitrary source, and the question of eigenvalues and eigenfunctions of the neutron transport equation is discussed briefly.

Modern computer codes for solving the neutron transport equation make it possible to obtain very accurate solutions of almost any actual problem of neutron thermalization so long as there is accurate enough information on the differential characteristics of the interactions of neutrons with matter, such as the scattering law and the absorption and scattering cross sections. However, the data on the neutron scattering law are still not complete or accurate even for the most thoroughly studied moderators. Therefore the calculations are to be trusted only to the extent that this incompleteness and inaccuracy has been analyzed. In addition it is frequently necessary to investigate the properties of neutron distributions for various geometric and other moderator parameters, as in problems of determining optimum values of parameters. The numerical solution of such problems requires extremely cumbersome calculations, not to mention the fact that results presented in numerical form are often difficult to interpret. Finally, problems arise in neutron thermalization when the neutron velocity distribution function has singularities (for example, in the problem of the eigenvalues of the neutron transport equation), and numerical methods of solving the transport equation become very inefficient.

On the other hand it is very probable that in most practically important cases the neutron distributions do not depend very much on the details of the scattering kernel but are determined mainly by a relatively small number of neutron characteristics of the medium, such as the total and transport cross sections, the first one or two moments of the energy (or velocity) transfer in scattering the absorption cross section, etc. This is especially true for steady-state neutron spectra which, as a rule are smooth curves of very simple form. In these cases the use of scattering kernels which bear little relation to actual scattering kernels but have the above characteristics may produce satisfactory results. At least these results may serve as a convenient zero approximation.

Therefore, it is of interest to consider scattering kernels which allow one to find solutions of the neutron transport equation for differences in absorption and moderator geometry and at the same time include arbitrary functions or parameters which may be varied to investigate the effect of different characteristics of the scattering law on the neutron distributions. This report presents such a model for a heavy moderator. A solution of the transport equation for the case of an arbitrary nonstationary source is found in the diffusion approximation.

1. THE NEUTRON TRANSPORT EQUATION AND THE GENERAL PROPERTIES OF THE SCATTERING KERNEL

The neutron velocity distribution as a function of space and time $N(\mathbf{r}, \mathbf{v}, t)$, that is, the number of neutrons per unit volume at point \mathbf{r} , per unit range of velocity about \mathbf{v} , and at time t , may be written in the diffusion approximation as

$$N(\mathbf{r}, \mathbf{v}, t) = \sum_B \chi_B(\mathbf{r}) N_B(\mathbf{v}, t), \quad (1)$$

Translated from *Atomnaya Énergiya*, Vol. 22, No. 2, pp. 100-107, February, 1967. Original article submitted August 20, 1966.

where the $\chi_B(\mathbf{r})$ forms an orthonormal set of eigenfunctions of the Laplacian operator which vanish at the extrapolated moderator boundary, the B^2 are the corresponding eigenvalues, and the functions $N_B(\mathbf{v}, t)$ satisfy the equation

$$\frac{\partial N_B}{\partial t} = - \left[\frac{1}{\tau_a} + D(\mathbf{v}) B^2 \right] N_B + \hat{H} N_B + S_B(\mathbf{v}, t). \quad (2)$$

Here τ_a is the neutron absorption lifetime and $D(\mathbf{v})$ is the diffusion coefficient:

$$S_B(\mathbf{v}, t) = \int \chi_B(\mathbf{r}) S(\mathbf{r}, \mathbf{v}, t) d\mathbf{r}, \quad (3)$$

$S(\mathbf{r}, \mathbf{v}, t)$ is the source density, and the scattering operator is given by

$$\hat{H} N(\mathbf{v}) = \int_0^\infty w(\mathbf{v}' \rightarrow \mathbf{v}) N(\mathbf{v}') d\mathbf{v}' - N(\mathbf{v}) \int_0^\infty w(\mathbf{v} \rightarrow \mathbf{v}') d\mathbf{v}', \quad (4)$$

where $w(\mathbf{v}' \rightarrow \mathbf{v})$ is the scattering kernel, that is, the probability that in one second a neutron will have its velocity changed from \mathbf{v}' to a unit velocity range about \mathbf{v} .

The scattering kernel should satisfy the following general requirements.

1) As $\mathbf{v}' \rightarrow \infty$ it goes over into the kernel for scattering from free stationary atoms, i. e., in the general case of a moderator consisting of a mixture of various isotopes:

$$\left. \begin{aligned} \lim_{\mathbf{v}' \rightarrow \infty} w(\mathbf{v}' \rightarrow \mathbf{v}) &= \sum_j w_j^{(f)}(\mathbf{v}' \rightarrow \mathbf{v}); \\ w_j^{(f)}(\mathbf{v}' \rightarrow \mathbf{v}) &= \begin{cases} \sum_{jf} \frac{(A_j+1)^2}{2A_j} \cdot \frac{v}{v'}, & \frac{A_j-1}{A_j+1} v' < v < v'; \\ 0, & v' < v \text{ or } \frac{A_j-1}{A_j+1} v' > v, \end{cases} \end{aligned} \right\} \quad (5)$$

where A_j is the mass number of an atom of type j , Σ_{jf} is the partial macroscopic cross section for scattering from such an atom if it is considered free and stationary. 2) The principle of detailed balance should be satisfied

$$M(\mathbf{v}') w(\mathbf{v}' \rightarrow \mathbf{v}) = M(\mathbf{v}) w(\mathbf{v} \rightarrow \mathbf{v}'), \quad (6)$$

where $M(\mathbf{v}) = 4\pi^{-\frac{1}{2}} v^2 e^{-v^2}$ is the Maxwell distribution. * 3) The function $w(\mathbf{v}' \rightarrow \mathbf{v})$ must be positive for all \mathbf{v}' and \mathbf{v} .

The question arises as to whether it is possible to find an expression for the scattering kernel which satisfies these requirements and at the same time leads to a solution of Eq. (2) of sufficiently simple analytic form. Unfortunately it turns out to be impossible as may be seen from the following argument. According to Eqs. (4) and (5) as $\mathbf{v}' \rightarrow \infty$ we have

$$\hat{H} N(\mathbf{v}) = \sum_j \left[\frac{(A_j+1)^2}{2A_j} \times v \Sigma_{jf} \int_{\frac{A_j-1}{A_j+1} v}^{\frac{A_j+1}{A_j-1} v} \frac{N(\mathbf{v}')}{v'} d\mathbf{v}' - v \Sigma_{jf} N(\mathbf{v}) \right]. \quad (7)$$

In the simplest case of a heavy moderator for which all the $A_j \gg 1$ and the function $N(\mathbf{v})$ is sufficiently smooth, or more precisely if $N(\mathbf{v}')/v'$ varies slowly over the range $v \leq v' \leq (A_j+1)v/(A_j-1)$, the integral on the right hand side of this equation may be written in the form

$$\begin{aligned} \int_{\frac{A_j-1}{A_j+1} v}^{\frac{A_j+1}{A_j-1} v} \frac{N(\mathbf{v}')}{v'} d\mathbf{v}' &= \frac{N(\mathbf{v})}{v} \int_{\frac{A_j-1}{A_j+1} v}^{\frac{A_j+1}{A_j-1} v} d\mathbf{v}' + \frac{d}{dv} \left[\frac{N(\mathbf{v})}{v} \right] \int_{\frac{A_j-1}{A_j+1} v}^{\frac{A_j+1}{A_j-1} v} (v' - v) d\mathbf{v}' + \dots \\ &= \frac{2}{A_j-1} N(\mathbf{v}) + \frac{2}{(A_j-1)^2} v^2 \frac{d}{dv} \left[\frac{N(\mathbf{v})}{v} \right] + \dots \end{aligned}$$

* It is assumed that velocities are measured in units of $(2kT/m)^{1/2}$ where T is the temperature of the moderator, k the Boltzmann constant, and m the mass of a neutron.

Thus neglecting terms of the order $1/A^2$ we obtain

$$\hat{H}N(v) = \sum_j v \frac{\Sigma_{jf}}{A_j} \left\{ 3N(v) + v^2 \frac{d}{dv} \left[\frac{N(v)}{v} \right] \right\} = \frac{d}{dv} \left[\sum_j \frac{v^2}{A} N(v) \right], \quad (8)$$

where

$$\Sigma_f = \sum_j \Sigma_{jf}; \quad \frac{1}{A} = \sum_j \frac{1}{A_j} \cdot \frac{\Sigma_{jf}}{\Sigma_f}. \quad (9)$$

It should be noted that the terms which have been dropped, although of higher order in $1/A$, may turn out to be very important in certain cases involving high velocities. A more exact argument shows that for $v \gg 1$ these terms may constitute a fraction of the order $(v/A) |d(\ln N)/dv|$. In particular it is of the order v^2/A for the Maxwell distribution; that is, the approximation cannot be applied to the Maxwell distribution when $v \sim A^{1/2}$.

Thus for a heavy moderator and a sufficiently smooth distribution function the operator \hat{H} reduces to a first order differential operator as $v \rightarrow \infty$. Analysis shows* that when the condition of detailed balance (6) is imposed, \hat{H} becomes a differential operator of at least the second order† and Eq.(2) cannot be solved in analytic form. A similar situation prevails for a hydrogenous moderator ($A_j = 1$) when the expression $w_j^{(f)}(v' \rightarrow v)$ is also simplified.

Therefore if we want to obtain an analytic solution of Eq.(2) it is necessary to give up one of the first two requirements (5) or (6). Thus giving up the correct asymptotic behavior as $v \rightarrow \infty$ allows us to replace the scattering kernel by one that is separable (degenerate, single term) or by a linear combination of separable kernels (N. Corngold et al. Proc. NBL Conf. on Neutron Thermalization, 1962, Vol. IV, p. 1103). Then it is easy to find a solution of Eq.(2). However this solution holds only if $v \lesssim 1$ and therefore there arises the problem of correctly joining it to the Fermi distribution and describing the intermediate region.

The second possibility consists in giving up the principle of detailed balance. At first glance it seems that abandoning this principle in the investigation of the phenomenon of thermalization is like "throwing out the baby with the bath water." However, as will be shown later, this is not at all the case. It turns out that Eq.(6) may be replaced by the appreciably less stringent integral condition

$$\int_0^{\infty} M(v') w(v' \rightarrow v) dv' = M(v) \int_0^{\infty} w(v \rightarrow v') dv', \quad (10)$$

that is, by the requirement that $\hat{H}M(v)$ vanish. Then it is possible to construct a scattering kernel for which Eq.(2) may be solved in analytic form, and the solution represents the main features of actual neutron distributions rather well. Of course it must always be kept in mind that any approximation based on the relinquishing of so important a principle as the principle of detailed balance must under some conditions lead to nonphysical results. The question as to when one may expect to realize these conditions in practice is discussed briefly at the end of the article.

2. MODEL OF A NEUTRON SCATTERING KERNEL IN A HEAVY MODERATOR

The differential equation (8) for the asymptotic ($v \rightarrow \infty$) form of the scattering operator shows that the asymptotic form of the scattering kernel may be written in terms of a δ -function of $v' - v$ and its derivative. For Eq.(8) follows directly from (4) if we assume

$$w(v' \rightarrow v) = \omega(v') \delta(v' - v) - \mu(v') \delta'(v' - v), \quad (11)$$

* The point is that when (6) is satisfied, the differential part of the operator \hat{H} when applied to the Maxwell distribution must yield zero. But at the same time it must also give zero when applied to a function which has the Fermi distribution as its asymptotic form and this is a function essentially different from $M(v)$. This is possible only if the differential part of the operator \hat{H} contains derivatives of the second or higher order.

† The so-called heavy monatomic gas model and its generalization leads to such an operator.

where

$$\left. \begin{aligned} \omega(v') &\equiv \lim_{v' \rightarrow \infty} \int_0^{\infty} w(v' \rightarrow v) dv = v' \Sigma_f; \\ \mu(v') &\equiv \lim_{v' \rightarrow \infty} \int_0^{\infty} w(v' \rightarrow v) (v' - v) dv = \frac{v'^2}{A} \Sigma_f. \end{aligned} \right\} \quad (12)$$

It is obvious that the right hand side of (11) has a meaning only when it occurs as a factor in integrations over v' or v . Here the condition that the terms dropped in Eq. (8) be small is equivalent to the statement that the integral containing $\mu(v')$ be small in comparison with the integral containing $\omega(v')$.

The scattering kernel (11) does not satisfy either of the conditions (6) or (10). The simplest generalization which makes it possible to satisfy just the latter condition consists in adding a separable part to Eq. (11). In addition, for generality the functions $\omega(v')$ and $\mu(v')$ may be considered arbitrary functions of v' such that

$$\lim_{v' \rightarrow \infty} \omega(v') = v' \Sigma_f; \quad \lim_{v' \rightarrow \infty} \mu(v') = \frac{v'^2}{A} \Sigma_f. \quad (13)$$

As a result we obtain a scattering kernel of the form

$$w(v' \rightarrow v) = \omega(v') \delta(v' - v) - \mu(v') \delta'(v' - v) + a(v') b(v), \quad (14)$$

where a and b are so far arbitrary functions. Without loss in generality one may require that

$$\int_0^{\infty} b(v) dv = 1. \quad (15)$$

Such a kernel corresponds to the macroscopic scattering cross section

$$\Sigma_s(v) \equiv \frac{1}{v} \int_0^{\infty} w(v \rightarrow v') dv' = \frac{1}{v} [\omega(v) + a(v)]. \quad (16)$$

According to (13) it will have the correct asymptotic behavior if

$$\lim_{v \rightarrow \infty} \frac{a(v)}{v} = 0. \quad (17)$$

Using (16) we find by direct substitution that Eq. (10) is satisfied for

$$b(v) = \frac{a(v) M(v)}{a_0} - \frac{1}{a_0} \cdot \frac{d}{dv} [\mu(v) M(v)]; \quad (18)$$

$$a_0 = \int_0^{\infty} M(v) a(v) dv. \quad (19)$$

The condition that the scattering kernel be positive imposes the following limitations: 1) the functions $a(v')$ and $b(v)$ must be everywhere nonnegative; according to (18) this gives

$$a(v) - \frac{d\mu(v)}{dv} + 2\mu(v) \left(v - \frac{1}{v} \right) \geq 0; \quad (20)$$

2) the function $\omega(v')$ must be everywhere nonnegative

$$\omega(v') \geq \left| \frac{d\mu(v')}{dv'} \right|. \quad (21)$$

In addition the kernel (14) may be multiplied only by a sufficiently smooth function of velocities $\Phi(v, v')$, so that

$$\begin{aligned} \omega(v) &\geq \left| \mu(v) \frac{\partial \ln \Phi(v, v')}{\partial v} \right|; \\ \omega(v') &\geq \left| \mu(v') \frac{\partial \ln \Phi(v, v')}{\partial v} \right|. \end{aligned} \quad (22)$$

Since Φ may be the Maxwell distribution these formulas imply that

$$\omega(v) \geq 2 \left| \frac{\mu(v)}{v} \right| \text{ for } v \rightarrow 0; \quad (23)$$

$$\omega(v) \geq 2 |v\mu(v)| \text{ for } v \gg 1. \quad (24)$$

Equation (24) when combined with (13) shows how our model is limited at large velocities* ($v^2 > A/2$).

Therefore we will suppose from now on that A is large enough so that

$$v^2 < A/2. \quad (25)$$

in the velocity range of interest. In other respects the requirements listed earlier obviously are not inconsistent with the possibility of replacing the asymptotic form of the scattering kernel by the differential operator (11) and Eqs. (13) and (17).

Thus, taking into account the limitations noted, there remain three arbitrary functions ω , μ , and a . From physical considerations it follows that they must be bounded for all finite velocities, and in particular for $v \rightarrow 0$; according to (23)

$$\lim_{v \rightarrow 0} \frac{\mu(v)}{v} \text{ is bounded.} \quad (26)$$

According to (14) and (18) the scattering operator (4) in our model has the form

$$\hat{H}N = \frac{d}{dv}(\mu N) - aN + I \left[aM - \frac{d}{dv}(\mu M) \right] \quad (27)$$

where the constant I is

$$I = \frac{1}{a_0} \int_0^{\infty} aN dv. \quad (28)$$

It should be noted that the operator \hat{H} does not depend on ω but is determined solely by a and μ .

3. SOLUTION OF THE NEUTRON TRANSPORT EQUATION

The transport equation (2) with the scattering operator (27) has the form

$$\frac{\partial N}{\partial t} = - \left(\frac{1}{\tau_a} + a + DB^2 \right) N + \frac{\partial (N\mu)}{\partial v} + I \left[aM - \frac{d(M\mu)}{dv} \right] + S, \quad (29)$$

where the subscript B has been omitted for brevity. It may be solved in the following way. We measure time from the instant \dagger the neutron source is turned on; that is $N=0$ for $t \leq 0$. Then the Laplace transform of Eq. (29) with respect to t reduces to

$$\frac{d}{dv}(\mu n) - \left(x + \frac{1}{\tau_a} + a + DB^2 \right) n = -i \left[aM - \frac{d}{dv}(\mu M) \right] + s, \quad (30)$$

where

$$n(v, x) = \int_0^{\infty} N(v, t) e^{-tx} dt, \quad (31)$$

i. e.,

$$N(v, t) = \frac{1}{2\pi i} \int_{\alpha-i\infty}^{\alpha+i\infty} n(v, x) e^{tx} dx, \alpha > 0; \quad (32)$$

* As may be seen from the discussion following Eq. (9) this has to do with the fact that we selected an inexact asymptotic scattering kernel.

† The steady state case may be obtained by supposing that for $t > 0$ S does not depend on t , and going to the limit $t \rightarrow \infty$.

$$s(v, x) = \int_0^{\infty} S(v, t) e^{-tx} dt; \quad (33)$$

$$i(x) = \frac{1}{a_0} \int_0^{\infty} a_n dv. \quad (34)$$

Equation (34) follows directly from (28) and (31). This is an ordinary first order differential equation whose general solution may easily be shown to have the form

$$n(v, x) = \frac{1}{\mu(v)} \int_v^{\infty} s(v', x) F(x; v', v) dv' + C \exp \left\{ \int_v^{\infty} \left[x + \frac{1}{\tau_a} + a(v'') \right. \right. \\ \left. \left. + D(v'') B^2 \right] \frac{dv''}{\mu(v'')} \right\} + i(x) \left\{ M(v) - \frac{1}{\mu(v)} \int_v^{\infty} \left[x + \frac{1}{\tau_a} + D(v') B^2 \right] M(v') F(x; v', v) dv' \right\} \quad (35)$$

where

$$F(x; v', v) = \exp \left\{ \int_{v'}^v \left[x + \frac{1}{\tau_a} + a(v'') + D(v'') B^2 \right] \frac{dv''}{\mu(v'')} \right\}; \quad (36)$$

C is an arbitrary constant which may be found from the following considerations. When v becomes larger than the maximum velocity of the neutrons emitted by the source, i. e., when S(v, t) and therefore also s(v, x) vanish, then neutron distribution N(v, t) and the corresponding n(v, x) must fall off with v as $v^2 e^{-v^2}$. Using (13) we find that C=0, i. e.,

$$n = \frac{1}{\mu(v)} \int_v^{\infty} s(v', x) F(x; v', v) dv' + i(x) \left\{ M(v) - \frac{1}{\mu(v)} \int_v^{\infty} \left[x + \frac{1}{\tau_a} \right. \right. \\ \left. \left. + D(v') B^2 \right] M(v') F(x; v', v) dv' \right\}. \quad (37)$$

The quantity i(x) may be found by substituting (37) into (34). As a result we obtain

$$i(x) = \frac{\int_0^{\infty} \frac{a(v)}{\mu(v)} dv \int_v^{\infty} s(v', x) F(x; v', v) dv'}{\int_0^{\infty} \frac{a(v)}{\mu(v)} dv \int_v^{\infty} \left[x + \frac{1}{\tau_a} + D(v') B^2 \right] M(v') F(x; v', v) dv'} \quad (38)$$

Equations (1), (3), (32), (33), (36)-(38) give the solution of the general problem of the space and time dependence of the neutron velocity distribution function in the diffusion approximation for the case of a scattering kernel of the form (14) when condition (10) is satisfied.

A detailed discussion of this solution is beyond the scope of the present work and will be carried out separately. We present below the results for some special cases.

A Steady Monochromatic Neutron Source. This case may be obtained by assuming (cf. last footnote)

$$S_B(v, t) = \sigma_B \delta(v - v_0), \quad t > 0, \quad (39)$$

i. e., by (33)

$$s(v, x) = \frac{1}{x} \sigma_B \delta(v - v_0), \quad (39')$$

and N(v) must be found in the limit $t \rightarrow \infty$. As a result of using Eqs. (32), (36)-(38) we obtain

$$N(v) \equiv \lim_{t \rightarrow \infty} N(v, t) = \frac{\sigma_B}{\mu(v)} \theta(v_0 - v) F(0; v_0, v) + \sigma_B \frac{\int_0^{v_0} \frac{a(v)}{\mu(v)} F(0; v_0, v) dv}{\int_0^{\infty} \frac{a(v)}{\mu(v)} dv \int_v^{\infty} \left[\frac{1}{\tau_a} + D(v') B^2 \right] M(v') F(0; v', v) dv'} \\ \times \left\{ M(v) - \frac{1}{\mu(v)} \int_v^{\infty} \left[\frac{1}{\tau_a} + D(v') B^2 \right] M(v') F(0; v', v) dv' \right\}, \quad (40)$$

where $\theta(x)$ is defined by the relations

$$\theta(x) = \begin{cases} 0, & x < 0; \\ 1, & x > 0. \end{cases}$$

Pulsed Monochromatic Neutron Source. In this case

$$S_B(v, t) = \sigma_B \delta(t) \delta(v - v_0), \quad (41)$$

i. e.,

$$s(v, x) = \sigma_B \delta(v - v_0).$$

In this case we obtain from (32), (36)-(38)

$$\begin{aligned} N(v, t) = & \sigma_B \delta \left\{ t - \int_v^{v_0} \frac{dv'}{\mu(v')} \right\} \exp \left\{ - \int_v^{v_0} \left[\frac{1}{\tau_a} + D(v'') B^2 \right] \frac{dv''}{\mu(v'')} \right\} + \frac{\sigma_B}{2\pi i} \int_{\alpha-i\infty}^{\alpha+i\infty} dx e^{xt} \\ & \times \left\{ M(v) - \frac{1}{\mu(v)} \int_v^{v_0} \left[x + \frac{1}{\tau_a} + D(v') B^2 \right] M(v') F(x; v', v) dv' \right\} \\ & \times \frac{\int_0^{v_0} \frac{a(v)}{\mu(v)} F(x; v_0, v) dv}{\int_0^{v_0} \frac{a(v)}{\mu(v)} dv \int_v^{v_0} \left[x + \frac{1}{\tau_a} + D(v') B^2 \right] M(v') F(x; v', v) dv'} \quad (42) \end{aligned}$$

Eigenvalues and Eigenfunctions of the Neutron Transport Equation. It is easy to show that the eigenvalues of Eq. (29) are the poles of $n(v, x)$ as a function of x , and the corresponding eigenfunctions are, aside from a normalization factor, the residues of the poles of (32). It may be seen from (36) and (37) that the poles x_j of the function $n(v, x)$ are identical with the poles of $i(x)$; i. e. they are solutions of the transcendental equation

$$\int_0^{v_0} \frac{a(v)}{\mu(v)} dv \int_0^{v_0} \left[x_j + \frac{1}{\tau_a} + D(v') B^2 \right] M(v') F(x_j; v', v) dv' = 0, \quad (43)$$

and the corresponding eigenfunctions, normalized to unity, are

$$\psi_j(v) = \frac{M(v) - \frac{1}{\mu(v)} \int_v^{v_0} \left[x_j + \frac{1}{\tau_a} + D(v') B^2 \right] M(v') F(x_j; v', v) dv'}{1 - \int_0^{v_0} \frac{dv}{\mu(v)} \int_v^{v_0} \left[x_j + \frac{1}{\tau_a} + D(v') B^2 \right] M(v') F(x_j; v', v) dv'} \quad (44)$$

We note that for sufficiently small values of B^2 there exists at least one solution of Eq. (43) close to $\frac{1}{\tau_a}$ for which the corresponding eigenfunction is close to the Maxwell distribution.

4. CONCLUSION

It was shown above that if the scattering kernel is taken in the form (14), satisfying the integral condition (10), it is possible to find an analytic expression, in terms of quadratures, for the solution of the neutron transport equation in the diffusion approximation for arbitrary functions of velocity $a(v)$ and $\mu(v)$ and the diffusion coefficient $D(v)$ (and also $\omega(v)$ on which the solution in general does not depend).

The question naturally arises as to how well the true scattering kernel may be described by expressions of the type (14) and (18), and when the flaws in the form we have been considering may be particularly serious.

Since Eq. (14) is a differential operator it is only meaningful to compare the integral characteristics of the true kernel and the form considered, such as the macroscopic scattering cross section, the moments of the energy (or velocity) transfer, etc. The fact that the solution does not depend on the form of $\omega(v)$ implies that the functions $a(v)$ and $\mu(v)$ may be chosen rather arbitrarily and $\omega(v)$ defined so as to make the macroscopic scattering cross section (16) agree with the true value.

The functions a and μ may, for example, be determined by requiring that the first and second moments of the velocity transfer agree with the true values. Analysis shows that such a procedure is in general not unique. The functions a and μ determined this way contain an arbitrary parameter which may be further varied for the best approximation (14) to the true scattering kernel. At the same time it turns out that in certain cases the functions a and μ determined by the first two moments of the velocity transfer do not satisfy condition (20) or some of the requirements listed in section 2 for any choice of the arbitrary parameter mentioned above.

Another way of choosing the functions a and μ is to require agreement with the actual first two moments of the velocity transfer, i. e., the quantities

$$\int_0^{\infty} (v' - v)^n w(v' \rightarrow v) dv' \quad (n = 1; 2), \quad (45)$$

if, of course, they exist.* For our model the integrals (45) converge only if the function $a(v)$ falls off faster than $1/v^3$ as $v \rightarrow \infty$.

Finally, a and μ may be determined by requiring agreement between the actual values and some integral characteristics of the scattering kernel which reflect the thermalization properties of the moderator better than do the moments of the velocity transfer, although they may not have a simple interpretation. For example it is well known that for a steady source $N(v)$ in a homogeneous, infinite, weakly absorbing moderator the neutron velocity distribution function may be expanded in a series in inverse powers of the neutron lifetime τ_a :

$$N(v) = \tau_a M(v) + N_0(v) + \frac{1}{\tau_a} N_1(v) + \frac{1}{\tau_a^2} N_2(v) + \dots,$$

where $N_1(v)$ does not depend on τ_a . There is still the possibility that if the functions a and μ are determined from the conditions that $N_0(v)$ and $N_1(v)$ be close to the actual values, it is possible to obtain an even better approximation to the scattering kernel than indicated above.

Thus there are rather extensive possibilities of approximating the most important characteristics of the true scattering kernel with our model. On the other hand, as has already been noted, neutron spectra found in neutron thermalization problems generally do not depend much on the fine details of the scattering kernel. Therefore one may hope that our model will allow us to obtain an approximate scattering kernel which is quite adequate for solving many problems in the theory of neutron thermalization.

At the same time, since this model is based on special assumptions, one must expect that in certain cases it may lead to incorrect results. Actually, according to the principle of detailed balance, if a scattering kernel contains a term of the form $\mu(v') \delta(v' - v)$, it must also contain a term of the form $\nu(v') \delta''(v' - v)$, where the functions μ and ν are connected by a definite relation. The essence of our model is the fact that the term $\nu(v') \delta''(v' - v)$ was replaced by another such that the sum over all the remaining components of the scattering kernel would convert it into a separable part. Such an approximation is valid when the contribution of this term is small in comparison with the contribution from $\mu(v') \delta'(v' - v)$, i. e., when the neutron velocity distribution function is sufficiently smooth and μ is not too small, or when the neutron spectrum is close to Maxwellian. Therefore one may expect good results when the model is used to calculate steady-state neutron distributions when absorption and leakage not very important and $\mu(v')$ does not vanish in the velocity range considered. † Somewhat worse results, it appears, must be expected in calculations of nonsteady-state neutron spectra, particularly for velocities much larger than thermal where the neutron velocity distribution function in a heavy moderator changes rapidly with velocity and our approximation of the term $\nu(v') \delta''(v' - v)$ is particularly rough.

However, a final solution of the problem of the optimum approximation of the scattering kernel by an expression of the type (14), (18) and a determination of its applicability to the problem of neutron thermalization obviously requires further investigation.

In conclusion the author considers it his pleasant duty to express his sincere thanks to A. V. Stepanov for his constant interest in the work and for valuable discussions.

* For example, for a homogeneous moderator the integrals (45) diverge for $n \geq 0$.

† The function $\mu(v')$ may vanish and change sign at certain points if, for example, it is determined from such integral characteristics of the scattering kernel as the moments of the velocity transfer. In this case, as may be seen from Eq. (3) the neutron spectrum has singularities at these points.

CALCULATING THE SPATIAL AND ENERGY DISTRIBUTION OF
THERMAL NEUTRONS IN A HETEROGENEOUS REACTOR

M. V. Fedulov

UDC 621.039.512.45

A method is presented for determining the spatial and energy distribution of thermal neutrons within the cells of a heterogeneous reactor. If the effect of the asymmetric part of the scattering cross section on the change in neutron energy is neglected, the problem of determining the integral parameters of a cell may, in many cases, be reduced to the solution of monoenergetic Boltzmann equations for a certain set of energy values with a subsequent determination of the neutron energy spectrum. The possibility of using an iterative process for refining the results of the first approximation is investigated.

Let us consider the problem of determining the steady-state spatial and energy distribution of thermal neutrons in an elementary cell of a heterogeneous reactor. Although the distribution of neutrons with energies above some limiting value E_{LI} is of interest only in so far as it is needed to obtain a sufficiently accurate distribution for $E < E_{LI}$, we shall formally seek a solution of the Boltzmann equation for neutrons of all energies. The resonance structure of the absorption cross section for $E > E_{LI}$ need be taken into account only in the energy region close to E_{LI} . In addition, since the spatial and energy distribution of sources (fission neutrons) does not affect the thermal group, the term describing the sources will be neglected as is usually done in determining thermal neutron spectra in an infinite homogeneous medium. We write the steady-state Boltzmann equation for the neutron density [1]:

$$\Omega \text{grad}_r n(E, \Omega, r) + \Sigma_a(E, r) n(E, \Omega, r) = \frac{1}{\sqrt{E}} \int_0^\infty \int \sqrt{E'} \Sigma_s(E' \rightarrow E, \cos \theta, r) \times n(E', \Omega', r) dE' d\Omega' - \Sigma_s(E, r) n(E, \Omega, r). \quad (1)$$

Here $n(E, \Omega, r)$ is the number of neutrons per unit interval of phase space, $\Sigma_s(E' \rightarrow E, \cos \theta, r)$ is the cross section for scattering through an angle θ with a change in energy from E' to E , $\Sigma_s(E, r)$ and $\Sigma_a(E, r)$ are the scattering and absorption cross sections, and Ω and r are the angle and spatial variables.

Let us write $\Sigma_s(E' \rightarrow E, \cos \theta, r)$ as the sum of an isotropic part $\Sigma_s^{(i)}(E' \rightarrow E, r) = \frac{1}{4\pi} \times \int \Sigma_s(E' \rightarrow E, \cos \theta, r) d\Omega$ and an anisotropic part $\Sigma_s^{(a)}(E' \rightarrow E, \cos \theta, r)$. The anisotropic part of the scattering cross section may be written approximately:

$$\Sigma_s^{(a)}(E' \rightarrow E, \cos \theta, r) \approx \Sigma_s^{(a)}(E, \cos \theta, r) \delta(E - E'), \quad (2)$$

where

$$\Sigma_s^{(a)}(E, \cos \theta, r) = \int_0^\infty \Sigma_s^{(a)}(E \rightarrow E', \cos \theta, r) dE'.$$

Let us write $n(E, \Omega, r)$ as the sum of isotropic and anisotropic parts and rewrite Eq. (1) taking account of approximation (2)

$$\Omega \text{grad}_r n(E, \Omega, r) + \Sigma_a(E, r) n(E, \Omega, r) = \int \Sigma_s^{(a)}(E, \cos \theta, r) n^{(a)}(E, \Omega', r) d\Omega' - \Sigma_s(E, r) n^{(a)}(E, \Omega, r) + Q(E, r), \quad (3)$$

where

$$Q(E, r) = \frac{4\pi}{\sqrt{E}} \int_0^\infty \sqrt{E'} \Sigma_s^{(i)}(E' \rightarrow E, r) \times n^{(i)}(E', r) dE' - \Sigma_s(E, r) n^{(i)}(E, r).$$

Equation (3) differs from the original Eq. (1) in the approximation made in the term determining the anisotropic scattering of neutrons belonging to the anisotropic component of the field:

$$\int_0^\infty \int \sqrt{E'} \Sigma_s^{(a)}(E' \rightarrow E, \cos \theta, r) n^{(a)}(E', \Omega', r) \times dE' d\Omega' \approx \sqrt{E} \int \Sigma_s^{(a)}(E, \cos \theta, r) n^{(a)}(E) d\Omega'. \quad (2')$$

Translated from *Atomnaya Énergiya*, Vol. 22, No. 2, pp. 108-113, February, 1967. Original article submitted November 11, 1965; revised March 28, 1966.

To estimate the error introduced by this approximation we must first take into account the fact that the contribution of the approximate term is most important for scattering in hydrogen and also for an increase in the asymmetry of the flux, i. e., in very inhomogeneous systems. As a consequence of the equality of the integrals over energy on the left and right hand sides of the approximate Eq. (2), the effect of the approximation is significantly decreased in the solution of a problem in which the main interest is in quantities characterizing the slow neutron group as a whole.

A quantitative estimate of the error introduced by an approximation essentially equivalent to Eq. (2) was made by Honeck [2] for the special case of a uranium-water slab lattice. It was shown that the approximation hardly affects the disadvantage factor.

The energy dependence of the solution of Eq. (3) is determined solely by the integral operator appearing in $Q(E, r)$. The other terms in the equation determine only the spatial and angular dependence of the neutrons of a given energy and the energy enters only as a parameter. It is important to emphasize that $Q(E, r)$ does not depend on the angle variables since it describes the change in density due to the isotropic scattering of neutrons belonging to the isotropic component.

Taking these remarks into account we write $n(E, \Omega, r)$ as a product of two functions

$$n(E, \Omega, r) = \nu(E) R_E(\Omega, r), \quad (4)$$

where $\nu(E)$ is the number of neutrons in a cell per unit energy range and $R_E(\Omega, r)$ is the spatial and angular distribution of the density of neutrons of energy E . Since by definition

$$\nu(E) = \int_V n(E, \Omega, r) d\Omega dr, \quad (5)$$

the normalization condition for $R_E(\Omega, r)$ is

$$\int_V R_E(\Omega, r) d\Omega dr = 1. \quad (6)$$

Substituting Eq. (4) into (3) and dividing by $\nu(E)$ we obtain

$$\begin{aligned} \Omega \text{ grad}_r R_E(\Omega, r) + \Sigma_a(E, r) R_E(\Omega, r) &= \int \Sigma_s^{(a)}(E, \cos \theta, r) R_E^{(a)}(\Omega', r) d\Omega' \\ &- \Sigma_s(E, r) R_E^{(a)}(\Omega, r) + Q_E(r); \end{aligned} \quad (7)$$

$$Q_E(r) = \frac{4\pi}{\sqrt{E}\nu(E)} \int_0^\infty \sqrt{E'} \Sigma_s^{(i)}(E' \rightarrow E, r) \times \nu(E') R_E^{(i)}(r) dE' - \Sigma_s(E, r) R_E^{(i)}(r), \quad (8)$$

where $R_E^{(i)}$ and $R_E^{(a)}$ (Ω, r) are the isotropic and anisotropic parts of $R_E(\Omega, r)$.

The set of equations (7) and (8) completely determines $R_E(\Omega, r)$ and $\nu(E)$, since it is equivalent to the original Eq. (1) to within the approximation (2). It is convenient, however, to use in addition the balance equation for $\nu(E)$:

$$\bar{\Sigma}(E) \nu(E) = \frac{1}{\sqrt{E}} \int_0^\infty \sqrt{E'} \bar{\Sigma}_s(E' \rightarrow E) \nu(E') dE', \quad (9)$$

which can be obtained either directly from balance considerations or by integrating Eq. (7) over the angle and spatial variables. The bars over letters in Eq. (9) denote averages over the cell volume.

$$\bar{\Sigma}(E) = \int_V [\Sigma_a(E, r) + \Sigma_s(E, r)] R_E^{(i)}(r) dr; \quad (10)$$

$$\bar{\Sigma}_s(E' \rightarrow E) = \int_V \Sigma_s^{(i)}(E' \rightarrow E, r) R_E^{(i)}(r) dr. \quad (10')$$

Let us consider the method of successive approximations for solving the system of Eqs. (7)-(10). If for any value of the energy the spatial dependence of the function $Q_E(r)$ on the right hand side of Eq. (7)

is supposed known, this equation breaks up into a continuum of monoenergetic Boltzmann equations. If some more or less real dependence of Q_E on r is specified, it is possible to obtain an approximate solution of any of these equations. We denote such a function by $Q_{1E}(r)$. It is important that for each energy the function $Q_{1E}(r)$ need be "guessed" only to within a constant factor since the normalization of R_E is known beforehand. Let us suppose that $Q_{1E}(r)$ corresponds to the normalization condition (6).

Let us solve Eq. (7) for a sufficiently large number of energy values and then determine intermediate values of $R_E(r)$ by interpolation. The choice of E values is made on the basis of the required accuracy and on the geometric and physical properties of the cell, i.e. principally on the assumed hardness of the spectrum and the energy dependence of the cross sections. After calculating the averages of the scattering and absorption cross sections over the cell Eq. (9) is solved and the energy dependence of ν is found for the average neutron spectrum over the cell.

The possibility of such a procedure follows from the fact that solutions of the one-velocity equations (7) depend only slightly on the source distribution $Q_E(r)$ since the neutron mean free path in the moderator before reaching the fuel is generally appreciably larger than the characteristic dimensions of the moderator region. In addition the dependence of Q_E on r averaged over the thermal group is determined by the slowing down power of the material in the epithermal region since the integral $\int_{E_{LI}}^{E_U} \sqrt{E} \nu(E) Q_E(r) dE$ describes the spatial distribution of the sources of the thermal group. In this connection it is natural to choose the dependence of Q_E on r in the first approximation to be the same as the distribution of slowing down power. In this case the first approximation may turn out to be quite sufficient if only the integral parameters of the thermal group in the cell are required.

The solution $\tilde{n}(E, \Omega, r) = \tilde{\nu}(E) \tilde{R}_E(\Omega, r)$ obtained in this way satisfies the Boltzmann equation for isotropic sources which alternate in sign and are therefore purely fictitious:

$$F(E, r) = \nu \tilde{\nu}(E) Q_{1E}(r) - \int_0^\infty \nu' \Sigma_s^{(i)}(E' \rightarrow E, r) \tilde{\nu}(E') \tilde{R}_E^{(i)}(r) dE' + \nu \Sigma_s(E, r) \tilde{\nu}(E) \tilde{R}_E^{(i)}(r), \quad (11)$$

where ν is the speed of a neutron of energy E . If the set of functions $Q_{1E}(r)$, $\tilde{R}_E(r)$, and $\tilde{\nu}(E)$ satisfy (8) as well as (7) and (9), $F(E, r)$ vanishes and $\tilde{n}(E, \Omega, r)$ is an exact solution of Eq. (3). Therefore one may take the integral of the square of $F(E, r)$ over the whole cell volume and over the energy from 0 to E_{LI} as a quantity characterizing the accuracy of the solution:

$$z = \int_0^{E_{LI}} \int_V F^2(E, r) dr dE. \quad (12)$$

In order to obtain a more accurate solution it is necessary in choosing the new functions $Q_{1E}(r)$ to take into account both the $Q_{1E}(r)$ used in the first approximation and the functions

$$Q_{2E}(r) = \frac{1}{\sqrt{E} \nu(E)} \int_0^\infty \sqrt{E'} \Sigma_s^{(i)}(E' \rightarrow E, r) \times \nu(E') \tilde{R}_E^{(i)}(r) dE' - \Sigma_s(E, r) \tilde{R}_E^{(i)}(r), \quad (13)$$

obtained by substituting the $\tilde{R}_E(r)$ into Eq. (8). The simplest expression for the new $Q_{1E}(r)$ is a linear combination of $Q_{1E}(r)$ and $Q_{2E}(r)$ of the first approximation. Denoting quantities referring to the first and second approximations by superscripts we write

$$Q_{1E}^{(2)}(r) = \alpha Q_{1E}^{(1)}(r) + \beta Q_{2E}^{(1)}(r). \quad (14)$$

If we substitute $Q_{1E}^{(2)}(r)$ into the right hand side of the Eq. (7) corresponding to energy E the solution thus obtained for $R_E(\Omega, r)$ will not in general satisfy (6). Therefore the sum of α and β may not be equal to unity; however if the first approximation solution is not too greatly different from the exact solution, β is close to $1 - \alpha$ and therefore one may write $1 - \alpha$ instead of β and then renormalize $R_E(\Omega, r)$.

The question of the existence of values of α for which the second approximation is more accurate than the first can apparently be discussed only in terms of specific calculations. However, some information about the values of α leading to the inequality $z^{(2)} < z^{(1)}$ may be obtained by neglecting the difference between $\nu^{(2)}(E)$ and $\nu^{(1)}(E)$ and supposing that the substitution of $Q_{1E}^{(1)}(r)$ into Eq. (7) gives the proper normalization for $R_E(\Omega, r)$. We write the expression for the function $F_\alpha^{(2)}(E, r)$ in the form

$$F_{\alpha}^{(2)}(E, r) = \alpha F_1^{(2)}(E, r) + (1 - \alpha) F^{(1)}(E, r),$$

where $F_{\alpha}^{(2)}(E, r)$ corresponds to $\alpha = 1$. Let us square $F_{\alpha}^{(2)}(E, r)$ and integrate over r and E . We obtain $z^{(2)}$ as a function of α :

$$z^{(2)}(\alpha) = \alpha^2 z^{(2)}(1) + 2\alpha(1 - \alpha)y + (1 - \alpha)^2 z^{(1)}, \tag{15}$$

where

$$y = \int_0^{E_k} \int_V F_{\alpha}^{(2)}(E, r) F^{(1)}(E, r) dr dE.$$

From Eq. (15) it is clear that if $y \neq z^{(1)}$ there is a range of values of α for which $z^{(2)}(\alpha) < z^{(1)}$:

$$\begin{aligned} 0 < \alpha < \alpha_0 & \text{ for } z^{(1)} > y; \\ 0 > \alpha > \alpha_0 & \text{ for } z^{(1)} < y, \end{aligned}$$

where

$$\alpha_0 = \frac{2(z^{(1)} - y)}{z^{(2)}(1) - 2y + z^{(1)}}.$$

In solving some problems one may suppose that the scattering kernel and the absorption cross section are independent of position within the neutron moderator. In this case Eqs. (10) may be written:

$$\bar{\Sigma}(E) = \Sigma_1(E) \psi_1(E) + \bar{\Sigma}_0(E) \psi_0(E); \tag{16}$$

$$\bar{\Sigma}_s(E' \rightarrow E) = \Sigma_{s1}(E' \rightarrow E) \psi_1(E') + \bar{\Sigma}_{s0}(E) \psi_0(E) \delta(E - E'). \tag{16'}$$

Here $\Sigma_1(E)$ and $\Sigma_{s1}(E' \rightarrow E)$ are the total differential scattering cross sections in the moderator, $\bar{\Sigma}_0$ the total cross section averaged over regions which do not contain moderator, $\psi_1(E)$ the ratio of the number of neutrons of energy E in the moderator to the total number of such neutrons in the cell, and $\psi_0 = 1 - \psi_1$. Substituting (16) into (9) we obtain

$$\left[\frac{\psi_0(E) \bar{\Sigma}_{a0}(E)}{\psi_1(E)} + \Sigma_1(E) \right] \nu_1(E) = \frac{1}{\sqrt{E}} \int_0^{\infty} \sqrt{E'} \Sigma_{s1}(E' \rightarrow E) \nu_1(E') dE'. \tag{17}$$

TABLE 1. Cell Dimensions and Total Cross Section of Fuel for $E = kT$

Cell Parameters	Cell Number				
	1	2	3	4	5
r_0 , cm	—	—	—	—	1
r_1 , cm	1.5	1.5	1.5	1.5	2
r_2 , cm	3	3	2	2	3
Σ_0 , cm ⁻¹	1	0.5	1	0.5	1

TABLE 2. The Parameter z as a Function of the Order of the Approximation

Order of the approximation	Method of characteristics	P_3 -approximation				
		Cell Number				
		1	2	3	4	5
1	0.0177	0.0169	0.0388	0.0040	0.0074	0.0168
2	0.0100	0.0098	0.0219	0.0030	0.0048	0.0096
3	0.0063	0.0061	0.0151	0.0024	0.0033	0.0059
4	0.0042	—	—	—	—	—
5	0.0027	—	—	—	—	—

The function $\nu_1(E) = \psi_1(E) \nu(E)$ is the neutron spectrum in the moderator.

We present below the results of calculating the thermal utilization for cells having cylindrical symmetry. Fuel is present only in the rod of radius $r_1 = 1.5$ cm or in a cylindrical layer of inner radius $r_0 = 1$ cm and outer radius $r_1 = 2$ cm. It is assumed that the remainder of the cell is filled with a hydrogenous moderator. Since the main purpose of the calculations is to find how the neutron density distribution depends on $Q_{1E}(r)$ and whether it is possible to apply the iterative method by using (14), several simplifying assumptions were made: 1) the scattering in the moderator is isotropic and the differential cross section $\Sigma_s(E' \rightarrow E)$ depends on the initial and final values of the neutron energy in the same way as in an ideal monatomic gas with mass number unity; 2) the absorption cross section is inversely proportional to the neutron velocity; 3) the temperature of the moderator, T , is constant over the whole moderator volume.

In all the cases considered the ratio of the absorption cross section to the total cross section at $E = kT$, where k is the Boltzmann constant, was taken as 0.8 for the

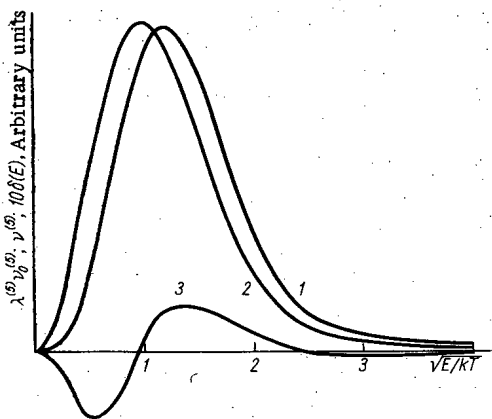


Fig. 1. Neutron spectra: 1) in the fuel ($\lambda^{(5)} \nu_0^{(5)}$); 2) in the moderator ($\nu_1^{(5)}$); 3) difference between spectra in fuel obtained in first and fifth approximations [$10 \delta(E)$].

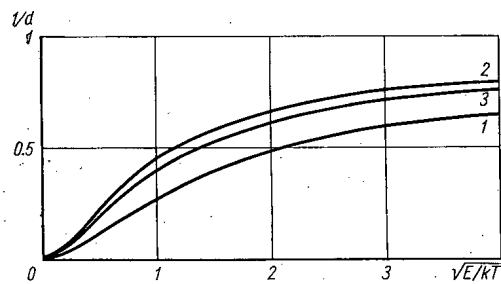


Fig. 2. The quantity $1/d$ as a function of E for three cells. The numbers on the curves indicate the cell numbers shown in Table 1.

TABLE 3. The Dependence of χ on the Order of the Approximation for Various Moderator Temperatures

Order of the approximation	Moderator temperature, °C				
	20	100	200	300	400
1	0.9415	0.9250	0.9116	0.9032	0.9069
5	0.9425	0.9262	0.9130	0.9044	0.9078

fuel and 0.01 for the moderator. Calculations were made for five cells in different geometrics and for various fuel cross sections Σ_0 (Table 1).

The value of r_2 in the table denotes the cell radius. The total cross section for the moderator at $E=kT$ was taken as 2 cm^{-1} . The monoenergetic equations (7) for all five cells were solved in the P_3 -approximation by the spherical harmonics method. In addition the first cell was calculated by the characteristics method (program [3]). It was found that the convergence of the iterative process was practically independent of the method used to solve Eq. (7). In calculating the third and fourth cells in which the moderator layer was very thin we used the method proposed by Honeck [4] of introducing an outer non-absorbing layer to simulate the isotropic reflection of neutrons from the cell boundary [4].

The first three approximations were calculated for each cell, and using the method of characteristics five approximations were computed for the first cell. The functions $Q_{1E}(r)$ in the first approximation were taken as constants in the moderator. For all cases considered $\alpha = 0.1$. Table 2 shows the values of z ; the normalization of ν in Eq. (11) corresponds to the absorption of one neutron per second in the cell, and $E_{LI} = 16 \text{ kT}$.

The calculations show that the first approximation gives a rather accurate value of the thermal utilization θ . The expression for θ in a two zone cell consisting of fuel and moderator when the absorption follows the $1/v$ law may be written in the form

$$\theta = \left[1 + \frac{\Sigma_{a1}}{\Sigma_{a0}} \frac{\int_0^{E_{LI}} \nu_1(E) dE}{\int_0^{E_{LI}} \nu_0(E) dE} \right]^{-1}, \tag{18}$$

where $\nu_0(E) = \frac{\psi_0(E)}{\psi_1(E)} \nu_1(E)$ is the number of neutrons in the fuel per unit energy. Using the method of characteristics in the first cell, the first approximation gives a thermal utilization of 0.8043 and the next four approximations give 0.8045. Similar results were obtained for the other cells.

Calculations showed that the spatial variation in $Q(E, r)$ hardly affected the neutron spectrum in the moderator, but it had a pronounced effect on the spatial distribution of neutron density at a given energy, and therefore on the spectrum in the fuel.

Figure 1 shows the neutron energy spectra in moderator and fuel obtained in the fifth approximation. Both curves are normalized to the same number of neutrons per unit volume, i. e., the function $\nu_0^{(5)}(E)$

is multiplied by

$$\lambda^{(5)} = \frac{\int_0^{E_{LI}} \nu_1^{(5)}(E) dE}{\int_0^{E_{FP}} \nu_0^{(5)}(E) dE}$$

The function $\delta(E) = \lambda^{(1)} \nu_0^{(1)}(E) - \lambda^{(5)} \nu_0^{(5)}(E)$ is plotted on Fig. (1) on a larger scale for convenience.

If the fuel absorption cross section does not follow the $1/v$ law, the error in the spectrum may decrease the accuracy of the calculated value of θ . To estimate the error when U^{235} is used, the ratio of the average absorption per unit time over the thermal group to the probability of absorption of a 2200 m/sec neutron was found:

$$\chi = \frac{\int_0^{E_{LI}} \nu \sigma_a^{235}(E) \nu_0(E) dE}{\sigma_a^{235}(E_0) \nu_0 \int_0^{E_{LI}} \nu_0(E) dE}$$

where $E_0 = 0.0253$ eV. Values of χ as a function of the temperature of the moderator t are given in Table 3. The listed values of χ cannot be considered as characteristic of a single cell since the values of the cross sections at $E = kT$ change with moderator temperature. Therefore, in spite of the fact that the ideal gas model was used in the calculations, ν_0 changes with E/kT .

The results listed in Table 3 show that the error in θ due to the deviation of the U^{235} absorption cross section from the $1/v$ law is of the same order as the error incurred in assuming that this law holds. However, this is an overestimate since the neutron spectrum used to average $\nu \sigma_a$ was calculated without taking into account deviations from the $1/v$ law.

The method described may turn out to be useful from two points of view. First, by refining the functions $Q_E(r)$ in a reasonable way it appears to be possible to obtain very detailed information on the spatial, angular, and energy distributions of neutrons in a cell. It should be noted however that such calculations require considerable machine time. On the other hand the main interest in reactor calculations is in the integral characteristics of the thermal group, and one might try using the first approximation for this purpose. One need only be convinced that the first approximation gives acceptable results if Q_E depends on r in the same way that the moderating power does. This latter fact may be ascertained by using the P_3 -approximation whereas it is reasonable to use integral methods such as that of Amouyal, Benoist, and Horowitz [5] or the first collision probability method [6] to obtain extensive solutions of Eq. (7) in the first approximation. Integral methods in most cases give higher accuracy for less calculating time than does the P_3 -approximation. However it is impossible to use them in second and higher approximations since they do not admit spatially inhomogeneous sources.

It should be noted that the ratio of the neutron density in the fuel to that in the moderator is a "smooth" function of energy except in the resonance region. Therefore, in order to obtain the first approximation it is sufficient to solve the monoenergetic equation for just a few energies and then to interpolate. Figure 2 shows the disadvantage factor

$$d(E) = \frac{\psi_1(E) V_1}{\psi_0(E) V_0}$$

as a function of energy, where V_1 and V_0 are the moderator and fuel volumes for the first three variations.

In conclusion the author wishes to thank G. A. Bat' for helpful discussions and Yu. P. Pushkarevoï, S. V. Obukhovoï, and A. S. Drozdovoï for performing the calculations.

LITERATURE CITED

1. A. Weinberg and E. Wigner, "The Physical Theory of Neutron Chain Reactors," [Russian translation], Moscow, Izd. Inostr. Lit. (1961).
2. H. Honeck, Nucl. Sci. Eng. 8, 49 (1964).
3. G. A. Bat' et al., Paper No. 373 presented by USSR at Third Intern. Conf. Peaceful Uses of Atomic Energy. Geneva, [in Russian] (1964).

4. Z. Weiss and I. Stammler, Nucl. Sci. Eng. 19, 374 (1964).
5. A. Amouyal, P. Benoist, and J. Horowitz, in: "Some Questions on Nuclear Power," M.A. Starikovich Ed., [in Russian], Moscow, Izd. Inostr. Lit. p.237 (1959).
6. J. Fukai, Nucl. Sci. Eng. 13, 345 (1962).

DETERMINATION OF THE EFFECTIVE MULTIPLICATION
(BREEDING) FACTOR OF NEUTRONS FROM THE MEASURED
DIFFERENTIAL REACTIVITY

T. S. Dideikin and B. P. Shishin

UDC 621.039.51

A relation is established between the effective multiplication factor of neutrons in a reactor and the experimental value of the reserve of reactivity, determined from measurements of differential reactivity. Correction terms are determined in integral form.

An experimental verification of the effective multiplication factor of neutrons in a reactor, k_{eff} , or its "reserve of reactivity" $\rho = 1 - \frac{1}{k_{\text{eff}}}$, constitutes an important problem, since a knowledge of the initial value of k_{eff} enables us to estimate the correctness of the selected composition of the active zone of the reactor in order to ensure the required period of operation.

The determination of small values of ρ or values of k_{eff} close to unity presents no special difficulties and may be carried out by measuring the established reactor starting period [1]. In determining large values of k_{eff} , wide use is made of the method of measuring the differential reactivity for a series of successive critical states of the reactor, established by varying the geometry, the composition of the active zone, and so on. In particular, wide use is made of the experimental arrangement in which the differential reactivity ($d\rho/dH$) associated with a variation in the height of the active zone is measured [2]. The successive critical states of the reactor for various heights of the active zone are established by varying the radius or the concentration of absorbent. However, considerable difficulties arise in making a strict transformation from the measured values of differential reactivity to the total reserve of reactivity or the value of k_{eff} , since the intermediate values of differential reactivity are determined, generally speaking, for an active zone differing in composition or geometry from the active zone under examination [3].

In this paper we establish a relation between the experimental values of differential reactivity with respect to any compensation parameter and the total reserve of reactivity or the value of k_{eff} of the reactor, and give a general criterion for estimating the correction terms, allowing for the difference between the intermediate critical states (in which the differential reactivity is measured) and the active zone for which it is required to determine k_{eff} or ρ . We shall analyze the value of the correction terms under specific experimental conditions for the "bare" reactor in the one-group diffusion approximation. As compensation parameters z_i we shall consider all quantities by varying which in the course of the experiment we may alter the k_{eff} of the reactor (particular compensation parameters include the geometric size of the active zone, the concentration of absorbent, the temperature, and so on). It is clear that k_{eff} and ρ may be regarded as functions of the compensation parameters:

$$k_{\text{eff}} = k_{\text{eff}}(z_i); \quad \rho = \rho(z_i).$$

Then the set of compensation parameters by which the critical state of the reactor may be realized is given by the equations

$$k_{\text{eff}}(z_i) = 1; \quad \rho(z_i) = 0. \quad (1)$$

The differential reactivity with respect to the compensation parameter is defined by the formula

$$\frac{d\rho(z_i)}{dz_k}$$

Translated from *Atomnaya Énergiya*, Vol. 22, No. 2, pp. 113-117, February, 1967. Original article submitted May 12, 1966.

As a rule, under actual experimental conditions, we are concerned with the variation of two compensation parameters; the differential reactivity is measured with respect to one of these, and the other is employed to bring the reactor into a new critical state. Thus, for example, in measuring $d\rho/dH$, where H is the height of the active zone, the critical state is achieved for various values of H by varying the radius of the active zone or the concentration of absorbent. In view of this we shall subsequently consider two compensation parameters, although the method described may easily be extended to any number of these.

Let us write down the expression for the differential reactivity with respect to parameter z_1 , considering only two compensation parameters z_1 and z_2 in the form

$$\frac{d\rho(z_1, z_2)}{dz_1} = \frac{1}{k_{\text{eff}}^2(z_1, z_2)} \cdot \frac{\partial k_{\text{eff}}(z_1, z_2)}{\partial z_1} + \frac{1}{k_{\text{eff}}^2(z_1, z_2)} \cdot \frac{\partial k_{\text{eff}}(z_1, z_2)}{\partial z_2} \cdot \frac{dz_2}{dz_1} \quad (2)$$

From the experimental conditions prevailing when measuring the quantity $d\rho(z_1, z_2)/dz_1$ it follows that $dz_2/dz_1 \equiv 0$, since in the course of a single measurement the compensation parameter z_2 remains constant. Allowing for this, we may write expression (2) for the measured differential reactivity in a single measurement in the form

$$\frac{d\rho(z_1, z_2)}{dz_1} = \frac{1}{k_{\text{eff}}^2(z_1, z_2)} \cdot \frac{\partial k_{\text{eff}}(z_1, z_2)}{\partial z_1} \quad (3)$$

The quantity $d\rho_e(z_1, z_2)/dz_1$ may be measured for several values of parameter z_1 in the range of variation between z_1^1 , defined by the condition

$$k_{\text{eff}}(z_1^1, z_2^0) = 1, \quad (4)$$

and the value z_1^0 defined by the condition

$$k_{\text{eff}}(z_1^0, z_2^1) = 1, \quad (5)$$

where z_1^0, z_2^0 are the values of parameters z_1 and z_2 corresponding to the reactor for which k_{eff} is being determined. The values of parameter z_2 corresponding to intermediate values of z_1 which are used in the measurement of $d\rho_e(z_1, z_2)/dz_1$, are determined from the critical condition

$$k_{\text{eff}}(z_1, z_2) = 1. \quad (6)$$

Then the experimental value of the total reserve of reactivity associated with the variation of z_1 in the range $z_1^1 - z_1^0$, will equal

$$\rho_e = \int_{z_1^1}^{z_1^0} \frac{d\rho_e(z_1, z_2)}{dz_1} dz_1. \quad (7)$$

Allowing for (3), expression (7) may be written in the form

$$\rho_e = \int_{z_1^1}^{z_1^0} \frac{1}{k_{\text{eff}}^2(z_1, z_2)} \cdot \frac{\partial k_{\text{eff}}(z_1, z_2)}{\partial z_1} dz_1. \quad (8)$$

Let us expand the integrand in a Taylor series in powers of the deviation of the parameter z_2 from the value corresponding to the reactor under consideration, $z_2 = z_2^0$:

$$\begin{aligned} \frac{1}{k_{\text{eff}}^2(z_1, z_2)} \cdot \frac{\partial k_{\text{eff}}(z_1, z_2)}{\partial z_1} &= \frac{1}{k_{\text{eff}}^2(z_1, z_2^0)} \times \frac{\partial k_{\text{eff}}(z_1, z_2^0)}{\partial z_1} + \sum_{n=1}^{\infty} \frac{(z_2 - z_2^0)^n}{n!} \cdot \frac{\partial^n}{\partial z_2^n} \\ &\times \left[\frac{1}{k_{\text{eff}}^2(z_1, z_2)} \cdot \frac{\partial k_{\text{eff}}(z_1, z_2)}{\partial z_1} \right]_{z_2=z_2^0} \end{aligned} \quad (9)$$

A strict proof of the applicability of expansion (9) may be given for any specific experiment if the analytical dependence of k_{eff} on the compensation parameters is known.

Expansion (9) is possible when the residual term

$$R_n = \frac{(z_2 - z_2^0)^{n+1}}{(n+1)!} \cdot \frac{\partial^{n+1}}{\partial z_2^{n+1}} \times \left[\frac{1}{k_{\text{eff}}^2(z_1, z_2)} \cdot \frac{\partial k_{\text{eff}}(z_1, z_2)}{\partial z_1} \right]_{z_2=\xi} \quad (9)$$

(ξ between z_2 and z_2^0)

tends to zero as $n \rightarrow \infty$. Substituting expression (9) into (8) and integrating, we obtain

$$\rho_e = \frac{1}{k_{\text{eff}}(z_1^0, z_2^0)} - \frac{1}{k_{\text{eff}}(z_1^0, z_2^0)} + \sum_{n=1}^{\infty} \rho_n, \quad (10)$$

where

$$\rho_n = \int_{z_1^0}^{z_1^0} \frac{(z_2 - z_2^0)^n}{n!} \cdot \frac{\partial^n}{\partial z_2^n} \times \left[\frac{1}{k_{\text{eff}}^2(z_1, z_2)} \cdot \frac{\partial k_{\text{eff}}(z_1, z_2)}{\partial z_1} \right]_{z_2=z_2^0} dz_1 \quad (11)$$

is a correcting term of the n-th order.

We note that in expression (10) $k_{\text{eff}}(z_1^0, z_2^0)$ is the unknown value of the effective multiplication factor of the neutrons in the reactor under consideration, which we call k_{eff}^0 . Then, allowing for (4), we obtain a relation for determining k_{eff}^0 from the measured reserve of reactivity ρ_e :

$$\rho_0 = \rho_e - \sum_{n=1}^{\infty} \rho_n, \quad (12)$$

where ρ_n is the correction of n-th order defined by relation (11) and $\rho_0 = 1 - 1/k_{\text{eff}}^0$. Let us consider expression (11) defining the value of the correction term ρ_n . We see from (11) that, in order to estimate the value of ρ_n in a specific experiment, we must know the law governing the variation of the parameter z_2 on varying z_1 in the range $z_1^0 - z_1^0$, and also the quantity

$$\frac{\partial^n}{\partial z_2^n} \left[\frac{1}{k_{\text{eff}}^2(z_1, z_2)} \cdot \frac{\partial k_{\text{eff}}(z_1, z_2)}{\partial z_1} \right]_{z_2=z_2^0} \quad (12a)$$

The law of variation of z_2 is determined directly in the course of the experiment, allowing for the critical condition (6). The character of the variation of expression (12a) may be obtained from a series of statistical calculations of the quantity $k_{\text{eff}}(z_1, z_2)$ for various values of the compensation parameter z_1 . It should be noted that relation (12) between the experimental value of the reserve of reactivity and the calculated value of k_{eff}^0 , and also the expression for the correction terms (11), are valid for reactors of any type, and do not depend on the method of calculating k_{eff}^0 . In cases in which there is a clear analytical dependence of k_{eff} on the compensation parameters, the determination of the corrections factors is greatly eased.

By way of an example of the use of the above principles, let us estimate the value of the correction terms for the two most commonly used methods of determining the reactivity reserve of a reactor. Both methods are connected with the measurement of the differential reactivity as a function of the height of the active zone. For each new height of the active zone, the critical state is achieved either by varying the zone radius or by varying the concentration of absorbent. If we suppose that, in the case considered, the model of the "bare" homogeneous reactor is applicable in the one-group diffusion approximation, then the expression for k_{eff} may be written in the form

$$k_{\text{eff}} = \frac{\nu \Sigma_f}{\Sigma_c [1 + (\kappa_R^2 + \kappa_H^2) M^2]}, \quad (13)$$

where Σ_f, Σ_c are the macroscopic cross sections for the fission and absorption of neutrons in the reactor, ν is the fission-neutron yield, κ_R^2, κ_H^2 are the radial and linear (height) dimensions of the reactor, and M^2 is the area of migration of the neutrons in the reactor.

It is assumed that Σ_c does not depend on $\nu \Sigma_f$ within the limits of the variations in reactor parameters associated with the carrying out of the experiment.

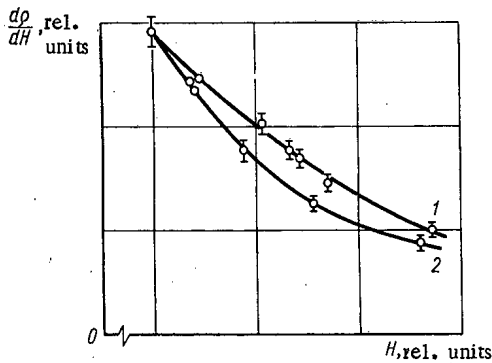


Fig. 1. Differential reactivity dp/dH as a function of the height H of the water level in the active zone of the reactor: 1) compensation by uniformly varying the absorbent distribution; 2) compensation by varying the radial leakage of neutrons from the active zone of the reactor.

If the critical state of the reactor for each new height of the active zone is attained by varying the radius, then the compensation parameter z_1 is $\kappa_H^2 M^2$, and the compensation parameter z_2 is $\kappa_R^2 M^2$. Then (13) may be written in the form

$$k_{\text{eff}} = \frac{\nu \Sigma_f}{\Sigma_c (1 + z_1 + z_2)}. \quad (13a)$$

Since it follows from (11) and (13a) that $\rho_n = 0$, we obtain a relation for determining k_{eff}^0

$$\rho_0 = \rho_e. \quad (14)$$

If the critical state is achieved by varying the absorption in the active zone, then the compensation parameter z_1 remains $\kappa_H^2 M^2$ as before, but z_2 becomes Σ_c . Then expression (13) takes the form

$$k_{\text{eff}} = \frac{\nu \Sigma_f}{z_2 (1 + z_1 + \kappa_R^2 M^2)}. \quad (13b)$$

Allowing for (13b), we obtain

$$\frac{1}{k_{\text{eff}}^2(z_1, z_2)} \cdot \frac{\partial k_{\text{eff}}(z_1, z_2)}{\partial z_1} = -\frac{z_2}{\nu \Sigma_f}. \quad (15)$$

The first derivative of (15) with respect to the second compensation parameter equals $1/\nu \Sigma_f$, and the derivatives of higher order equal zero, i.e.,

$$\rho_2 = \rho_3 = \dots = \rho_n = 0. \quad (15a)$$

Allowing for condition (6), let us find the first correction term ρ_1 :

$$\rho_1 = - \int_{z_1^0}^{z_1^1} (z_2 - z_2^0) \frac{dz_1}{\nu \Sigma_f} = - \int_{z_1^0}^{z_1^1} \frac{dz_1}{1 + \kappa_R^2 M^2 + z_1} + \frac{z_2^0}{\nu \Sigma_f} \int_{z_1^0}^{z_1^1} dz_1 = - \ln \frac{1 + \kappa_R^2 M^2 + z_1^1}{1 + \kappa_R^2 M^2 + z_1^0} + \frac{z_2^0 (z_1^1 - z_1^0)}{\nu \Sigma_f} = \ln k_{\text{eff}}^0 - \rho_0. \quad (15b)$$

Then relation (12) for determining k_{eff}^0 takes the form

$$k_{\text{eff}}^0 = \exp \rho_e. \quad (16)$$

Thus, depending on the method of experimentally determining the total reactivity reserve of the reactor, we obtain a variety of relations between the calculated and experimental values.

The diffusion one-group model of a homogenized reactor is often used for treating experimental results associated with the determination of reactivities. Here the influence of the reflector, as a rule, reduces to a corresponding increase in the dimensions of the active zone of the reactor. On this principle, the conclusions reached for the "bare" reactor may be extended to reactors with reflectors also.

The above-mentioned relationship between the experimental results and the methods of compensating excess reactivity is in fact observed experimentally. The figure shows the experimental values of the differential reactivity dp/dH as functions of the height of the water level H in the active zone of a reactor having a composite neutron spectrum.

According to the one-group model, the reactivity reserve of the reactor is determined by integration along curve 2 (formula 14). Direct integration along curve 1 gives an overestimated value of the reactivity reserve of the system (by 10 to 15%). However, the use of formula (16) in this case yields results coinciding with the results of integration along the lower curve.

LITERATURE CITED

1. P. Liewers, *Kernenergie*, H. 8, 593 (1961).
2. S. Krasnik and A. Radkovskii, In: "Transactions of the International Conference on the Peaceful Use of Atomic Energy (Geneva, 1955)" [in Russian], Vol. 5, Moscow, Izd. AN SSSR, p. 248 (1958).
3. A. Henry, *Nucl. Sci. Eng.* 3, 52 (1958).

ABSTRACTS

SLOWING DOWN OF NEUTRONS IN A HYDROGENOUS MEDIUM

Yu. A. Platovskikh

UDC 539.125.523.5

We have obtained equations for the slowing down of neutrons in a hydrogenous medium which differ from the familiar Goertzel-Greuling and Goertzel-Selengut equations. As the initial equation for the Fourier transform of the neutron flux $\Phi(k, u)$, where k is the Fourier transform variable, we use the equation in the diffusion approximation for a medium containing hydrogen and a heavy element. The first equation is obtained by differentiating the initial equation with respect to the lethargy u , and then expanding $\Phi(u-\xi)$, where ξ is the maximum increase in lethargy per collision, in a Taylor's series about point u . If two terms are retained in the expansion we obtain the following equation:

$$\frac{d}{du} [(\Sigma_t + k^2 D) \Phi] + (\Sigma_a + k^2 D) \Phi = S + \frac{dS}{du}, \quad (1)$$

where D is the diffusion coefficient, $S = S(u)$ is the source spectrum, $\Sigma_t = \Sigma_a + \Sigma_H + \xi \Sigma_A$ where Σ_H and Σ_A are the scattering cross sections for hydrogen and the heavy element, and ξ is the average increase in lethargy per collision.

Another equation is found by using an approximate Green's function for an infinite nonabsorbing medium. This function includes an expression for first collision neutrons and an asymptotic part. The equation has the form

$$\frac{d}{du} [\bar{\xi} (k^2 D + \Sigma) \Phi] + (\Sigma_a + k^2 D) \Phi = S + \frac{d}{du} \bar{\xi} S, \quad (2)$$

where

$$\bar{\xi} = \frac{\Sigma_H + \xi \Sigma_A}{\Sigma_s}, \quad \Sigma_s = \Sigma_H + \Sigma_A.$$

Equation (2) leads to the following formula for the neutron age:

$$\tau(u) = \int_{-\infty}^u S(u') \frac{D(u') du'}{\Sigma(u')} + \frac{D(u)}{\Sigma(u)} + \int_{-\infty}^u S(u') du' \int_u^{\infty} \frac{D(u'') du''}{\bar{\xi}(u'') \Sigma(u'')}, \quad (3)$$

and Eq. (1) corrects the first and subsequent collisions. The results of calculating the neutron age to indium resonance are presented in the table.

As may be seen from the table, Eq. (2) [Formula (3)] shows good agreement with the moments method and with experiment, while Eq. (1) is not suitable for calculating the neutron age. Calculations show that Eq. (2) leads to better results for the nonleakage probability for water than the Goertzel-Selengut method does.

Neutron Age to Indium Resonance

Calculational method	Be	C	H ₂ O	Reference
Moments method	80.0	318.4	26.0	[1]
Goertzel-Selengut Method	74.6	304.1	30.9	[2]
Equation (2)	80.7	322.2	26.0	—
Equation (1)	101.2	402.8	—	—
Goertzel-Greuling Method	79.1	316.5	28.3	—
Experiment	80.0 ± 2.0	311.0 ± 3.0	26.5 ± 0.3	[1, 2]

At large distances from a plane source the spatial and energy distribution of neutrons $\Phi_0(x, u)$ which is obtained from Eqs. (2) and (1) has nearly the same form as the rigorous solution obtained by Wick. Thus if the scattering cross section depends on lethargy, the solution of Eqs. (1) and (2) has the form

$$\varphi_0(x, u) = G(u) |x|^a \exp(-\Sigma^* |x|),$$

where a is a constant depending on the rate of change of Σ with lethargy, and Σ^* differs from Σ by a factor.

Analysis of the solutions shows that Eq. (1) gives a better description of neutron slowing down far from the source than other diffusion equations do.

Translated from Atomnaya Energiya, Vol. 22, No. 2, p. 118, February, 1967. Original article submitted March 17, 1965; abstract September, 1966.

LITERATURE CITED

1. V. P. Kochergin and V. V. Orlov, *Atomnaya Énergiya* 6, 34 (1959).
2. R. Paschall, *Trans. Am. Nucl. Soc.* 6, No. 2 (1963).

DIFFRACTION OF SLOW NEUTRONS BY STRATIFIED SYSTEMS

V. F. Turchin

UDC 539.125.5:539.121.72

For work with cold neutrons it would be interesting to produce a stratified system with a periodic space variation of the slow neutron scattering amplitude. One can obtain such a system, for example, by depositing alternately, on some backing, layers of equal thickness d of materials, or isotopes, characterized by scattering amplitudes of opposite signs. The three dimensional diffraction grating thus obtained will reflect neutrons satisfying the Bragg relation, like a system of crystal planes at distances $2d$ apart. For layer thicknesses d of the order of tens of interatomic distances the diffraction grating will reflect ordinary cold neutrons ($\lambda \approx 5 \text{ \AA}$) at rather large angles.

However, an artificially produced stratified system will hardly have the high degree of periodicity characteristic of crystals, and therefore the degree of monochromatization in reflection from it will be less than in reflection from a crystal. If we deliberately seek to worsen the degree of monochromatization we could probably obtain an "all-wave" mirror reflecting neutrons of widely different wave lengths incident at any angle. An all-wave mirror might be made by slowly changing the grating period with depth. One might expect such mirrors to be very useful since, unlike crystals, they could easily be made in any shape, such as a paraboloid of revolution, and in large sizes. By using such mirrors one might produce neutron beams of large cross section and focus them; one might even try to develop a cold neutron reflection optics.

In this connection a theory of the scattering of slow neutrons from arbitrary stratified systems is developed in the present report. The Lax procedure serves as the starting point (M. Lax, *Rev. Mod. Phys.* 23, No. 4, (1951); *Phys. Rev.*, 85, 621, 1952). A system of differential equations is obtained for the amplitude of the incident wave $A_+(z)$ and the reflected wave $A_-(z)$

$$A'_+(z) = -i \frac{\hbar}{2} [\bar{V}(z) A_+(z) + \tilde{V}_+(z) A_-(z)] + \left(\frac{\hbar}{2}\right)^2 [\bar{V}(z) A_+(z) + \tilde{V}_+(z) A_-(z)];$$

$$A'_-(z) = i \frac{\hbar}{2} [\bar{V}(z) A_-(z) + \tilde{V}_-(z) A_+(z)] + \left(\frac{\hbar}{2}\right)^2 [\bar{V}(z) A_-(z) + \tilde{V}_-(z) A_+(z)],$$

where $\bar{V}(z)$, $\tilde{V}_+(z)$, and $\tilde{V}_-(z)$ are certain integral transforms of functions of the scattering amplitudes representing the slow and fast components. By solving the equation for the case of a semiinfinite periodic medium we obtain the reflection and absorption coefficients. These allow us to find the thickness of the stratified system which makes the reflection coefficient close to maximum. These results are applicable to any stratified system, in particular to a crystal.

Ignoring technical questions one might note that a diffraction grating would best be produced by using the isotopes Ni^{62} ($a^{\text{coh}} = -0.87 \times 10^{-2} \text{ cm}$) and Ni^{58} ($a^{\text{coh}} = 1.44 \times 10^{-12} \text{ cm}$). Calculations performed for this case show that a total of several tens of ideally placed layers would be required to obtain a reflection coefficient of the order of unity. Nonideal laying down of the layers leads to an increase in the required

Translated from *Atomnaya Énergiya*, Vol. 22, No. 2, p. 119, February, 1967. Original article submitted April 5, 1966; revised October 5, 1966.

grating thickness, which can be estimated if one knows the departure from the ideal arising from the imperfections of the technological process and the diffusion of atoms from one layer to another.

SHIELDING PROPERTIES OF STONE CONCRETE

V. B. Dubrovski, M. Ya. Kulakovski,
P. A. Lavdanski, V. I. Savitski,
V. N. Solov'ev, and A. F. Mirenkov

UDC 621.039.538

Using stone concrete for biological shields allows one to make the most effective use of local building materials such as stone or ore, and to make new mixtures which strike the best balance between density and cost. Depending on the aggregate used, stone concretes, like ordinary concrete, may have various densities and water content.

For the stone concrete and ordinary concrete shields studied (Table 1) the spatial distribution of neutrons and capture γ -radiation and the distribution of dose rate outside the shield were computed for an attenuation of the total dose rate of 5×10^9 .

The results of the experiments showed that a change in the hydrogen content of stone concrete had only a small effect on the fast neutron removal length. Because of the large densities of stone concrete the relaxation length in them is smaller than in ordinary concretes (compositions 1-4, 7-8 cf. Table 1). For stone concrete and ordinary concrete of the same density (compositions 5 and 6) the relaxation length in stone concretes is also smaller due to the large fraction of light elements composing them. Stabilization of the neutron spectrum occurs at practically the same depth in stone concrete and ordinary concrete shields and therefore at large shield thicknesses λ for thermal and intermediate neutrons in stone concrete shields is equal to λ for fast neutrons. As a consequence of the smaller hydrogen content

TABLE 1. Contribution of Individual Forms of Radiation of Total Dose Outside the Shield, %

Com- posi- tion no.	Kind of Material	Density kg/m ³	Water content kg/m ³	$\lambda = \frac{1}{\Sigma_{rem}}$	D_F^*	D_I	D_T	L_{γ}^{cap}	Total Dose	Shield thickness cm
1	Ordinary concrete with granite	2350	74	13.42	14.24	8.7	37.4	39.66	100	325
2	Stone concrete with granite	2400	48	13.38	15.18	14.4	32.9	37.4	100	318
3	Hematite concrete	3300	60	11.6	50.5	44.2	3.73	2.07	100	280
4	Stone hematite concrete	3750	39	10.43	33.6	62.6	3.13	1.3	100	247
5	Stone hematite concrete with shot	4600	60	9.3	30.0	65.5	2.48	1.95	100	211
6	Stone concrete with shot	4600	39	9.15	19.9	76.8	1.71	1.62	100	213
7	Serpentine concrete	2050	198	13.4	53.5	12.4	29.3	5.5	100	312
8	Stone Serpentine concrete	2225	234	12.3	37	8.3	24.5	30.2	100	272

* D_F , D_I , D_T , and D_{γ}^{cap} are the doses due to fast, intermediate, and thermal neutrons, and capture γ -radiation respectively.

Translated from Atomnaya Énergiya, Vol. 22, No. 2, pp. 119-120, February, 1967. Original article submitted June 9, 1966; abstract November 2, 1966.

TABLE 2. Relaxation Lengths of Neutrons and γ -Ray Dose cm (numerator) as a Function of Shield Thickness in cm (denominator)

Kind of material	p^{21}		In without Cd		In in Cd		BF ₃ without Cd		BF ₃ in Cd		Exp. value of λ for γ -ray dose rate at reactor power	
	Exp.	Calc.	Exp.	Calc.	Exp.	Calc.	Exp.	Calc.	Exp.	Calc.	0	1 kW
Concrete $p=2.2$ tons/m ³ water content 4.5%	12.5 20-80	12.7	10.4 20-120	11.0	10.2 20-180	—	12.5 50-100	13.0	12.5 50-100	13.1	9.7 20-80	13.75 60-120
Stone concrete $p=2.3$ tons/m ³ , water content 3.64%	12.3 20-80	12.5	10.4 20-120	11.3	10.2 20-180	—	12.5 50-100	12.0	12.3 50-100	12.6	9.5 20-80	13.3 60-120

in stone concrete of compositions 2, 4, and 6, the buildup factor for the thermal neutrons is smaller than that for intermediate neutrons is larger than in concretes 1, 3, and 5. In stone concrete of composition 8 the hydrogen content is larger than in concrete of composition 7 and therefore the buildup factor for thermal neutrons is larger and that for intermediate neutrons is smaller than in ordinary concrete. Due to the smaller λ of thermal and intermediate neutrons in all stone concretes investigated, their buildup does not make a significant contribution to the total dose outside the shield and does not lead to an increase in its thickness. Because of the larger density of stone concretes, the total γ -flux in them is smaller than in ordinary concretes. If the thickness of the shield is determined by the external γ -radiation, the advantage of stone concretes of larger density is obvious.

The report also presents results of an experimental investigation of the shielding properties of stone concrete performed in the beam of the VVR-TS research reactor at the L. Ya Karpov Physics and Chemistry Institute, the calculated spatial distribution of neutrons, and the readings of detectors used in performing the experiments (Table 2).

It was established that, in addition to its technical and economic advantages stone concrete has somewhat better shielding properties than ordinary concrete and may find application as a material for biological shields.

SHIELDING PROPERTIES OF BORATED HEAT-RESISTANT CHROMITE CONCRETES

D. L. Broder, V. B. Dubrovski,
M. Ya. Kulakovski, P. A. Lavdanski,
V. I. Savitski, V. N. Solov'ev, and A. F. Mirenkov

UDC 621.039.538

Results of the experimental investigation of the shielding properties of borated chromite heat-resistant concrete are presented and compared with the results of theoretical calculations.

Translated from Atomnaya Énergiya, Vol. 22, No. 2, p. 121, February, 1967. Original article submitted June 9, 1966.

Neutron and γ Dose Rate Relaxation Lengths in cm (numerator) as a Function of Shield Thickness in cm (denominator)

Kind of concrete	P_{31}		In without Cd		BF_3		Exp. value of λ for γ -ray dose rate at reactor power	
	Exp.	Calc.	Exp.	Calc.	Exp.	Calc.	0	1 kW
Chromite without boron	$\frac{10.4}{40-80}$	11.15	$\frac{13.5}{50-120}$	13.6	$\frac{14.5}{50-100}$	14.7	$\frac{8.0}{20-80}$	$\frac{12.45}{60-120}$
Chromite with 32 kg/m ³ of boron	$\frac{10.4}{40-80}$	11.8	$\frac{12.5}{40-80}$	12.2	$\frac{13.5}{40-90}$	13.0	$\frac{8.0}{20-80}$	$\frac{11.3}{60-120}$
Chromite with 65 kg/m ³ of boron	$\frac{10.4}{40-80}$	10.95	$\frac{12.5}{40-80}$	12.2	$\frac{13.5}{40-80}$	13.0	$\frac{8.0}{20-80}$	$\frac{11.3}{60-120}$
Ordinary*	$\frac{12.5}{20-80}$	12.7	$\frac{10.4}{20-120}$	—	$\frac{12.0}{50-100}$	—	$\frac{9.7}{20-80}$	$\frac{13.75}{60-120}$

* Density 2.2 tons/m³.

The experimental study of shielding properties was made in the horizontal beam of the VVR-TS reactor at the L. Ya. Karpov Physics and Chemistry Institute using boron trifluoride counters, phosphorus threshold detectors, and indium resonance detectors.

A method for calculating the spatial distribution of neutrons from a monodirectional source is described. The calculated neutron spectrum at the outer edge of the VVR-TS core is given as are the results of the calculation of the neutron penetration through the concretes performed by this method, and also the results of calculating the readings of the detectors used in the experimental part of the work. The data obtained are listed in the table.

It was established that the introduction of more than 30 kg/m³ of boron into the chromite concrete is useless since it does not lead to any significant improvement in shielding properties. The good agreement between the calculated and experimental results shows that the calculational method described in the report is accurate enough and gives a correct description of the spatial distribution of neutrons from monodirectional sources in shields.

HEAT RELEASE IN BORATED CONCRETE SHIELDS

V. B. Dubrovski, M. Ya. Kulakovski,

P. A. Lavdanski, V. I. Savitskii, and V. N. Solov'ev

UDC 621.039.538.4

Results of an investigation of the heat release due to the absorption of the capture γ - and α -particles from the $B^{10}(n, \alpha) Li^7$ reaction in five concretes having different boron concentrations are described. The average energy liberated in the capture of a neutron by boron is less than half that liberated in the capture of a neutron by most of the other constituents of concretes. Therefore the addition of boron to concrete leads to a decrease in heat release and to a redistribution of it over the thickness of the shield (cf. table).

Translated from Atomnaya Energiya, Vol. 22, No. 2, pp. 121-122, February, 1967. Original article submitted June 9, 1966.

Heat Release $Q(\times 10^{-13} \text{ w/cm}^2)$ and Distance from Inner Surface of Shield to Point of Maximum Heat Release x_{max} in Borated Concretes*

Boron concentration in kg/m^3	Kind of concrete									
	Ordinary		Hematite		Chromite		With scrap		Magnesite	
	Q	x_{max}	Q	x_{max}	Q	x_{max}	Q	x_{max}	Q	x_{max}
0	1.52	12	1.46	18	1.175	33	1.185	15	1.091	36
15	0.634	15	0.661	12	0.410	18	0.640	12	0.503	16.5
60	0.661	12	0.585	9	0.462	15	0.607	9	0.553	12

* Normalized to one neutron entering the concrete shield.

The study included ordinary concrete, concretes with iron ore and metallic scrap added, and also heat-resistant chromite and magnesite concretes which may be used in shields up to temperatures of 1700° C.

Graphs showing the distribution of heat release allow the shield designer to determine the efficacy of such concretes in various structural elements of the shield for hard spectra.

On the basis of an analysis of the data recommendations are made for the boron concentration in shielding concretes. (15 kg/m^3 of natural boron).

DIFFERENTIAL ALBEDO OF A NARROW BEAM OF FAST NEUTRONS FROM A SEMIINFINITE WATER SCATTERER

L. Ya. Gudkova, V. G. Zolotukhin,
V. P. Mashkovich, and A. I. Mis'kevich

UDC 539.125.52:539.121.72

The differential spectral, number and dose albedos of a narrow beam of neutrons from a semiinfinite water scatterer were calculated on a high speed computer using the Monte Carlo method. The neutron sources were square pulses with narrow energy widths ΔE_0 equal to 0.4-0.8; 0.8-1.4; 1.4-2.5; 2.5-4.0; 4.0-5.0; 5.0-6.5; 6.5-8.5; 8.5-10.5; 10.5-12 and 12-14 MeV.

In contrast to calculations in other reports [1-3], in our work: 1) differential albedos were studied, including the azimuthal dependence; 2) the neutron sources were square pulses with narrow energy widths ΔE_0 ; 3) the dependence of the number albedo on the threshold energy of the detectors E_{THR} was investigated; to do this the differential albedo of monoenergetic neutrons of energies E_0 equal to 1 and 3 MeV was studied.

From 2000 to 4000 histories were run for each variation of the problem. The energy intervals were taken equal to 1/16 the maximum energy of the source neutrons.

Translated from *Atomnaya Énergiya*, Vol. 22, No. 2, pp. 122-123, February, 1967. Original article submitted September 14, 1966.

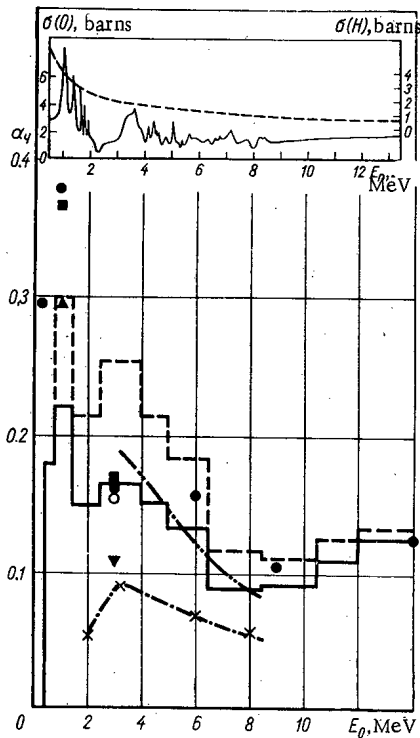


Fig. 1. Integrated number albedo α_N for normal incidence: Square pulse sources:— this report ($E_{\text{THR}} = 1$ keV) ---- this report (reduced to $E_{\text{THR}} = 0.5$ eV), \times - - - \times - - - [3] ($E_{\text{THR}} = 0.1$ MeV) - . - . - [3] (reduced by authors of this report to $E_{\text{THR}} = 0.5$ eV); monoenergetic sources; \bullet [1] ($E_{\text{THR}} = 0.5$ eV), \circ [2] ($E_{\text{THR}} = 0.5$ eV), \blacktriangle this report ($E_{\text{THR}} = 0.15$ keV), \blacktriangledown this report ($E_{\text{THR}} = 1$ keV), \blacksquare this report (reduced to $E_{\text{THR}} = 0.5$ eV). The total interaction cross sections for oxygen (solid curve) and hydrogen (dotted curve) are shown at the top of the figure.

The results of the calculations of number and dose albedos as functions of the polar and azimuthal angles of reflection and the angle of incidence are presented.

Certain regularities in the results obtained may be illustrated by the calculated magnitudes of the integrated neutron albedos for normal incidence (cf. Fig. 1).

Analysis of the data plotted on the figure shows the following: 1) the magnitude of the number albedo is strongly dependent on the choice of threshold energy for the detectors E_{THR} ; increasing, for example, at $E_0 = 3$ MeV by a factor of 1.9 for a decrease in E_{THR} from 0.1 MeV to 0.5 eV; for the dose albedo the contribution of neutrons with energies below 1 keV may be neglected; 2) the considerable irregularities in the behavior of the interaction cross section with water is attributed to the existence of differences, at certain source energies, in the magnitudes of the albedos for square pulsed sources and monoenergetic sources whose energies lie within the boundaries of the square pulses. For example, the number albedo for a source with $E_0 = 3$ MeV is smaller by a factor of 1.53 than that for a source with energy width $\Delta E_0 = 2.5 - 4$ MeV.

The information on monoenergetic sources is in good agreement with data in the literature [1-3].

LITERATURE CITED

1. M. Berger and J. Cooper, J. Res. Natl. Bur. Stds. 63A, 101 (1959).
2. M. Leimdörfer, "The Backscattering of Fast Neutrons from Plane and Spherical Reflectors," Stockholm (1964).
3. L. M. Shirkin, Atomnaya Énergiya 20, 267 (1966).

USE OF ALBEDO BOUNDARY CONDITIONS TO REDUCE
THE REGION OF ITERATION*

V. S. Shulepin

UDC 539.125.52:621.039.51

The source iteration method is widely used to obtain numerical solutions of the homogeneous reactor equations. However, it is not always expedient, and sometimes not even possible to apply this method over the whole range of the spatial variable. For example, in calculating many variations of a reactor which differ in the physical properties of the core but have the same reflector composition and thickness it is advisable to use the iteration method only in the core and to take the reflector properties into account by an albedo. Further, if the core has a complex composition and the reflector or shield consists of a large number of different layers, the iteration method cannot always be used because of limitations of computer memory. In this case the use of the albedo method allows one to solve the problem since the number of albedo quantities for the reflector or shield is relatively small.

Albedos may be determined, for example, by a method described by V. V. Orlov (In: "Neutron Physics", Moscow, Gosatomizdat, 1961, p. 179 [in Russian]). The equations in that report allow one to determine the magnitudes of albedos of a nonmultiplying medium adjacent to the outer surface of the core (reflector) and also the corresponding albedos for a central nonmultiplying region of the reactor. Having found the albedo values it is then possible to write the boundary conditions for the solution of the diffusion equation using the source iteration method in the core. The use of albedos of multiplying media is complicated by the fact that the albedos of these media depend on the effective multiplication constant k_{eff} . The region of applicability of albedos of multiplying media is limited to the calculation of some reactor dimension and the spatial and energy distribution of the neutrons for a given magnitude of k_{eff} . The introduction of albedos of multiplying regions into boundary conditions makes it impossible to iterate on the multigroup neutron fluxes in the boundary conditions.

The use of albedo boundary conditions and a finite difference scheme for solving the reactor equations are discussed in this report. An example is presented of a calculation with a decreased region of iteration. It is shown that the convergence of the iterative process depends on the number of calculational intervals in the region where the iteration is carried out.

VARIABLE-THICKNESS, PREMODERATING, HIGH-
SENSITIVITY NEUTRON DETECTOR†

Yu. A. Vakarin, L. N. Veselovskii,
B. S. Gribov, A. V. Kolotkov,
V. G. Kuznetsov, and V. A. Sakovich

UDC 539.107.4:539.125.5

A detector intended for use in a collimator with an entrance hole 10 cm in diameter is described. A water-filled cylinder is inserted into the cylinder; a thermal neutron scintillation counter is free to

* Translated from *Atomnaya Énergiya*, Vol. 22, No. 2, p. 123, February, 1967. Original article submitted May 19, 1966; revised September 15, 1966.

† Translated from *Atomnaya Énergiya*, Vol. 22, No. 2, p. 124, February, 1967. Original article submitted April 28, 1966; revised September 26, 1966.

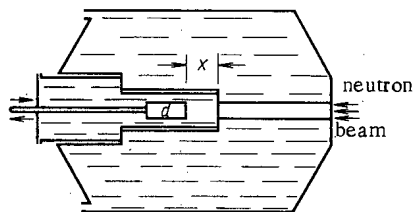


Fig. 1. Geometry of the arrangement: d) Thermal neutron detector; x) variable layer of neutron premoderator.

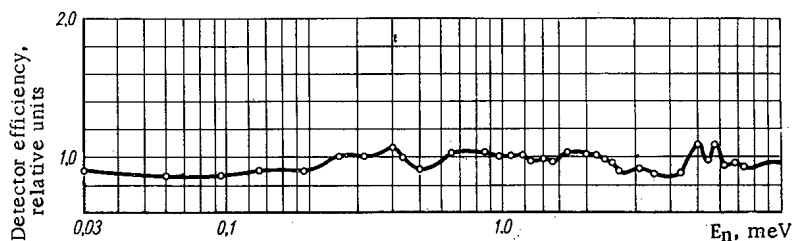


Fig. 2. Detector recording efficiency plotted vs. neutron energy, at 80 mm moderator thickness.

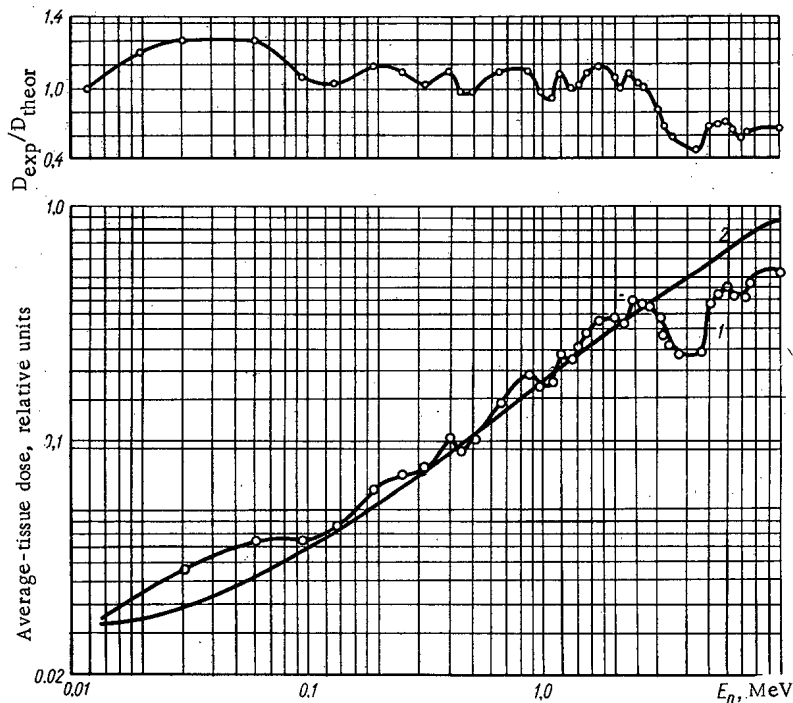


Fig. 3. Detector recording efficiency plotted vs. neutron energy, at 150 mm moderator thickness: 1) spectral sensitivity of detector at 150 mm moderator thickness (D_{exp}); 2) average-tissue dose (rem) per unit neutron flux (D_{theor}).

move along the cylinder axis (Fig. 1). The recording efficiency of the detector was studied by using monoenergetic neutrons in the 30 - 19 MeV range at premoderator layer thicknesses of 0 to 20 cm.

The use of different moderator thicknesses made it possible to measure both flux levels of neutrons of from 30 to 18 MeV energy, and the biological dose due to them (Figs. 2 and 3).

THERMAL COLUMN CONVERTER FOR SHIELDING STUDIES

V. P. Mashkovich, A. N. Nikolaev,
B. I. Sinitsyn, V. K. Sakharov, and S. G. Tsypin

UDC 539.16.08:621.039.538

The article deals with the design and radiation characteristics of the thermal column converter in the BR-5 reactor facility. This converter was designed to study radiation transmission through non-uniformities in the shielding.

The converter assembly consists of a tank of stainless steel $2 \times 2 \times 2.5$ m, the front face 2 m^2 and adjacent to the reactor thermal column. The converter, extracted from its shielded container (a source-holder combination, U^{235} -enriched uranium dioxide), is set into operating position by remote control. A 2-cm thick boron carbide filter is placed on the outer surface of the front face of the tank. The filter has a hole 250 mm in diameter and a cadmium sheet 1 mm thick on the inner surface for absorbing thermal neutrons. The radiation detectors can be arranged at any point in the experimental tank by means of a special remote positioning device.

Thermal flux distribution was measured at the exit of the thermal column and on the inner surface of the experimental tank. The thermal flux at the converter operating position was $1.78 \cdot 10^8 \pm 0.10 \cdot 10^8$ neutrons/cm²·sec. The axial and radial fast distributions in the experimental tank were studied at the exit from the converter.

The measurements showed that the converter functions as a disk type isotropic source 250 mm in diameter with a capacity of $1.57 \cdot 10^8 \pm 0.07 \cdot 10^8$ neutron fission events per cm² sec at a reactor power rating of 5 MW.

Corrections taking into account the γ -photons and fast neutrons entering the experimental tank from the reactor thermal column were introduced into the indicator readings in the treatment of the experimental results.

It was found that γ -emission from the thermal column of the reactor must be taken into account when working with γ -sensitive detectors. Suppression of γ background by placing a bismuth plug at the thermal column exit was judged feasible.

Translated from *Atomnaya Énergiya*, Vol. 22, No. 2, p.125, February, 1967. Original article submitted June 4, 1966.

LETTERS TO THE EDITOR

STOPPING POWER OF NICKEL FOR PROTONS AND He_4^+ IONS
IN THE ENERGY RANGE 20 TO 95 keVG. F. Bogdanov, V. P. Kabaev,
F. V. Lebedev, and G. M. Novikov

UDC 539.9

The use of nickel foils in diagnostic apparatus designed for the study of plasma necessitates determining their stopping power with respect to particles with energies from a few kiloelectron volts to hundreds of kiloelectron volts. We have therefore determined the specific energy losses of 20-95 keV protons and 30-90 keV He_4^+ ions.

Energy analysis of the particle beams before and after passing through a foil of known thickness was carried out by means of an electrostatic analyzer with a resolving power of 1.5%. Particle beams of the required energy were separated out by means of a magnetic separator with a similar resolving power.

Nickel films were obtained by depositing nickel vapor on a copper substrate, the latter then being dissolved (the foils were not annealed). The foil thickness was determined by weighing.

The specific energy losses were determined for five batches of foils, the thicknesses being 21.2 ± 1.2 ; 23.9 ± 1.2 ; 30.0 ± 1.3 ; 60.5 ± 1.6 and $70.0 \pm 1.7 \mu\text{g}/\text{cm}^2$. Measurements were made on three or four foils of each batch and the results were averaged. The experimental errors, consisting of the errors in determining the foil thicknesses, the energy losses in the foils, and the energy of the incident particles, ranged from 6% for foils $70.0 \mu\text{g}/\text{cm}^2$ thick to 11.6% for foils $21.2 \mu\text{g}/\text{cm}^2$ thick. The specific losses obtained with foils of different thicknesses varied by not more than 14%, which was no greater than the experimental error. Hence the absolute value of the specific losses was determined as the weighted mean of the five (unequally-accurate) measurements. The error thus obtained was $\pm 5\%$.

The experimental values of the specific energy losses of protons in nickel are given in Table 1 and Fig. 1 (dark circles). The same figure shows the specific losses obtained by other authors as functions of energy. The continuous line corresponds to the proton energy losses in nickel [1-3]. Our own results agree closely with those of [2, 3] and rather less well with those of [1]. The points indicated by triangles were taken from [4], in which the specific energy losses of tritons in nickel were determined. The energies given for these points represent 1/3 of the energy of the tritons. We see from Fig. 1 that the points thus obtained lie close to the curve representing the specific energy losses of protons, except for

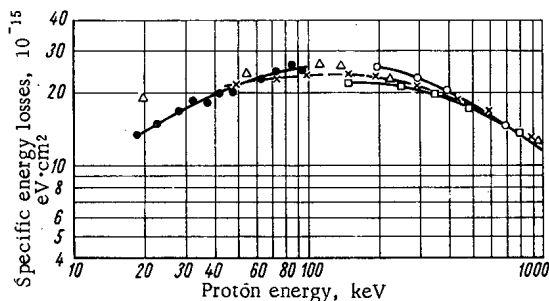


Fig. 1. Stopping power of nickel and copper as a function of the energy of the incident particles.

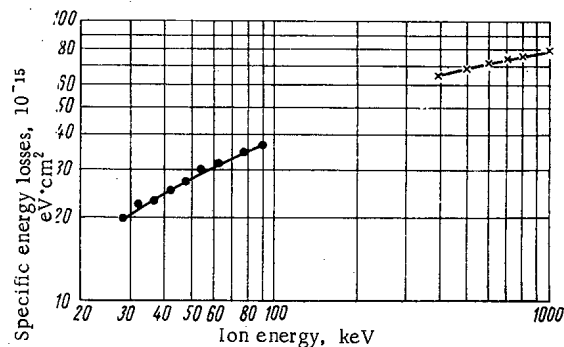


Fig. 2. Specific energy losses of He_4^+ ions in nickel as a function of their mean energy.

Translated from *Atomnaya Énergiya*, Vol. 22, No. 2, pp. 126-127, February, 1967. Original article submitted October 11, 1966.

TABLE 1. Specific Energy Losses of Protons in Nickel

E, keV	$dE/dx, \text{keV}\cdot\text{cm}^2/\text{mg}$	E, keV	$dE/dx, \text{keV}\cdot\text{cm}^2/\text{mg}$
19	140	65	234
23.5	157	68	250
28	170	70	240
34	190	73	232
39	186	75	244
43.5	202	78	255
49	202	80	248
54	222	83	249
59	235	88	255
60	230	91.5	265
63.5	235	95	255

TABLE 2. Energy Losses of He_4^+ Ions in Nickel

E, keV	$dE/dx, \text{keV}\cdot\text{cm}^2/\text{mg}$	E, keV	$dE/dx, \text{keV}\cdot\text{cm}^2/\text{mg}$
28.5	204	57.5	300
32.5	238	63	325
38	238	72	346
42.5	258	78	356
48	280	83	356
54.5	304	91	376

the point at 20 keV. However, this point corresponds to the lower boundary of the range of energies in which Wolke worked [4], and this probably explains the discrepancy in the values of the losses. The agreement between the specific energy losses of protons and tritons for corresponding particle velocities indicates that the specific losses do not depend on the mass of the incident particles. In the same figure, the broken line gives the stopping power of copper taken from [3, 5]. In the energy range studied, the specific energy losses of protons in nickel and copper coincide to an accuracy equal to the measuring error.

The results of measurements of the specific energy losses of He_4^+ ions in nickel are shown in Table 2 and Fig. 2 (dark circles). The crosses in Fig. 2 show the stopping power of nickel with respect to α -particles [6]. The data obtained in the present investigation for He_4^+ ions may be used for determining the energy losses of α -particles, since at this energy the losses are determined by the effective charge, independently of the charge state of the incoming particles [7], and our foils are "thick" in the sense that charge equilibrium is capable of being established in them. This may be seen from the following rough calculation. The electron capture cross section for He_4^{++} ions in hydrogen at 100 keV approximately equals $3 \cdot 10^{-16} \text{ cm}^2$. Hence the free path of 100-keV α -particles in the metal is no greater than $4 \cdot 10^{-8} \text{ cm}$, which is many times smaller than the thickness of the foils studied. We see from Fig. 2 that our own data are in good agreement with the results of [6].

LITERATURE CITED

1. G. M. Osetinskii, Supplement No. 5 to Atomnaya Énergiya. [in Russian], Moscow, Atomizdat, p. 94 (1957).
2. A. Chilton et al., Phys. Rev., 93, 413 (1954).
3. M. Bader et al., Phys. Rev., 103, 32 (1956).
4. R. Wolke et al., Phys. Rev., 129, 2591 (1963).
5. S. Allison and S. Warshaw, Rev. Mod. Phys., 25, 779 (1953).
6. D. Porat and K. Ramavataram, Proc. Roy. Soc., A 232, 394 (1959).
7. S. Allison, Rev. Mod. Phys., 30, 1137 (1958).

NUCLEAR PROPERTIES OF THE ISOTOPES OF ELEMENT
102 WITH MASS NUMBERS 255 AND 256

V. A. Druin, G. N. Akap'ev,
A. G. Demin, Yu. V. Lobanov, B. V. Fefilov,
G. N. Flerov, and L. P. Chelnokov

UDC 546.799.92

We know of two papers [1, 2] relating to the synthesis and presumed properties of the isotope 102^{255} . According to the earlier of these [1], the isotope 102^{255} may be an α -emitter with a half-life of 10 min and α -particle energy 8.5 MeV. According to [2], however, isotope 102^{255} has quite different properties; its half-life is 15 sec, and the α -particle energy 8.2 MeV. All this calls for new experiments in order to establish the properties of this isotope, and this is the object of the present investigation. There is also considerable interest in determining the α -decay energy of isotope 102^{256} , which has so far never been measured.

Synthesis of the isotopes of element 102 was achieved by irradiating a target of natural uranium with Ne^{22} ions, using the reactions $\text{U}^{238}(\text{Ne}^{22}, 5n) 102^{255}$ and $\text{U}^{238}(\text{Ne}^{22}, 4n) 102^{256}$. The experimental method was described in detail earlier [3]. In these experiments, irradiation was carried out in the inclined beam of the 310-cm cyclotron of the United Institute of Nuclear Research; this enabled a large target (35×20 mm) to be used after slightly modifying the construction of the target chamber. The energy of the ions was varied by means of aluminum foils. The efficiency of collecting the product nuclei and the energy of the ions were checked continuously by recording the yield of the well-known isotope Ac^{214} formed in the reaction $\text{Au}^{197}(\text{Ne}^{22}, \text{rn}) \text{Ac}^{214}$ between the incident ions and slight gold traces deliberately introduced for this purpose into the uranium layer of the target. (Preliminary experiments showed that this produced no serious increase in the background for the α -particle-energy range under consideration.)

Measurements were made under a variety of timing conditions with ion energies of 177 to 137 MeV; these enabled the following α groups to be sharply recorded: * 8.08 MeV (about 3 min); 8.23 MeV (more than 5 min); 8.35 MeV (composite group with half-lives of about 30 sec and more than 5 min); 8.41 MeV (6 ± 2 sec); 8.87 MeV (25 sec); 11.65 MeV (45 sec). In order to identify these α -emitters, their yields were measured as functions of the energy of the incident ions (see figure).

The characteristics of the high-energy α -groups 8.87 and 11.65 MeV are in good agreement with data relating to the isomers $\text{Po}^{214\text{m}}$ and $\text{Po}^{212\text{m}}$. The formation of these isomers in our experiments was probably due to the presence of lead impurities in the target (these not having been eliminated in the purification of the target and substrate material).

The group with α -particle energy 8.41 MeV only appeared sharply for ion energies of 110 MeV, corresponding to the maximum of the reaction $\text{U}^{238}(\text{Ne}^{22}, 4n) 102^{256}$. The half-life agreed with existing data for the 102^{256} isotope [4].

The maximum cross section of the reaction leading to the formation of an α -emitter with an energy of 8.41 MeV equalled approximately $2 \cdot 10^{-32}$ cm², which is close to the value of $4 \cdot 10^{-32}$ cm² given in [4] for the maximum of the excitation function of the reaction $\text{U}^{238}(\text{Ne}^{22}, 4n) 102^{256}$. Thus we may conclude that the 8.41-MeV α -group belongs to the isotope 102^{256} . It thus follows that the α -decay energy of isotope 102^{256} is 8.58 MeV, since, for an even-even isotope, the most intense α -group corresponds to a transition of the ground state of the daughter nucleus.

* Alpha groups of energies higher than 7.9 MeV are given. Bracketed figures indicate the measured half-lives. The error in determining the energies of the α -particles was ± 0.03 MeV.

Translated from *Atomnaya Énergiya*, Vol. 22, No. 2, pp. 127-128, February, 1967. Original article submitted October 1, 1966.

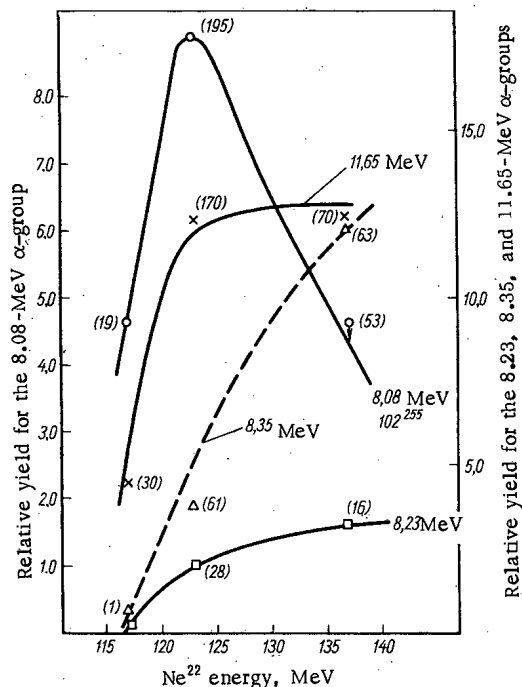


Fig. 1. Excitation functions of $U^{234} + Ne^{22}$ reactions leading to the formation of emitters with α -particle energies of 8.08, 8.23, 8.35, and 11.65 MeV. (Bracketed figures give total number of recorded α -particles).

By comparing the illustrated excitation functions of reactions leading to the formation of α -emitters with 8.08, 8.23, and 8.35 MeV, we see that the reaction reminiscent of $U^{238}(Ne^{22}, 5n) 102^{255}$, (as regards the shape and position of the maximum) only gives an α -emitter with an energy of 8.08 MeV and a half-life of about 3 min, which may thus be the isotope 102^{255} . The maximum yield of the α -group 8.08 MeV is roughly five times that of the α -group 8.41 MeV. This agrees with known experimental data relating to the excitation functions of the reactions $U^{238}(Ne^{22}, 5n) 102^{255}$ and $U^{238}(Ne^{22}, 4n) 102^{256}$ [5].

The rise in the yield of α -emitters 8.23 and 8.35 MeV with increasing energy of the bombarding ions over the whole range of ion energies studied indicates that these α -emitters are formed in reactions of a different type (apparently without the formation of a composite nucleus) and cannot relate to element 102. The identification of these reactions is difficult on the basis of available data. The results show that the properties of isotope 102^{255} differ considerably from those hitherto published.

The authors are grateful to I. V. Kolesov for the construction of particular components of the apparatus, to V. M. Plotko, Yu. V. Poluboyarinov, V. I. Krashonkin, and G. Ya. Sung Ching-yang for help in the measurements, and to A. F. Linev, B. A. Zanger, and I. A. Shelaev for making the necessary arrangements for the experiments on the accelerator.

LITERATURE CITED

1. P. Fields et al., *Arkiv Fys.*, **15**, 225 (1959).
2. A. Ghiorso et al. *Phys. Rev. Letters*, **6**, 473 (1961).
3. G. N. Akap'ev et al., Preprint OIYaI R-2704, Dubna (1966).
4. E. D. Donets, V. A. Shchegolov, and V. A. Ermakov, *Atomnaya Énergiya*, **16**, 195 (1964).
5. E. D. Donets, V. A. Shchegolev, and V. A. Ermakov, *Yadernaya fizika*, **2**, 1015 (1965).

BEAM OF HELIUM IONS WITH A CURRENT OF 200 mA
AND AN ENERGY OF 70 keV

N. V. Pleshivtsev, V. I. Martynov,
G. G. Tomashev, Yu. F. Grigorovich,
and B. K. Shembel'

UDC 539.107.6:621.384.6:621.038

In order to solve certain problems in the physics of elementary particles and nuclear physics, the intensity of accelerated ions must be increased [1-3]. In this paper we shall present the results of experiments on obtaining an intense beam of helium ions under continuous conditions.

The arrangement of the experimental apparatus is shown in Fig. 1. The ion source was a duoplasmatron with electron oscillations in the anode region of the plasma [4]. The ions were initially formed into a beam by means of the specially-shaped plasma surface, the electric field of a single-gap lens, and a magnetic field. Subsequent focusing of the ion beam was effected by two magnetic lenses.

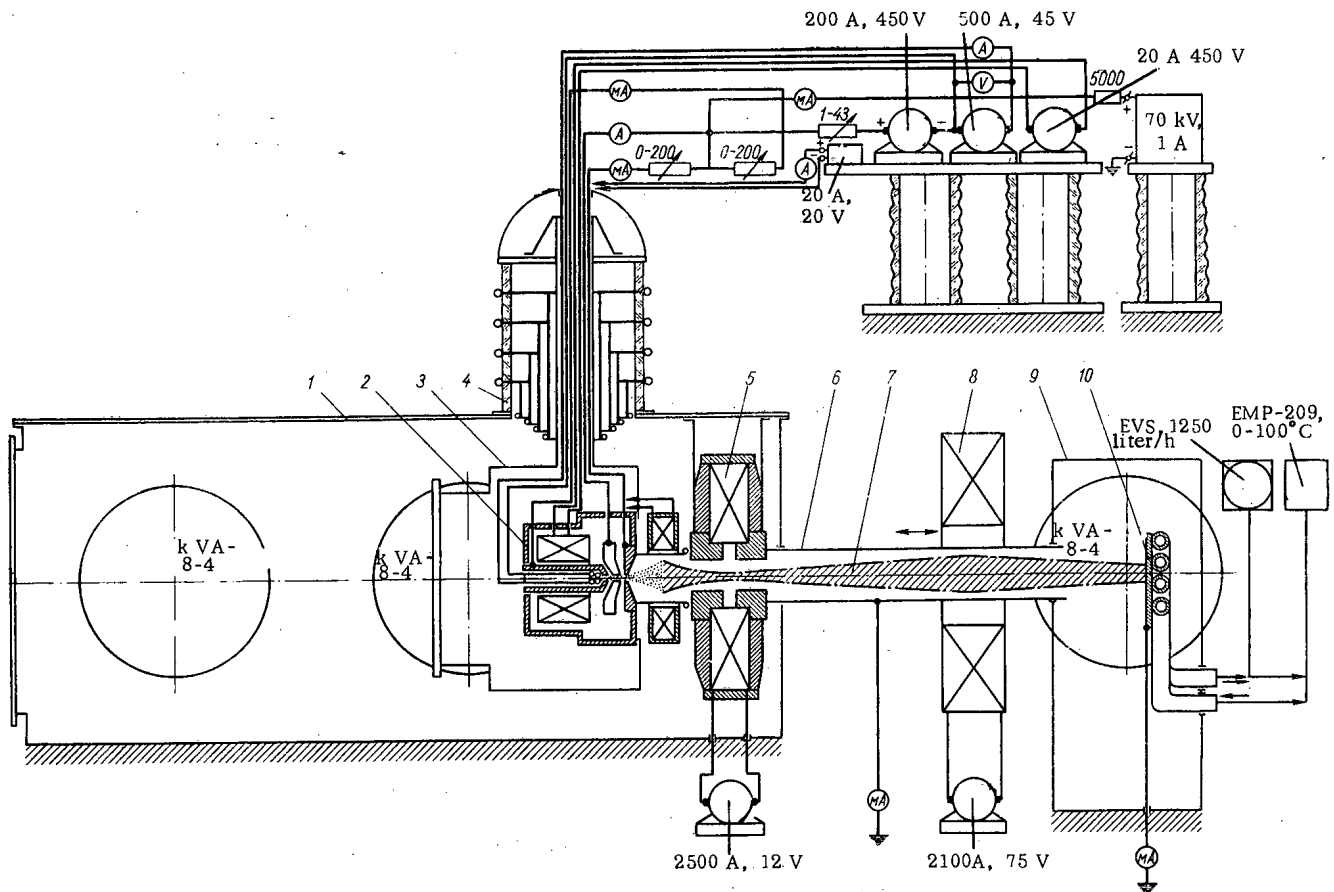


Fig. 1. Principle of the experimental apparatus: 1) injector container; 2) ion source; 3) vacuum-tight container; 4) procelain insulator; 5) first magnetic lens; 6) ion guide; 7) helium-ion beam (200 mA, 60 keV); 8) second magnetic lens; 9) container for current receiver; 10) current receiver.

Translated from *Atomnaya Énergiya*, Vol. 22, No. 2, pp.128-131, February, 1967. Original article submitted June 24, 1966.

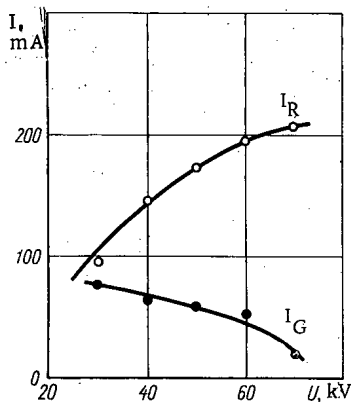


Fig. 2. Currents of helium ions reaching the current receiver (I_R) and ion guide (I_G) as functions of accelerating voltage.

The geometry and position of the plasma boundary extending out from the ion source into the vacuum depends on many factors: the plasma concentration, the electron temperature, and the electric and magnetic fields [5]. The optimum conditions for focusing a helium-ion beam with the greatest current possible were therefore found experimentally.

The current receiver was placed at a distance of 1.6 m from the ion-source emission aperture. The ion currents to the current receiver and ion guide (the latter being 880 mm long and 150 mm in internal diameter) were measured calorimetrically.

Figure 2 shows the helium-ion current as a function of accelerating voltage. We see from the figure that, with increasing accelerating voltage, the number of ions falling on the ion guide becomes smaller. At a potential of 70 kV, the ion losses represent 10% of the current in the focused beam.

The geometry of the ion beam was studied on emergence from the ion guide (Fig. 3). By determining the diameter of the beam and its angular convergence, and using the well-known laws of geometric and electron optics, we may calculate the geometry of the beam in the reverse direction from the current receiver to the accelerating gap (see Fig. 1).

The agreement between the calculated and observed beam dimensions in the accelerating gap, and also the small number of ions falling on the ion guide (as compared with the calculated number for an uncompensated beam), indicate fairly complete self-compensation of the space charge of the ions in the region between the median plane of the first magnetic lens and the current receiver.

In conclusion, we present the main operating parameters of the injector for focusing a 210-mA, 70-keV ion beam.

Parameters of Ion Source

Arc current	10 A
Arc voltage	100 V
Pressure in arc chamber, measured with an LT-2 tube	0.2 mV
Pressure in anode-anticathode region, measured with an LT-2 tube	4.0 mV

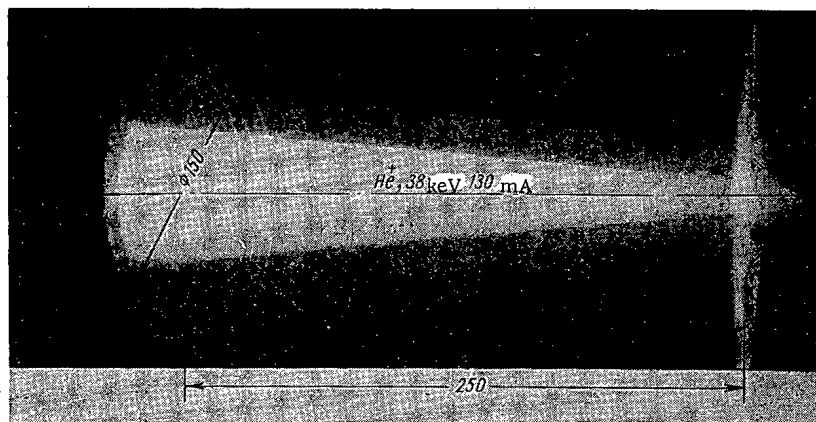


Fig. 3. Photograph of helium-ion beam (130 mA, 38 keV) at the exit from the ion guide.

Parameters of Focusing System

Accelerating voltage	70 kV
Current of high-voltage rectifier	370 mA
Number of ampere-turns on first magnetic lens	22,000
Number of ampere-turns on second magnetic lens	120,000
Pressure in injector container	$1.6 \cdot 10^{-5}$ mm-Hg
Pressure in current-receiver chamber	2 to $3 \cdot 10^{-5}$ mm-Hg

Parameters of Helium-Ion Beam

Helium-ion current to current receiver	210 mA
Ion current falling on ion guide	20 mA
Beam diameter at current receiver	8.5 cm
Beam-convergence semiangle	$1^{\circ} 15'$

For comparison, we note that the current of hydrogen ions was 420 mA for an energy of 80 keV (from calorimetric measurements) and that of argon ions (from electrical measurements) 35 mA at 60 keV.

We wish to thank A. S. Vlasov, I. F. Kukuev, E. A. Vlasenko, A. I. Martynov, and I. A. Shlafshtein for participation in the preparation and carrying out of the experiments.

LITERATURE CITED

1. D. I. Blokhintsev et al., In: "Trans. Intern. Conf. Accelerators (Dubna, 1963)" [in Russian], Moscow, Atomizdat, p. 21 (1964).
2. L. Teng, IEEE on Nucl. Science, NS-11, 17 (1964).
3. J. Richardson, see [2], p. 5; NS-12; The first Nat. particle accelerator Conf. Washington (10-12 March), p. 1012 (1965).
4. R. A. Demirkhanov et al., Pribery i Tekh. Éksp., No. 2, p. 19 (1964).
5. M. D. Gabovich, "Plasma Ion Sources" [in Russian], Kiev, Naukova dumka (1964).

PULSE METHOD FOR MEASURING HOW NEUTRON SPECTRA
OF FINITE-SIZED WATER SAMPLES DEVIATE FROM THE
EQUILIBRIUM MAXWELL SPECTRA

S. B. Stepanov

UDC 539.121.64+539.125.5+539.16.08

To exactly estimate the extrapolated length in experiments on nonstationary diffusion, and ultimately to improve the accuracy of our estimates of the measured constants, we need to know the mean energy of the neutrons in the specimen. Since neutron losses by escape are proportional to the velocities of the neutrons, it follows that in a specimen of finite size the neutron spectrum will be depleted of fast neutrons. Thus the smaller the specimen, the colder will be the spectrum of the neutrons within it. This effect has been studied experimentally by various authors [1, 2]. One group [1] used the method of poisoning of an absorber whose capture cross section does not obey the $1/v$ law; another group [2] used the effect of sensitivity of the detector to the spectrum. The first method is basically applicable only to liquids; the second requires experiments with several detectors of which the sensitivities vary with the neutron energy according to different laws.

Information on the temperature of a Maxwell spectrum can be obtained directly in a pulse experiment based on the effect of "stretching" with time of a spectrum recorded by a detector which is placed at some flight distance l from the surface of the specimen.

Suppose that at the initial moment $t=0$ we switch on a source of thermal neutrons with Maxwell distribution; then the number of neutrons recorded by a detector at time t can be written as follows:

$$N(t) = N_0 e^{-\alpha t} \int_0^{\infty} e^{-\frac{l}{v} - \left(\frac{v}{v_0}\right)^2} \frac{A}{v^2 v} D(v) B(v) dv, \quad (1)$$

where v is the velocity of the neutrons; v_0 is the most probable velocity; $v' = 1/t$; A/v is the detector efficiency; $D(v)$ is the diffusion coefficient; $B^2(v)$ is a geometrical parameter; and α is the decay constant.

Introduce the dimensionless parameter $\tau = (v_0/v) = (v_0/e) t$ and rewrite (1) with $D(v)$ in the form

$$D(v) = D(v_0) \left(\frac{v}{v_0}\right)^a.$$

We can neglect the dependence of B^2 on v :

$$N(\tau) = N_0 e^{-\frac{\alpha l}{v_0} \tau} \left[\int_0^{\tau} e^{-\frac{l}{v_0} \tau - \frac{1}{\tau^2}} \frac{d\tau}{\tau^{4+a}} \right] = N_0 e^{-\frac{\alpha l}{v_0} \tau} f(\tau). \quad (2)$$

For given $l \neq 0$, $N(\tau)$ a complicated function of t and v_0 . The occurrence of the functions $\exp(-\frac{\alpha l}{v_0} \tau)$

(which decreases with increasing τ) and $f(\tau)$ (which increases with τ) leads to the appearance of a maximum on the $N(\tau)$ curve: its position depends on the value of v_0 .

Let us find an equation for the value of τ at which $N(\tau)$ takes its maximum value (τ_0):

$$\frac{\partial N(\tau)}{\partial \tau} = N_0 e^{-\frac{\alpha l}{v_0} \tau} \left[\frac{\partial f(\tau)}{\partial \tau} - \frac{\alpha l}{v_0} f(\tau) \right] = 0.$$

TABLE 1. t_{\max} (μ sec)

l, cm	h, cm		
	3.25	4.5	7.00
23±3	(128±6)	(136±6)	(152±8)
18±3	(104±6)	(112±5)	(120±6)
13.0±2.5	(96±4)	(96±5)	(104±6)
8.0±2.5	(72±4)	(80±5)	(88±5)
0±1	(45±8)	(49±7)	(51±9)

Translated from Atomnaya Énergiya, Vol. 22, No. 2, pp. 131-132, February, 1967. Original letter submitted June 3, 1966; revised September 26, 1966.

TABLE 2. Values of v_0 for Various Values of B^2

h , cm	α , $\times 10^{-4} \text{sec}^{-1}$	$\bar{\lambda}_{tr}$, cm	B^2 , cm^{-2}	v_0 , $\times 10^{-5}$ cm/sec	kT , eV
3.25	2.63 ± 0.04	0.332 ± 0.016	0.738 ± 0.026	1.98 ± 0.18	0.0205 ± 0.0038
4.50	1.85 ± 0.03	0.345 ± 0.018	0.421 ± 0.012	2.08 ± 0.16	0.0226 ± 0.0034
7.00	1.18 ± 0.02	0.356 ± 0.019	0.201 ± 0.004	2.14 ± 0.14	0.0240 ± 0.0030

Finally we get

$$\left. \frac{\partial f(\tau)}{\partial \tau} \right|_{\text{for } \tau=\tau_0} = \frac{\alpha l}{v_0} f(\tau_0). \quad (3)$$

Our measurements were made with water at 20°C in a cylindrical vessel of diameter 30 cm, for three different values of the water layer thickness h . The value of $N(t)$ was measured for four different flight distances l . In each case we determined the position of the maximum on the $N(t)$ curve, so that by extrapolation we could find the exact position of the maximum when $l=0$; this cannot be found directly, because there is always some distance between the detector and the neutron-emitting surface. The position of the maximum when $l=0$ determines the moment of "switching on" of the source of thermal neutrons.

Since for water $a=2$ [3, 4], therefore $f(\tau)$ can be written as

$$f(\tau) = \int_0^\tau e^{-\alpha \frac{l}{v_0} \tau - \frac{1}{\tau^2}} \frac{d\tau}{\tau^6}.$$

Thus the equation for v_0 (3) will become

$$\frac{\frac{\alpha l}{v_0} \tau_0 - \frac{1}{\tau_0^2}}{\tau_0^6} = \frac{\alpha l}{v_0} \int_0^{\tau_0} \frac{e^{-\frac{\alpha l}{v_0} \tau - \frac{1}{\tau^2}}}{\tau^6} d\tau. \quad (4)$$

Table 1 gives measured values of t_{max} for various flight distances l and thicknesses h .

The error in l is governed by the inaccuracy of collimation of the neutron flux by the cadmium collimator and by the finite thickness of the detectors.

The last row of this table gives t_{max} for $l=0$, obtained by extrapolation. The relation $t_{\text{max}}=f(l)$ was approximated to by a first-degree polynomial. The calculation was performed by the method of least squares. The error in t_{max} was governed by the channel width of the time analyser ($2 \mu\text{sec}$) and the width of the fast-neutron pulse ($\sim 6 \mu\text{sec}$). Besides the error in t_{max} shown in Table 1, for $l=0$ we allowed for error caused by the fact that the position of the maximum depends on the higher-energy harmonics, whose damping rates are characterized by the thermalization time. The quantity ($4.1 \pm 0.4 \mu\text{sec}$ [4]) was also used in estimating the error in t_{max} when $l=0$. From the value of $t_{\text{max}}(l)$ when $l \neq 0$ we calculated $t_{\text{max}}(0)$ and the result substitution in $\tau_0 = \frac{v_0}{1} [t_{\text{max}}(l) - t_{\text{max}}(0)]$. We then calculated v_0 from (4) by an iteration method. The decay constant α was measured experimentally at the minimum flight distance $l=(3 \pm 1)$ cm. The result was used in the calculations based on (4).

Table 2 gives measured values of v_0 for various values of B^2 . It also gives the corresponding values of kT . In calculating B^2 we made use of the relation between v_0 and the transport length $\bar{\lambda}_{tr}$. The values of $\bar{\lambda}_{tr}$ were calculated [3] from the formula

$$\bar{\lambda}_{tr} = 3\bar{D} \frac{m(a-1)}{v_0 m(a)},$$

where $m(a-1)$ and $m(a)$ are coefficients obtained in averaging λ_{tr} and D over the Maxwell spectrum. The relation between \bar{D} and v_0 was taken from [5]. Table 2 gives the values of $\bar{\lambda}_{tr}$ used in the calculations. The indeterminacy of B^2 arose mainly owing to the uncertainty of $\bar{\lambda}_{tr}$. If the relation between kT and B^2 is approximated by a first-order polynomial, calculation gives the following result:

$$kT(B^2) = [(0.0253 \pm 0.0042) - (0.0065 \pm 0.0089) B^2] \text{eV}. \quad (5)$$

This expression agrees with the results in [1] obtained by the poisoning method; here the relation between kT and B^2 was also given by a first-degree polynomial:

$$kT(B^2) = [(0,0253 \pm 0,0021) - (0,0065 \pm 0,0049) B^2] eV. \quad (6)$$

Comparing (5) and (6), we see that the result of the poisoning method is more accurate. However, a simple calculation reveals that the method described above can yield greater accuracy if we modify the initial time parameters. For this purpose it is necessary that the width of the fast-neutron pulse and the width of the time analyser channel should be much less than the thermalization time, on which the accuracy of v_0 will then mainly depend.

The author would like to thank G. A. Alimov, who collaborated in the preparatory part of the work. He also thanks L. N. Yurova for valuable advice.

LITERATURE CITED

1. E. St. Andrea et al., In: Proc. Second Intern. Conf. Peaceful Uses of Atomic Energy (Geneva 1958): Selected reports of foreign scientists. Vol. 2, Moscow, Atomizdat, p. 518 (1959).
2. E. Starr and J. de V. L. Villers, "Thermalization of Neutrons." Moscow, Atomizdat, [Russian translation], p. 183 (1964).
3. L. N. Yurova, Report No. 356 presented by the USSR to the Third Inter. Conf. Peaceful Uses of Atomic Energy, Geneva (1964).
4. Möller and N. Sjöstrand, Arkiv. Fys. 27, 501 (1964).
5. A. V. Antonov et al., Atomnaya Énergiya, 12, 22 (1962).

DOSE RATE OF γ -RADIATION DUE TO CAPTURE IN WATER

V. M. Mordashev

UDC 539.121.72:539.122

References [1, 2] give graphical tables of calculated dose rates P of γ -radiation due to capture by water of neutrons from a point unidirectional source emitting 1 neutron/sec: they plot the results vs. the neutron energy E , the angle φ between the flight direction of the neutrons and the source-detector line, and the distance r between the source and detector.

Below we give an approximation of these graphical tables in the form of a product of two functions,

$$P(E, \varphi, r) = P_0(E, r) \cdot k(\varphi, r) \quad (1)$$

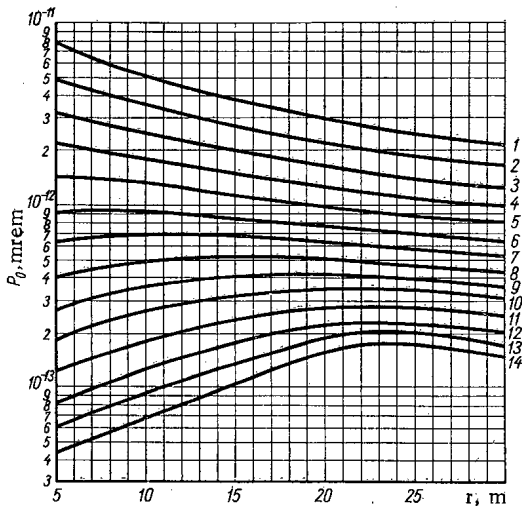


Fig. 1. Graph of function $P_0(E, r)$ for the following values of E in eV: 1) 0.208 - 0.5; 2) 0.5 - 1.18; 3) 1.18 - 2.68; 4) 2.68 - 6.04; 5) 6.04 - 13.6; 6) 13.6 - 29.9; 7) 29.9 - 72.6; 8) 72.6 - 159; 9) 159 - 340; 10) 340 - 706; 11) 708 - 1375; 12) 1375 - 2560; 13) 2560 - 4560; 14) 4590 - 7950.

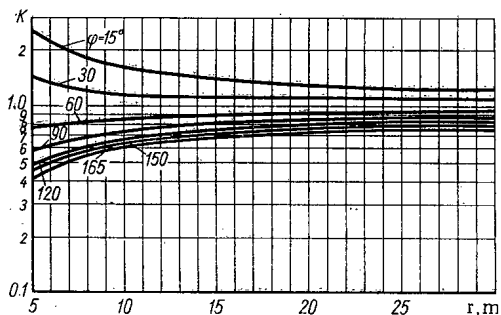


Fig. 2. Graph of function $k(\varphi, r)$.

in the ranges $E=(0.208-7950)$ eV, $\varphi=(15-165)^\circ$, $r=(5-30)$ m. Figures 1 and 2 are the graphs of $P_0(E, r)$ and $k(\varphi, r)$. The relative rms deviations of the values of P given by (1) from the tables in [1, 2] are equal to 9%; the maximum deviation is 30%.

The author wishes to thank A. G. Klimenko for carrying out the calculations.

LITERATURE CITED

1. R. Beissner, Report NARF-61-4T (FZK-9-151). Convair (1961).
2. Biological Shielding of Nuclear Reactors. Handbook. Translated from the English. Moscow, Atomizdat (1964).

Translated from *Atomnaya Énergiya*, Vol. 22, No. 2, p.133, February, 1967. Original letter submitted July 23, 1966.

MEASUREMENT OF REACTOR ABSORPTION CROSS
SECTIONS OF Gd¹⁵⁴ AND Gd¹⁵⁶

E. I. Grishanin, G. M. Kukavadze,
V. I. Lependin, L. Ya. Memelova,
I. G. Morozov, V. V. Orlov, and D. T. Pilipets

UDC 539.17.012

We have measured the reactor absorption cross sections of Gd¹⁵⁴ and also made a more detailed analysis of the absorption cross section of Gd¹⁵⁶; the measurement method was described in [1].

We used samples of gadolinium oxide weighing 10 mg, which were irradiated in the "dry" port of a VVR-M reactor by an integrated neutron flux of $2.8 \cdot 10^{19}$ to $2.7 \cdot 10^{20}$ neutron/sec. The self-shielding effect of the specimens was reduced as far as possible. The integral flux of thermal neutrons was monitored by means of the concentration changes of Li⁶⁰.

The isotopic compositions of the irradiated specimens were analysed with an MI-1311 mass-spectrometer, using GdO⁺ ions. Table 1 gives the results, corrected for the contents of O¹⁷ and O¹⁸.

Table 2 gives the measured equilibrium concentrations and reactor cross sections of Gd¹⁵⁴ and Gd¹⁵⁶. The errors in the measured reactor cross sections of Gd¹⁵⁴ and Gd¹⁵⁶ are due to errors in measuring the equilibrium concentration for given isotopic composition and in the calculated values of the reactor cross sections of Gd¹⁵⁵ and Gd¹⁵⁷.

To confirm that the Gd¹⁵⁵ and Gd¹⁵⁷ concentrations were close to their equilibrium values, we estimated the concentration of "unburnt" primary nuclei of these isotopes in specimens irradiated with the maximum integral neutron flux. In the absence of screening, the concentration of unburnt primary

TABLE 1. Isotopic Compositions of Gadolinium Specimens Subjected to Various Integral Thermal-Neutron Fluxes

Sample	$\int_0^t \Phi(t') dt'$ $\times 10^{-19}$ neutron/cm ²	Isotopic composition of gadolinium, %				
		Gd ¹⁵⁴	Gd ¹⁵⁵	Gd ¹⁵⁶	Gd ¹⁵⁷	Gd ¹⁵⁸
Enriched with Gd ¹⁵⁶	0	0.14 ± 0.02	0.830 ± 0.017	94.86 ± 0.11	2.93 ± 0.06	0.89 ± 0.04
	2.8	0.058 ± 0.003	0.396 ± 0.020	95.39 ± 0.14	0.183 ± 0.004	3.61 ± 0.08
	4.11	0.061 ± 0.003	0.287 ± 0.015	95.60 ± 0.04	0.033 ± 0.004	3.69 ± 0.08
	5.48	0.060 ± 0.001	0.152 ± 0.003	95.44 ± 0.04	0.0142 ± 0.0002	4.01 ± 0.03
	9.14	0.182 ± 0.005	0.040 ± 0.001	95.67 ± 0.10	0.00738 ± 0.00129	3.77 ± 0.08
Enriched with Gd ¹⁵⁴	0	66.2 *	21.7 *	5.7 *	2.3 *	2.3 *
	9.14	66.50 ± 0.22	2.80 ± 0.02	24.49 ± 0.19	—	4.64 ± 0.05
	13.2	66.51 ± 0.19	1.40 ± 0.01	25.75 ± 0.16	—	4.66 ± 0.04
	16.3	66.39 ± 0.61	0.50 ± 0.02	26.92 ± 0.46	—	4.50 ± 0.22
	27.0	65.58 ± 0.12	0.1900 ± 0.0045	27.81 ± 0.010	—	4.77 ± 0.03
Natural gadolinium	0	1.98 ± 0.05	15.03 ± 0.13	20.71 ± 0.11	15.53 ± 0.06	24.84 ± 0.08
	9.14	2.14 ± 0.06	3.29 ± 0.03	31.64 ± 0.43	0.110 ± 0.008	41.01 ± 0.36
	13.2	2.15 ± 0.02	1.99 ± 0.02	33.46 ± 0.19	0.0350 ± 0.0003	40.50 ± 0.14
	16.3	2.21 ± 0.02	0.708 ± 0.005	34.22 ± 0.13	0.0069 ± 0.0012	40.53 ± 0.10
	27.0	2.26 ± 0.02	0.020 ± 0.001	35.19 ± 0.08	0.00261 ± 0.00054	40.53 ± 0.04

*Manufacturers' specifications

Translated from Atomnaya Énergiya, Vol. 22, No. 2, pp. 133-135, February, 1967. Original letter submitted April 8, 1966.

TABLE 2. Measured Values of ρ_5/ρ_4 and ρ_7/ρ_6 , Equilibrium Concentration Ratios, and Reactor Cross Sections of Gd¹⁵⁴ and Gd¹⁵⁶

Sample	ρ_7/ρ_6	ρ_5/ρ_4	σ_6 , barn	σ_4 , barn
Enriched with Gd ¹⁵⁶	$(7.70 \pm 1.30) \cdot 10^{-5}$	—	11.5 ± 2.0	—
Enriched with Gd ¹⁵⁴	—	$(2.80 \pm 0.08) \cdot 10^{-3}$	—	100 ± 5
Natural gadolinium	$(7.42 \pm 1.54) \cdot 10^{-3}$	$(3.5 \pm 0.9) \cdot 10^{-3}$	11.1 ± 2.3	125 ± 32

TABLE 3. Equilibrium Concentrations and Unburnt Primary-Nucleus Concentrations of Gd¹⁵⁵ and Gd¹⁵⁷ in Samples Subjected to Maximum Irradiation

Sample	Equilibrium concentrations		Concentrations of unburnt primary nuclei	
	Gd ¹⁵⁵	Gd ¹⁵⁷	Gd ¹⁵⁵	Gd ¹⁵⁷
Enriched with Gd ¹⁵⁶	—	$(7.37 \pm 1.30) \cdot 10^{-3}$	—	$(1.44 \pm 0.54) \cdot 10^{-5}$
Enriched with Gd ¹⁵⁴	0.183 ± 0.006	—	$(7.0 \pm 1.3) \cdot 10^{-3}$	—
Natural gadolinium	$(8.0 \pm 2.0) \cdot 10^{-3}$	$(2.61 \pm 0.54) \cdot 10^{-3}$	$(12 \pm 3) \cdot 10^{-3}$	$\sim 10^{-12}$

nuclei is given approximately by the exponential law

$$N_7 = N_7^i \exp \left\{ -\sigma_7 \int_{t_i}^T \Phi dt \right\},$$

where N_7 is the concentration of Gd¹⁵⁷ nuclei at time T for a specimen with maximum irradiation, N_7^i is the concentration of unburnt primary Gd¹⁵⁷ nuclei at time t_i . Owing to errors in the determination of the integral neutron flux, the values of N_7 (or N_5) have a certain scatter for specimens with different amounts of irradiation. These values were therefore averaged over three specimens of a single type but with different amounts of irradiation.

Table 3 gives the results obtained for the equilibrium concentrations and the numbers of primary unburnt Gd¹⁵⁵ and Gd¹⁵⁷ nuclei. The errors in the isotopic compositions were taken as equal to the statistical values.

The errors in the measured Gd¹⁵⁵ and Gd¹⁵⁷ concentrations rose rapidly as the concentrations of these isotopes decreased in the irradiated specimens; this was especially due to the corrections for O¹⁷ and O¹⁸, which were present in the specimens in concentrations comparable with those of Gd¹⁵⁵ and greater than those of Gd¹⁵⁷ by a factor of three to four. The isotopic composition of oxygen was taken from [2].

The reactor absorption cross sections of Gd¹⁵⁵ and Gd¹⁵⁷ are mainly due to the presence in the thermal region of resonances whose contribution to the cross sections can be determined within 1% [3]. The spectrum of a reactor in the thermal region is determined by the temperature of the neutron gas, while the error made in measuring this temperature is due to variations in the temperature of the reactor water and to errors of measurement. During irradiation of the specimens, the temperature of the water in the reactor did not vary by more than 10° C around its mean temperature of 60° C. The law of this temperature variation is unknown, and therefore the rms error was represented by the maximum error. Following [4], we took the error in the experimentally measured neutron-gas temperature as $\pm 6^\circ$ C in this case. Allowing for the indeterminacy in the reactor water temperature and in the measured core characteristics, the rms error in the neutron gas temperature was taken as $\pm 15^\circ$ C.

There is agreement, within the experimental error, between the reactor absorption cross sections of Gd¹⁵⁴ and Gd¹⁵⁶ measured for specimens with different isotopic compositions. Further improvement in the measurement accuracy is possible if we carry out experiments on specimens with lower contents of the other rare earths (especially of samarium and praseodymium), which would enable us to work with Gd⁺

ions. This would obviate the necessity for correcting for the oxygen isotopes, and would substantially improve the accuracy of measurement of small Gd^{157} and Gd^{155} concentrations.

The values obtained for the cross sections of Gd^{154} and Gd^{156} enable us to make fairly accurate determinations of the residual poisoning of natural gadolinium when it is used as a self-screened burning-up absorber. The mean value of the isotopic reactor cross section per gadolinium nucleus after burn-up was 15 ± 1 barn, where the absorption cross sections of Gd^{156} and Gd^{154} have been doubled so as to allow for subsequent neutron absorption in the product nuclei Gd^{155} and Gd^{157} .

The authors are grateful to A. A. Belonozhenko, I. M. Gorbach, L. I. Moseev, L. A. Stepanova, and N. G. Uverov for help with the measurements and chemical treatment of the specimens, and to G. I. Toshinskii and V. G. Zolotukhin for discussing the results and for valuable remarks.

LITERATURE CITED

1. E. I. Grishanin et al., *Atomnaya Énergiya*, 19, 459 (1965).
2. A. Nier, *Phys. Rev.*, 77, 789 (1950).
3. H. Moller et al., *Nucl. Sci. and Engng* 8, 183 (1960).
4. K. Burkhart and V. Reichhardt, In: "Thermalization of Neutrons" (Proc. Brookhaven Conf.), Moscow, Atomizdat, [Russian translation], p. 314 (1964).

TURBULENT THERMAL DIFFUSIVITY IN A CURRENT OF
LIQUID WITH HIGH THERMAL CONDUCTIVITY

V. M. Borishanskii and T. V. Zablotskaya

UDC 621.039.517

In the present study, coefficients of turbulent thermal diffusivity a_T were calculated on the basis of earlier measurements made at the TsKTI [1, 2] on temperature fields in currents of molten light and heavy metals. The calculation was carried out according to the formula

$$a_T = \frac{qr_0}{c\gamma \frac{dt}{d\xi}} - a_1, \quad (1)$$

where q is the specific heat flow; r_0 is the radius of the pipe; c , γ , and a_1 are, respectively, the specific thermal capacity, the density, and the thermal diffusivity of the coolant (a_T is the turbulent analogue of a_1); $\xi = r/r_0$ is a dimensionless radius; t is the temperature of the current at a distance r from the axis of the pipe.

The distribution of the heat flow q over the cross section of the pipe was calculated by using the logarithmic profile of the velocities. To calculate the derivative $dt/d\xi$ in formula (1), the measured temperature fields were approximated by means of the formula

$$\theta = \frac{b}{a} \sqrt{a^2 - \xi^2} - c. \quad (2)$$

Here $\theta = \frac{t_{wall} - t}{t^*}$, where $t^* = \frac{q_0}{c\gamma v^*}$, and $v^* = \bar{w} \sqrt{\frac{\xi}{8}}$; \bar{w} is the velocity of the liquid, and ξ is the friction factor, i.e., the coefficient of resistance to flow. The constants a , b , c for each measured profile were determined from experimental data by using the three boundary conditions:

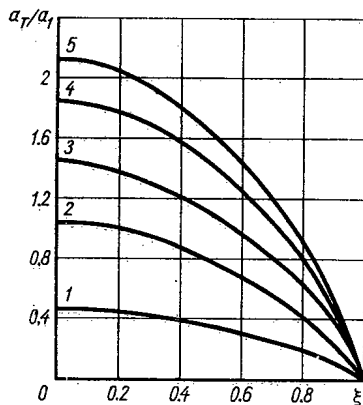


Fig. 1. a_T/a_1 as a function of ξ for various values of Re (Pr = 0.0075): 1) Re = 26,500; 2) Re = 69,200; 3) Re = 91,400; 4) Re = 98,200; 5) Re = 105,500.

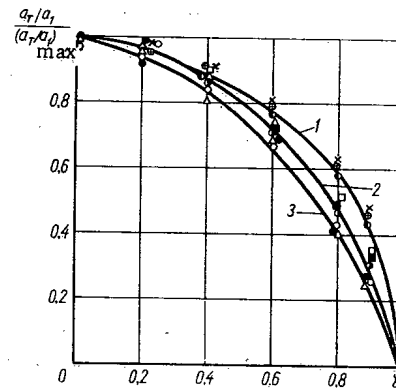


Fig. 2. Graph of $\frac{a_T/a_1}{(a_T/a_1)_{max}} = f(\xi)$:

- 1) Pr = 0.027, (x) Re = 22,200, (⊕) Re = 95,100, (●) Re = 158,000;
2) Pr = 0.022, (□) Re = 46,200, (■) Re = 114,900, (●) Re = 202,000;
3) Pe = 0.0075, (○) Re = 26,500, (Δ) Re = 91,400, (●) Re = 105,000;
—) average curves.

Translated from Atomnaya Énergiya, Vol. 22, No. 2, pp.135-137, February, 1967. Original article submitted July 25, 1966.

$$\left. \begin{aligned} &\theta|_{\xi=0} = \theta_0 \text{ (}\theta_0 \text{ found experimentally); } \theta|_{\xi=1} = 0; \\ &\frac{d\theta}{d\xi} \Big|_{\xi=1} = -\frac{r_0 q_0}{t^* \lambda} \equiv -\frac{Pe}{2} \sqrt{\frac{\xi}{8}} \end{aligned} \right\} \quad (3)$$

The fourth condition, $\frac{d\theta}{d\xi} \Big|_{\xi=0} = 0$, which is required for a more accurate approximation of the measured temperature field, was kept identical for all values of a, b, c.

Substituting the approximation formula (2) into the original Eq. (1), we obtain a calculation formula for computing the turbulent heat transfer coefficient

$$\frac{a_T}{a_1} = \frac{a}{b} Pe \sqrt{\frac{\xi}{8}} \sqrt{\frac{a^2 - \xi^2}{\xi^2}} \int_0^{\xi} \omega \xi d\xi - 1. \quad (4)$$

By using the analytical expression (2) to approximate the experimental data, we were able to avoid the need for graphical differentiation on the temperature fields, which could cause considerable errors that would be difficult to estimate. On the basis of the measured temperature fields, formula (4) can be used for calculating the coefficients of turbulent thermal diffusivity for any value of ξ between 0 and 1. Using the experiments of [1, 2], carried out with three liquids in the Prandtl number range of $0.0075 < Pr < 0.027$, we calculated the relationships $a_T/a_1 = f(\xi, Re)$. The results of the calculations of the coefficients a_T for one coolant are shown in Fig. 1.

Figure 2 shows the values of the turbulent thermal diffusivity coefficients for each coolant in the coordinates $a_T/(a_T)_{max} = f(\xi)$. The experimental data corresponding to different Re values for $Pr = const$

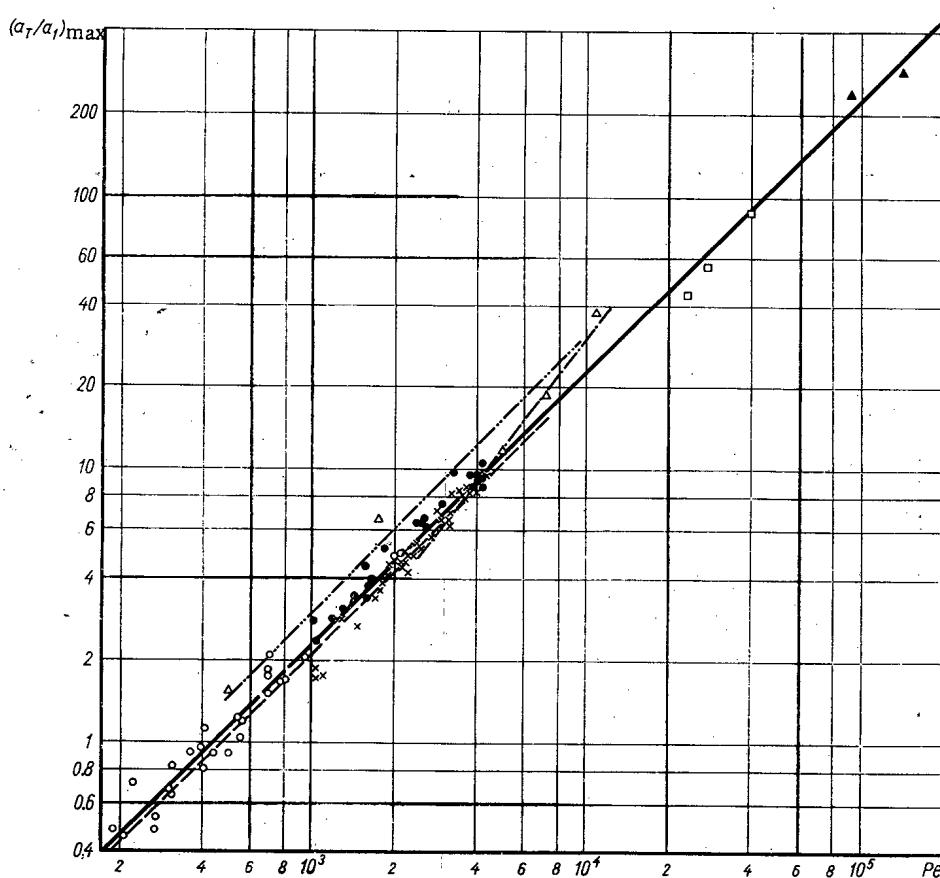


Fig. 3. Graph of $(a_T/a_1)_{max} = f(Pr)$: Δ) data from [3]; \square) $Pr \approx 1$ [4]; \blacktriangle) $Pr = 5$ [1, 2]; \bullet) $Pr = 0.027$ [1, 2]; \times) $Pr = 0.022$ [1, 2]; \circ) $Pr = 0.0075$ [1, 2]. Calculations from empirical formulas: --- $(a_T)_{max} = 2.695 \cdot 10^{-8} Re^{1.29}$ [5]; --- $(a_T/a_1)_{max} = 7.5 \cdot 10^{-5} Re$ [3]; --- $a_T/\nu = 2.04 \cdot 10^{-3} (1 + \xi^2 - 2 \xi^3)$ evaluated at $\xi = 0.25$ [3]; --- $(a_T/a_1)_{max} = 2.2 \cdot 10^{-3}$ (data of present study).

lie close to the same curve. This indicates that there is no functional relationship between $a_T / (a_T)_{\max}$ and Re .

Figure 3 shows the results in the coordinates $(a_T/a_1)_{\max} = f(Pe)$. It also shows the calculated data for water [2] and air [4]. In the last two cases the fields were differentiated graphically. In addition, Fig. 3 shows the result of the calculation for $(a_T/a_1)_{\max}$ according to empirical formulas from [3, 5]. It should be noted that a linear relationship exists between $(a_T/a_1)_{\max}$ and Pe .

The equation of the curve drawn through all the experimental points in Fig. 3 is of the form

$$\left(\frac{a_T}{a_1}\right)_{\max} = 2,2 \cdot 10^{-3} Pe. \quad (5)$$

Formula (5) essentially expresses the law characterizing a well-developed turbulent flow of any liquid. This law may be written in the form

$$\frac{\bar{w}d}{a_T} = Pe_T = \text{const.} \quad (6)$$

Consequently, for values of ξ corresponding to $a_T = (a_T)_{\max}$, turbulent heat transfer will preferentially take place in the current of coolant. For this range of ξ values the situation is correctly described by the Reynolds analogy between heat transfer and momentum for the flow of liquids (including liquid metals) in pipes.

In conclusion, it should be noted that in the original Eq. (1) the mutual influence of the processes of molecular and eddy thermal diffusivity reduced to simple superposition. In the flow of liquids with high thermal conductivity it is apparently possible to have a secondary influence of molecular thermal diffusivity on the value of a_T calculated by formula (1). This may explain the difference between the average curves in Fig. 2 for experiments with liquids having different Prandtl numbers. The maximum difference is observed for $\xi = 0.8$ and amounts to 30%.

The possible influence of the Prandtl number on the value of a_T calculated by formula (1) is noted, for example, in [6]. On the other hand, the authors of [3] found no such relationship. The final solution of this problem, which is of considerable theoretical importance for the development of the theory of heat transfer in turbulent flow, can be found by thorough investigation of the structure of turbulent flow in various liquids.

LITERATURE CITED

1. V. M. Borishanskii, T. V. Zablotskaya, and N. I. Ivashchenko, In: "Convective Heat Transfer in Two-Phase and One-Phase Flows", [in Russian]. Edited by V. M. Borishanskii and I. I. Paleev, M. -L., Énergiya, p. 363 (1964).
2. V. M. Borishanskii et al., *Ibid.*, p. 350.
3. V. I. Subbotin, M. Kh. Ibragimov, and E. V. Nomofilov, *Teploénergetika*, No. 6, 70 (1963); *Atomnaya Énergiya*, 14, 414 (1963); *Teplofiz. Vysok. Temp.* 3, 421 (1965).
4. N. I. Ivashchenko, *Teploénergetika*, No. 2, 72 (1958).
5. S. Isakoff and T. Drew, *Proc. General Disc. Heat Transfer*, London, 405 (1951).
6. L. Yu. Artyukh, L. A. Vulis, and B. P. Ustinenko, *Izv. AN KazSSR, Seriya Énerg.*, No. 2/16, 102 (1959).

CALCULATION OF THE STORED ENERGY IN IRRADIATED GRAPHITE, FROM X-RAY DATA

M. S. Koval'chenko and V. V. Ogorodnikov

UDC 621.039.553:621.039.532.2

The elastic energy associated with the appearance of microstresses in graphite irradiated with doses of up to $5 \cdot 10^{19}$ neutrons/cm² was calculated in [1] by the harmonic analysis of diffuse (110) x-ray diffraction reflections; it was shown that, in order of magnitude, the elastic energy agreed with results obtained by other authors. On annealing, however, the values of elastic energy fell regularly with increasing temperature. Taken together with the results of a detailed study of irradiated graphite described in [2], these results suggest that the stored energy in irradiated graphite is made up of the elastic energy of the microstresses and the potential energy of the static displacements of atoms in the lattice. The first of these quantities is associated with the development of linear defects (chiefly dislocations) and the second with the appearance of point defects; in irradiated materials the latter should play the major part, both in producing changes of properties and in restoring these on thermal annealing [3].

Static displacements, mainly associated with the occurrence of interstitial atoms, lead to a change in lattice parameters [4]. On the basis of an analogy between the expansion of the lattice resulting from the static displacements of the atoms in irradiated materials and the dynamic displacements of the atoms in thermal vibrations, we may estimate the stored energy due to the formation of interstitial atoms. Vacancies have a much smaller effect on the change in lattice parameters, and their influence may therefore be neglected.

The analogy between the static displacements associated with the radiation damage of solids and the dynamic displacements (associated with heating) is supported not only by thermodynamic considerations [5] but also by the fact that, both on heating and on irradiation, the displacement of the atoms leads to an anisotropic expansion of the lattice. In both cases there is a sharp change in the *c* parameter of graphite and a very slight change in the *a* parameter. Hence for calculation purposes we may consider simply the variation in the *c* parameter with temperature, as given by the formula

$$c = c_0 \exp \left(\int_{T_0}^T \alpha_c dT \right), \quad (1)$$

where c_0 is the initial value of parameter *c*, corresponding to temperature T_0 , α_c being the thermal-expansion coefficient along the *c* axis. For a small range of temperature variation $\Delta T = T - T_0$, the change

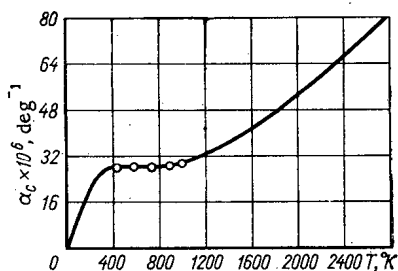


Fig. 1. Temperature dependence of the linear-expansion coefficient of graphite in the *c* direction: ○) experimental data from [8].

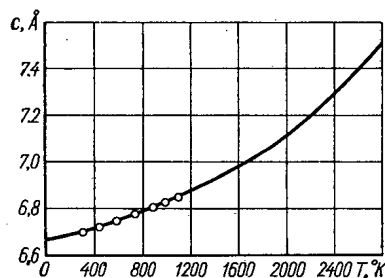


Fig. 2. Temperature dependence of the *c* parameter of graphite: ○) experimental data from [8].

Translated from *Atomnaya Énergiya*, Vol. 22, No. 2, pp. 138-140, February, 1967. Original article submitted May 26, 1966.

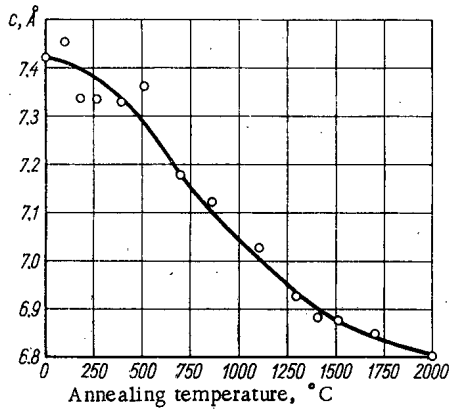


Fig. 3. Variation of the c parameter of irradiated graphite with annealing temperature.

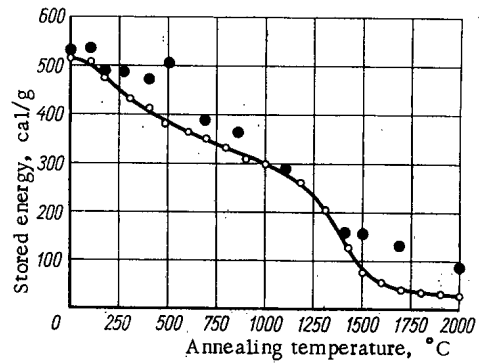


Fig. 4. Variation in the stored energy of irradiated graphite with annealing temperature: ○) experiment ●) calculation.

in the parameter is given by the formula

$$c = c_0 (1 + \alpha \Delta T). \quad (1a)$$

The use of relation (1a) enables us to determine the effective temperature ΔT from the change in the parameter of the irradiated graphite. The energy stored in the form of static displacements of the atoms may be estimated from a formula analogous to that relating to the change in the enthalpy of a body on heating [6]

$$\Delta U = \frac{1}{2} C_P \Delta T, \quad (2)$$

where C_P is the specific heat at constant pressure (in the absence of external stresses in the case considered [7]) and the factor $\frac{1}{2}$ is introduced because only potential energy is under consideration. For larger values of effective temperature it is necessary to consider the temperature dependence of α_c and C_P , when the stored energy may be calculated from the formula

$$\Delta U = \frac{1}{2} \int_{T_0}^T C_P(T) dT. \quad (2a)$$

The lattice parameter c and the stored energy (measured calorimetrically on annealing) vary in similar ways with the annealing temperature of neutron-irradiated graphite [2]. A preliminary estimate of the effective temperature by formula (1a) showed that the change in lattice parameter in [2] corresponded to heating the graphite above the melting point. In order to obtain acceptable values of effective temperature and also correct values of stored energy, we must use expressions (1) and (2a), which allow for the temperature dependence of α_c and C_P .

The thermal expansion of graphite in the temperature range 400 to 1000° K was studied in full detail in [8]. In accordance with the theory developed by Riley in [9] for graphite, the temperature dependence of α_c is described by the equation

$$\alpha_c = LC_{V_x} + MC_{V_z} + NT, \quad (3)$$

where L , M , and N are constants; C_{V_x} and C_{V_z} are the components of the specific heat at constant volume, C_V , respectively relating to the thermal vibrations of atoms perpendicular and parallel to the hexagonal axis of the graphite crystal.

The components of specific heat are expressed in terms of the Debye function

$$D\left(\frac{\theta}{T}\right) = 3 \left(\frac{T}{\theta}\right)^3 \int_0^{\theta/T} \frac{\xi^4 e^{\xi}}{(e^{\xi} - 1)^2} d\xi \quad [10];$$

$$C_{V_x} = 3RD \left(\frac{\theta_x}{T}\right); \quad C_{V_z} = 3RD \left(\frac{\theta_z}{T}\right), \quad (4)$$

where R is the universal gas constant, while $\theta_x = 2280^\circ \text{K}$ and $\theta_z = 760^\circ \text{K}$ are the characteristic temperatures relating to the vibrations of the atoms perpendicular and parallel to the hexagonal axis.

The experimental data of [8], after allowing for the variation of α with temperature [11], agree with calculations based on equation [3] for the following values of the coefficients: $L = -1.640 \cdot 10^{-9} \text{ kg-atom/J}$, $M = 1.314 \cdot 10^{-9} \text{ kg-atom/J}$, $N = 3.090 \cdot 10^{-8} \text{ deg}^{-2}$.

The temperature dependence of α_c is shown in Fig. 1. This enables us to plot the parameter c as a function of heating temperature (Fig. 2) and thus determine the effective temperature for calculating the stored energy associated with static distortions. The irradiation of graphite with a neutron flux of about 10^{21} neutrons/cm² increases the c parameter from 6.70 to 7.45 Å, which corresponds to a temperature rise from 300 to 2650° K, i. e., $\Delta T = 2350^\circ \text{K}$. The mean-square displacement of the atoms in the direction of the hexagonal axis on heating, as calculated from the formula

$$x = \sqrt{\frac{9\hbar^2 T}{Mk\theta_z^2 r_c^2}} \quad (5)$$

(x is the displacement in fractions of $r_c = \frac{1}{2}c$, $\hbar = \frac{h}{2\pi}$ is Planck's constant, M is the mass of the atom, k is Boltzmann's constant) [12], equals $\sqrt{x^2} = 0.8 \text{ \AA}$.

Since the temperature dependence of specific heat is given by the expression $C_p(T) = a + bT + cT^{-2}$, we find that, after integration, expression (2a) takes the form

$$\Delta U = \frac{1}{2} \left[a + \frac{1}{2} b (T_1 + T_0) + \frac{c}{T_1 T_0} \right] \Delta T, \quad (6)$$

where for graphite $a = 17165.88$; $b = 4.27054$; $c = 8792.28 \cdot 10^5$ [11]. For these values of coefficients, the stored energy is expressed in J/kg-mole.

The stored energy calculated in this way is $2.7 \cdot 10^7 \text{ J/kg-mole}$, or 525 cal/g [2]. For calculating the change in the stored energy associated with the annealing of irradiated graphite we use data from the same paper [2] relating to the thermal recovery of the c parameter (Fig. 3). Comparison between theory and experiment (Fig. 4) indicates satisfactory agreement. A certain deviation of the computed values from the experimental results for high annealing temperatures may be due to the fact that at these temperatures annealing of linear as well as point defects takes place, and this introduces another term into the expression for the reduction in stored energy.

LITERATURE CITED

1. A. Austin and R. Harrison, *Phys. Rev.*, **100**, 1225 (1955).
2. W. Woods, L. Bup, and J. Fletcher, In: "Metallurgy of Nuclear Power and the Effects of Irradiation on Materials." *Trans. Inter. Conf. Peaceful Use of Atomic Energy (Geneva, 1955)* [Russian translation], Moscow, Metallurgizdat, p. 563 (1956).
3. Van Bueren, *Defects in Crystals* [Russian translation], Moscow, IL, p. 250 (1962).
4. J. Eshelby, *Continuum Theory of Dislocations* [Russian translation], Moscow, IL, p. 57 (1963).
5. M. A. Matveev, G. M. Matveev, and F. Ya. Kharitonov, *Neorganicheskie Materialy*, **2**, 395 (1966).
6. G. S. Zhdanov, *Solid-State Physics* [in Russian], Moscow, izd. MGU, p. 447 (1964).
7. H. Leibrid, *Microscopic Theory of the Mechanical and Thermal Properties of Crystals* [Russian translation], Moscow-Leningrad, Fizmatgiz, p. 188 (1963).
8. J. Nelson and D. Riley, *Proc. Phys. Soc.*, **57**, 477 (1945).
9. D. Riley, *Proc. Phys. Soc.*, **57**, 486 (1945).
10. Ch'ien Hsueh-sen, *Physical Mechanics* [in Russian], Moscow, Mir, p. 220 (1965).
11. G. V. Samsonov et al., *Physico-Chemical Properties of Elements* [in Russian], Kiev, Naukova Dumka, **236**, 202 (1965).
12. J. Zeiman, *Principles of Solid-State Theory* [Russian translation], Moscow, Mir, p. 82 (1966).

RADON EMANATION FROM URANIFEROUS ORES
AND MINERALS IMMERSSED IN LIQUID

M. I. Prutkina and V. L. Shashkin

UDC 553.495

Radon emanation from solids immersed in a liquid is a process which has been subjected to relatively little study. Emanation from minerals and ores is the same in water and in air, according to data reported by V. I. Spitsyn [1] and I. E. Starik [2], and the effect of moisture observed in some instances is due to the solubility of the uranium-bearing minerals. The same holds for the enhanced liberation of radon when specimens were treated with a blast of moist air in [3]. I. E. Starik and O. S. Melikova [4] have concluded that emanation of powder samples undergoes no change as the moisture is varied. Lower emanation of samples immersed in organic liquid has been reported [1], but no interpretation was ventured.

The authors studied radon emanation in water, alcohol, and kerosene, from pulverized samples of several uraniumiferous minerals and ores.

The sample studied (weighing not more than 5 g) was placed in a bubbler and 10-20 ml liquid were poured over the sample. Radon was allowed to build up for a month in the sealed bubbler. γ -scintillation measurements were then taken [5].

The experiments revealed that the emanation coefficient of monazites in air is 0.17-0.33%, and that it is 10-20% higher in water. The ratio of emanation coefficients in water and air for large pitchblende grains is 1.3, but can be raised to 2.2 by pulverizing the sample with a simultaneous increase in the respective coefficients.

Emanation coefficients increase 1.45-fold and 2.12-fold in air and water respectively as silicate uranium samples sized from -1 mesh to +2.4 mesh are ground to powder.

The table lists emanation coefficients of ore samples ground to 150 mesh. In all instances, the emanation coefficients are higher in water than in air, and the emanation coefficients occupy practically the same intermediate values in alcohol and in kerosene. No appreciable dissolution of radium was observed.

Emanation Coefficients of Ore Samples in Air and in Liquid

Mineralogical makeup	Emanation coefficient, %			
	air	water	kerosene	alcohol
Limestones	14	38	19	18
Carboniferous sandstones	26	41	34	33
Clays, sandstones with organic matter	37	54	35	34
Coaly-clay shales with carbonates and sulfides	16	32	23	22
Aluminosilicates with carbonates	13	29	22	20
Ferruginated albitites	9	26	15	16
Quartz sulfide ore	20	24	28	26
Aluminosilicates	31	60	42	40
Clays with sandstones	32	48	38	40

Translated from Atomnaya Énergiya, Vol. 22, No. 2, pp. 140-141, February, 1967. Original article submitted June 24, 1966.

Other experiments demonstrated that moisture increases up to 5% or higher raise the emanation coefficient in air to values practically equal to the emanation coefficients in water, while 5-15% changes in moisture have no affect on the emanation coefficient. If the samples are heavily moistened and then dried at 105° C, the emanation coefficient typical of a dry sample will be restored.

A blast of moist air causes samples to release additional radon [3]. This effect was confirmed by the authors through V. I. Baranov's experiment on minerals sparingly soluble in water. This proves that the effect observed cannot be due to dissolution of the minerals.

Note also a transitional effect involving additional radon release when water acts on a dry de-emanated sample. If a powder sample carefully blown in a bubbler is immersed in water, an additional amount of radon emanates from the sample, and this amount may be anywhere from 5% to 23% of the amount of radon bound in the dry sample, depending on the type of ore. Radon emanation in response to water poured on the sample rises exponentially with a half-life of 30-45 min. Additional radon emanation is independent of whether or not the sample is blown with air during the experiment. This effect is observed only in relation to water. Analogous experiments on kerosene demonstrated no additional radon release.

Note that radon emanation in response to water acting on an ore sample can be a source of error in the determination of the emanation coefficient in water. When the buildup time is short, the additional amount of radon emanated will be taken as the amount accumulated during the time leading to a higher emanation coefficient.

Phenomena associated with emanation in a liquid are indicative of the significant role played in emanation by surface processes. In a dry sample, part of the radon appears to be sorbed on the capillary walls. The radon is desorbed in response to water which wets the surface of the capillaries and penetrates into the pores. This is due to additional radon release as the moist air blows by, and to the action of the water. If the sample is left for a protracted time in water, the water will fill up the capillaries and thereby reduce the possibility of newly formed radon becoming adsorbed.

The different effects of water, alcohol, and kerosene appear to be due to the different degrees to which these liquids succeed in wetting the surface of the minerals.

The effect of moisture on emanation in ores and minerals should be taken into account in measuring the radioactivity of ore and mineral samples.

LITERATURE CITED

1. V. I. Spitsyn, Radium research papers, Vol. II, [in Russian], Moscow, USSR Academy of Sciences press, p. 264 (1926).
2. I. E. Starik, Radioactive Techniques in Geological Dating, [in Russian], Moscow, GONTI press (1938).
3. V. I. Baranov and A. P. Novitskaya, Radiokhimiya, 2, No. 4, 485 (1960).
4. I. E. Starik and O. S. Melikova, Trudy RIAN, [Proc. Radium Inst. USSR Academy of Sciences], 5, No. 2, 184 (1957).
5. V. L. Shashkin, Methods in the Analysis of Natural Radioactive Elements, [in Russian], Moscow, State Atom press (1961).

VI INTERNATIONAL CONFERENCE ON NUCLEAR PHOTOGRAPHY

N. A. Perfilov

The VI International Conference on Nuclear Photography was held in Florence, July 19 through July 23. Tutorial review papers and original research reports were heard and discussed. About 120 delegates representing 20 countries were in attendance at the conference.

The following major topics were discussed: 1) properties of nuclear emulsions; 2) automated measurements of particle tracks in nuclear emulsions; 3) applications of the nuclear emulsions method; 4) development and applications of solid-state dielectric charged particle detectors. Here we review briefly the contributions on these topics.

1. A review paper by P. Cuer (Strasbourg, France) was devoted to research on the latent image obtained when photographic emulsion layers are bombarded by different particles. The reporter stressed the importance of studying the nature of the latent image, the topography, the dimensions of the development centers, and other factors, in order to produce improved emulsions (improved sensitivity and discrimination), and gave an account of work accomplished in this direction at the Strasbourg nuclear center. This work includes: 1) the study of the surface structure of AgBr grains with the electron microscope; 2) inspection and analysis of developed particle stars with the aid of the electron microscope, so that events occurring closely in time can be separated, for example in the study of decay of hypernuclei; 3) the use of AgCl single crystals as particle detectors.

Cuer also reported on some basic results obtained in laboratories in other countries, particularly at the Institute of Atomic Physics (Bucharest, Rumania) on the effect of a pulsed electric field on latent images created by α -particles, protons, and electrons. He mentioned the work done at the V. G. Khlopin Radium Institute of the USSR Academy of Sciences (Leningrad): determination of the efficiency, radiolytic yields, topography, size of development centers in relation to the nature of the particles and the magnitude of specific losses; study of AgBr single-crystal distribution in sensitivity, changes in emulsion sensitivity at low temperatures. These results were reported in detail by the authors during the discussion.

New methods in the preparation of nuclear emulsions were covered in a review report by E. Meuser (West Germany). The bulk of his report was devoted to joint efforts by two leading firms, Agfa of West Germany and Gevaert of Belgium, on the study of the physicochemical processes underlying the mechanism of silver bromide microcrystal formation. The report also covered the work by J. Markocki and W. Romer (Poland) on synthesis of a uniform high-speed emulsion based on the Lipmann emulsion. The nature of emulsion sensitivity was discussed in relation to the structure of the AgBr microcrystals.

A report on experiments studying replacement of gelatine by synthetic polymers in photographic emulsion layers, resulting in emulsion layers with new properties (permanence in vacuum, fast development, etc.), now being conducted at the V. G. Khlopin Radium Institute stimulated deep interest.

K. S. Bogomolov (NIKFI [Motion Picture and Photography Sci. Res. Inst.], USSR) reviewed the state of the art in processing of nuclear emulsions. He gave an account of recent work on improving photographic processing of emulsion layers with the object of improving photographic properties, uniform development in depth, and minimizing regression of charged particle tracks, as well as methods of electrolytic development and the use of ultrasonic vibrations to speed up processing (developing and fixing steps).

A review paper by G. B. Zhdanov (Lebedev Institute of Physics) on nuclear emulsions in high-strength magnetic fields shed light on two major areas of application of emulsions in strong magnetic fields (200 kG and higher): a) measurement of the magnetic moments of hyperons and study of muon polarization; b) study of nuclear interactions of fairly high energies (~ 20 GeV and higher).

Translated from Atomnaya Énergiya, Vol. 22, No. 2, pp. 142-144, February, 1967.

A paper by R. Schmitt (Strasbourg, France) gave an account of experiments on the analysis of nuclear disintegration tracks in photographic emulsion layers by means of an electron microscope. Thin slices (on the order of 10 microns thick) were prepared from emulsion layer containing the object under study, and investigations were conducted on development of the emulsion layers to obtain a sufficiently compact grain without enlarging grain size too much as a result of the development. Only under this condition will electron microscope inspection of the specimen yield additional information on the event recorded in the emulsion layer beyond that obtainable with an optical microscope.

2. The author of a review paper on this problem, B. Stiller (Washington, USA), discussed the underlying principles in the design of devices for automating measurements of particle tracks in nuclear photographic emulsions. In the view of the reporter, all work on automation in nuclear photography could be divided under two headings: 1) automation of geometrical measurements; 2) the search for necessary events (stars, tracks in a given direction) or counts of the number of specified events in a given emulsion volume.

Reviewing automation of geometrical measurements, the reporter gave an account of the instruments used by V. Barkas and associates at the University of California. Their arrangements make use of the digital-travel and "Brover" microscopes. Rotating encoders mounted on the x- and y-axes of the microscope stage, and recording devices, transfer measurement data to punched cards for subsequent processing on an IBM-650 computer. This arrangement can be used to solve any of ten or so problems (measuring energy-range relationships for heavy ions, measurement of pion and proton ranges, etc.).

The more complicated system has been proposed by A. E. Voronkov, G. E. Belovitskii and colleagues (P. N. Lebedev Institute of Physics, USSR Academy of Sciences, Moscow). Their arrangement features a signal-to-digital converter working on all three axes. The microscope stage is moved automatically. A handle controlling microscope stage advance speed is used by the operator to follow the particle track and compute coordinates. The authors used the arrangement to measure the energy spectrum of scattered 14 MeV neutrons.

An arrangement devised by the P. Benjamin et al. group (Aldermaston, Britain) features rotating encoders on all three axes of the microscope. Signals from the encoders are supplied to a visual data reproducer and to punched cards for subsequent IBM computer processing. Each coordinate is measured to within 0.1 micron. The sweep rate covered 100 to 150 tracks an hour in experiments on fission neutron energy spectra.

Another solution has been suggested by a CERN team. They employed a Leitz Ortholux microscope with a specially fabricated object stage. Linear optically magnifying encoders are aligned with the three axes. Coordinates are printed and recorded on punched tape, and can be displayed visually. Each coordinate is determined to within 2.5 microns. The prototype of this system has been in operation for about a year. A similar arrangement was used by the reporter to process stacks of nuclear emulsions on board the Gemini spaceship. Scientists were confronted with the problem of separating out a large number of background tracks due to trapped particles from the comparatively small number of tracks due to primary heavy nuclides. This required automatic recording of coordinates during the sweep and analysis by a computing device.

A second group of papers on discrimination and counts of a specific type of tracks was discussed in connection with concrete problems.

3. Applications of the nuclear photographic emulsion method were discussed in four review papers delivered by known specialists. N. Hertz (Switzerland) reported on applications of nuclear emulsions in high energy physics research at CERN. He made a summary comparison of the photographic emulsion method and rival techniques, and noted that reliance on a variety of techniques is advantageous in many lines of research, and that the use of pulsed magnetic fields and of emulsions loaded with the elements under study is profitable. The reporter announced that an arrangement is being built at CERN which generates a pulsed 300 kG magnetic field. 99% copper and 1% chromium alloy is used in the pulse coil.

M. Shapiro (Washington, USA) discussed several problems solved with the aid of nuclear photographic emulsions, in a report on applications of photographic emulsions in cosmic ray research. These problems include the study of the energy spectrum of light nuclei in cosmic radiation, the azimuthal variation of light nuclides, the isotopic makeup of hydrogen and helium, information on which is vital to the study of the origin of cosmic rays.

V. Barkas (Riverside, USA) attempted, in a review paper entitled "Possible role of emulsions as detectors in future high-energy accelerator experiments," to outline the scope of problems which might be solved in the future by this method.

M. Stevenson (Berkeley, USA) briefly discussed experiments by the Alvarez group which is now studying interactions between cosmic rays ($E > 10^{11}$ eV) and balloon-borne equipment at heights above 30 km. The experiment involves the use of a voluminous liquid hydrogen target, a combination of rows of photographic emulsions and spark chambers in the field of a superconducting magnet. The spark chambers are triggered by Cherenkov counters which react to high-energy particles.

During the discussion, R. Fitch (USA) reported on some photographic emulsion research in oriented re-entry satellite experiments, and on temporal variations of proton intensity in the inner radiation belts from August 1961 through September 1965. D. Lord (USA) reported on an emulsion spectrograph designed for studying interaction of high-energy particles, and capable of measuring momenta to 300 GeV/c.

4. A review paper on this subject was presented by R. Walker (USA), one of the authors of a new particle recording technique. The most important findings were obtained by Walker and colleagues using cellulose nitrate to detect particles. Walker reported measurement of pile neutron flux at exposures lasting as long as 104 hours, using glass detectors and calibrated uranium preparations. This method offers significant advantages over more involved and laborious radiometric techniques for measuring neutron flux.

A review paper by M. Debovet (Strasbourg, France) compared nuclear photographic emulsions and organic polymers used to record charged particles.

We can infer from the papers and reports presented at the conference, and from the ensuing discussion, that the method of photographic emulsions occupies a prominent place alongside other techniques currently in use in nuclear physics, cosmic radiation, and elementary process research (spark chambers and bubble chambers, solid state detectors). Some experiments involve combined use of nuclear emulsions and rival techniques.

The nuclear emulsion technique is by no means limited to physics problems. It is also employed with success by biologists studying the effect of radioactive radiations on living cells, by geologists studying the distribution of radioactive elements in minerals, and in several other fields as well.

Investigations must be continued to improve photographic emulsions, to improve their ability to discriminate between different particles, and to improve their stability to high vacuum and low temperatures. We also have to seek out and develop methods capable of extracting more information from the events recorded in the emulsion layers (use of an electron microscope for inspection, study of the effect of an electric field on latent images, etc.). Attention must be given to the task of devising improved devices for inspecting and measuring particle tracks in emulsion layers with a built-in option for transfer of source information to a computer for processing. The use of pulsed magnetic fields on the order of 3000 kG or higher is important for higher precision in energy measurements and for determining the nature of particles.

Solid-state detectors (glass, plastics, AgCl crystals) are now being used, along with photographic emulsions, to record charged particles. These two techniques successfully complement one another in those experiments where not only light particles but high-energy multiply charged ions (fission fragments) are to be recorded. Intensified research is called for to seek out new materials (among the plastics) for recording charged particles and for charge discrimination and energy discrimination.

ENGINEERING COST FACTORS AND OUTLOOK FOR THE
USE OF FIELD RADIOMETRIC MOISTURE GAGES AND SOIL
DENSITY GAGES IN CROP LAND IMPROVEMENT

V. A. Emel'yanov and V. I. Sinitsyn

A sweeping program of land and soil improvement was projected in the program of the Communist Party of the Soviet Union and in the resolutions of the May Plenum of the CPSU Central Committee. The program and resolutions cover the next few years of agricultural work. The basic problem in land and soil improvement is one of achieving a proper salt regime in arid zones and water regime in the root habitant layer of the soil, so as to guarantee top harvests of cultivable crops. But the required water and salt regimes depend on the density of soils, since density affects porosity and moisture variations. This explains the need for mass determinations to obtain density and moisture values for soils. The thermo-gravimetric and weight-by-volume methods developed at the close of the past century for this purpose are very laborious, inefficient, and do not yield reproducible results. Furthermore, the errors in these methods are quite large and very difficult to discern. Many new techniques for determining moisture and density of ground and soils based on the use of a variety of physical and chemical principles have been proposed and tested in recent years. We could mention, e.g.: nuclear magnetic resonance, ultrasonics, interaction between nuclear radiations and ground samples, etc.

But the most suitable of all the new methods are neutron and γ -ray methods [1] which render measurements of absolute moisture and density of soils possible with ease and rapidity, no matter what the moisture, density, or granulometric makeup of the soils. These methods have provided a basis for the design of field deep-hole neutron NIV-1 moisture gages [2], deep-hole and surface γ - γ density gages, GGP-1 and PGP-1 [3, 4], available from the All-Union Izotop organization. The NVU surface-and-depth neutron moisture gage, experimental samples of which have been run through successful production tests, is being prepared for quantity manufacture. These moisture gages and soil density gages are intended primarily for land improvement research.

The All-Union Research Institute for Hydraulics and Land Improvement (VNIIGiM) has developed a scintillation γ -scopic density gage for precision measurements of the density of soils and ground types in horizontal layers about 5 cm thick down to depths of 1.5 - 2 m and with boreholes spaced 30-40 cm apart. Gamma-ray emitter and detector units are designed so they can be coupled together to form a probe for a scintillation γ - γ density gage. The probe of a scintillation neutron moisture gage can then be joined to the density gage. This allows for measurements using γ -scopic, neutron-neutron, or γ - γ techniques, depending on the purpose in mind and on the specific conditions encountered in the work.

TABLE 1. RMS Errors in Soil Moisture Measurements (abs%) and Soil Density Measurements (g/cm^3) with the NIV-1, GGP-1, PGP-1 gages

Type of error	NIV-1		GGP-1	PGP-1
	Range of measurements			
	2-30%	30-40%	$1.0\text{-}2.2\text{ g}/\text{cm}^3$	$1.0\text{-}2.3\text{ g}/\text{cm}^3$
Error in unit measurement	± 1.1	$+2.1$	± 0.043	± 0.041
Including components corresponding to:				
errors in count rate measurements	± 0.42	± 1.42	± 0.013	± 0.013
calibration errors	± 0.50	± 0.70	± 0.014	± 0.012
effect of changes in chemical composition, in weight by volume of solids, in air gaps	± 0.18	None det.	—	—
effect of changes in chemical composition, moisture, and air gaps	—	—	± 0.016	± 0.016

Translated from Atomnaya Énergiya, Vol. 22, No. 2, pp. 144-146, February, 1967.

TABLE 2. Engineering Cost Factors in Mass Measurements of Soil Moisture and Density under Natural Conditions*

Method of measurement	Cost of one soil moisture and density measurement (with porosity calculation), rubles		Time spent in one soil moisture and density measurement (with porosity calculation), man-days	
	boreholds to 25 mm in depth †	in boreholds and natural outcrops	boreholds to 25 mm in depth †	in boreholds and natural outcrops
Measurements by technical means based on use of the thermogravimetric and volume-weight methods with assay of monoliths and delivery of monoliths to non-portable laboratories ‡	3.93	4.11	1.76	1.63
Same, based on field-laboratory samples	2.35	0.71	1.13	0.24
Measurements taken with neutron moisture gages, surface and deep-hole γ - γ density gages	0.25	0.36	0.043	0.10

* Table compiled on basis of data reported by V.I. Osipov.

† Borehole sinking costs and sinking time not counted.

‡ Time required to transport monolith samples to laboratories not counted.

This institute has also developed a neutron density gage and a γ - γ soil density gage for monitoring moisture and density of alluvial soils to depths of 2-3 m during the alluviation process. The probes for these instruments are hollow dural tubes tapered on bottom and housing both emitters and detectors. The detector in the density gage probe is made up of three STS-5 particle counters, while the probe in the moisture gage is made up of three STS-5 cadmium-shielded counters (to measure moisture levels below 40%) and a STS-6 counter with a cylindrical movable silver activation indicator (for measuring moisture levels from 40-100%). The probes are tamped down to a preset level in the soil. These devices will soon be in regular production.

Errors affecting the performance of neutron moisture gages and γ - γ density gages depend on a lot of different factors, and in the first instance depend on statistical and instrumental errors.

Widespread comparative measurements of soil moisture and density by radiometric, thermogravimetric, and weight-by-volume methods have been carried out in different climatic zones throughout the country. Moisture was measured over a range from 2 to 45%, and density was measured over a range from 1.0 to 2.3 g/cm³. These comparative measurements showed that: 1) discrepancies of over ± 1 abs % in moisture measurements amounted to only 20%, and discrepancies of over ± 2 abs % amounted to only 7%; 2) discrepancies of over ± 0.02 g/cm³ in density measurements amounted to 56%, while discrepancies of over ± 0.05 g/cm³ amounted to only 16%, and discrepancies of over ± 0.08 g/cm³ amounted to only 5%; 3) in measurements of soil moisture and density, the number of positive and negative deviations was almost identical, and we found no effect of the granulometric composition of the soils on the final results. In evaluating these discrepancies, we have to bear in mind the errors inherent in the thermogravimetric and weight-volume methods, which are commensurate with the errors incurred in the use of radiometric soil moisture gages and density gages. Maximum absolute error was not established in general for the thermogravimetric or weight-volume methods.

V. I. Osipov (Moscow State University) and L. I. Beskin (VNIIGiM) carried out a special mathematical treatment of the results of 60 comparative moisture measurements and 93 soil density measurements under natural conditions, utilizing data from 20 precision measurements of soil moisture and density where values were known by other means. This treatment revealed the root mean square errors in the unit measurements made with radiometric moisture gages and density gages, and to separate out the components of these errors to locate major sources of error (Table 1).

A comparison of errors in unit measurements made with the NIV-1 soil moisture gage and errors in the thermogravimetric method, when determinations were repeated 10-30 times, showed that NIV-1 errors are not greater than the errors in the thermogravimetric method, which can now be regarded as a standard method. Rms errors of unit density measurements by the volume-weight method, carried out by highly trained operators, were ± 0.05 g/cm³, which is in excess of the rms errors in measurements taken with GGP-1 and PGP-1 soil density gages (see Table 1). The volume-weight method can also be utilized as a standard reference method.

Mass measurements of soil moisture and density by means of radiometric moisture gages and density gages can be of advantage in greatly reducing losses in time, labor, and cost (Table 2).

The cost of mass measurements of soil moisture and humidity was cut 10-fold, and time losses were cut from 4 to 8 times, in land improvement field research using borehole radiometric soil moisture gages and density gages to depths of 1.5-2.0 m, according to Giprovodkhoz production test data.

The Central Asian Irrigation Research Institute carried out 5250 measurements of soil moisture, using a NIV-1 soil moisture gage, in hydrogeological surveys of the Kel'te-Sai river basin, and of these 255 were comparative measurements conducted simultaneously with the NIV-1 and by thermogravimetric means. Discrepancies greater than 5% in relative errors of soil moisture measurements were encountered in only 11 cases.

During the 1963-1966 period, a VNIIGiM expedition operating on the Barren Steppe utilized a NIV-1 gage. The problem was to investigate a seepage flow from a channel, the gradual change in the moisture profile around the channel, to fix the point where the filtration profile joins with the groundwater level, and to gather information on the subsequent interaction between the seepage flow and groundwater flow (underground water was flowing at a depth of 20 meters at the start of the investigations). It was impossible to solve this problem by the thermogravimetric method. The NIV-1 soil moisture gage was employed in daily measurements of soil moisture at all required depths, i. e., "snapshots" of the moisture profile were taken. About 5000 measurements were taken in 1963, yielding material sufficient to plot the soil moistening network around two channels with water seeping from them. This led to solution of a problem which had resisted efforts of investigators for several decades.

The Volga-Akhtuba expedition of the Moscow Hydrology and Land Improvement Institute initiated a study, in 1964, of moisture changes on irrigated lands down to 30-m depths, with special emphasis on the distribution of irrigation water. A NIV-1 gage was used in this work. The results of systematic soil moisture measurements have uncovered an impressive array of new factors of crucial importance for arriving at practical recommendations on flooding and irrigation conditions and techniques.

The All-Union Hydraulics and Land Improvement Research Institute monitored the density and moisture of alluvial soils at the Khauzkhan dam, at the high-head guard dams of the Voskresenskoe ore processing combine, and at the dam of the Cherepet hydroelectric power plant, by means of radiometric density gages and moisture gages. Errors in density measurements did not exceed $\pm 0.04 \text{ g/cm}^3$, and errors in moisture measurements did not exceed $\pm 1.5 \text{ abs}\%$, and this is several times lower than the errors associated with the volume-weight and thermogravimetric methods. The results provided a basis for recommendations on raising labor productivity during the alluviation.

The NIV-1 moisture gage and the GGP-1 and PGP-1 density gages have been employed successfully in research practice and at the Kazakh Water Management Research Institute, at zone experimental land reclamation stations in the Zavolzh'e region (territory to the east of the Volga) and on the Meshchera, and also by many other organizations.

The practice of using field radiometric moisture gages and soil density gages in our country, plus foreign experience in performing radiometric measurements of soil density and moisture, have provided convincing evidence to the effect that radiometric soil density gages and moisture gages are not only competitive with thermogravimetric moisture gages and volume-weight density gages in land improvement studies and measurements of moisture by mass, but also provide indisputable economic advantages.

LITERATURE CITED

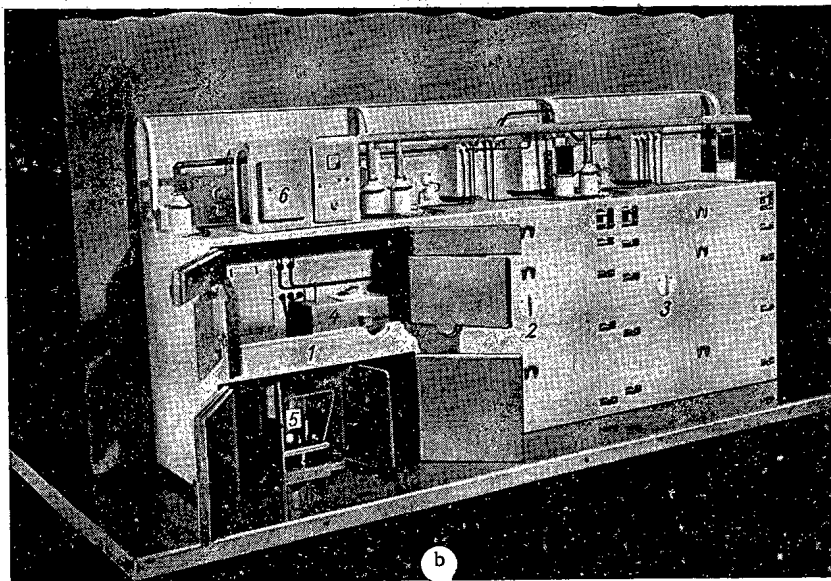
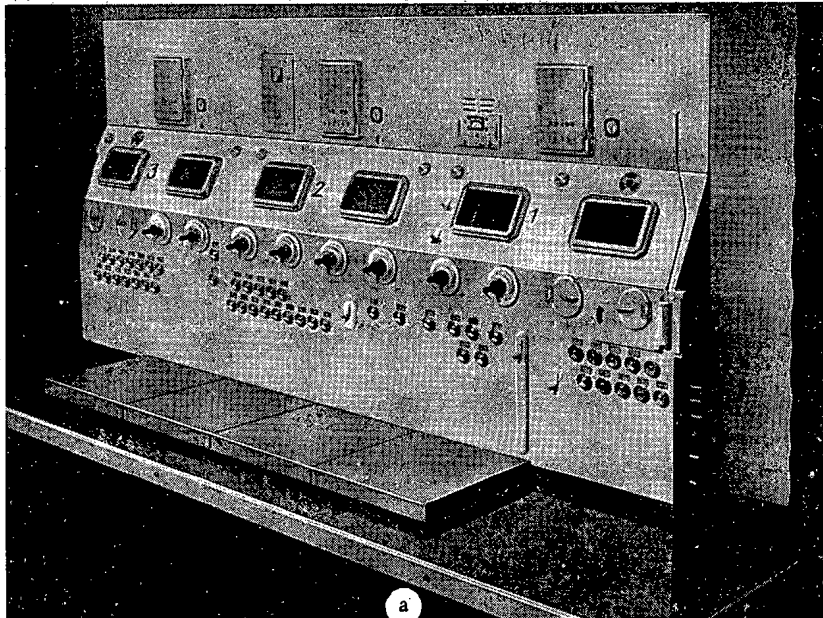
1. V. A. Emel'yanov, Gamma Rays and Neutrons in Field Soil Improvement Research, [in Russian], Moscow, State atom press, (1962).
2. Gidrotekhnika i melioratsiya, No. 9, 34 (1964).
3. Gidrotekhnika i melioratsiya, No. 1, 17 (1965).
4. Izotopy v SSSR, No. 1, 33 (1965).

TRAIN OF GLOVE BOXES FOR HANDLING γ -ACTIVE MATERIALS

G. I. Lukishov, K. D. Rodionov, and G. U. Shcherbenok

The TsBShch TsBSh-1 glove box train, differing from the TsBP-1* glove box line in its ability to continuously handle γ -ray emitters with a maximum Co^{60} activity of 5.4 g-eq of radium over a 6-h period, has been developed for nuclear facilities.

* For information on this line, see: *Atomnaya Énergiya*, 19, 486 (1965).



TsBSh-1 train of glove boxes: a) front view; b) rear view. 1) transfer box; 2) packing and crating box; 3) weighing box; 4) carrier; 5) transfer unit; 6) attachment for heatsealing PVC casings.

Translated from *Atomnaya Énergiya*, Vol. 22, No. 2, pp. 146-147, February, 1967.

The TsBSh-1 line of glove boxes (see photograph) is a modular assembly consisting of three glove boxes; 1) one box for receiving and removing preparations, 2) a second box for packing and crating, and 3) a third box for weighing. Each glove box spans two work stations.

The controls, display and readout instruments, and control boards are located on the front panels of the boxes. Access to the boxes is through a maintenance zone via doors and assembly handholes. The thickness of the shielding plates on the front face is 100 mm, and the thickness on the back of the box is 80 mm, 30 mm on the walls between adjacent boxes (for a total of 60 mm), 85 mm on the end faces, and 55 mm on top.

Work is performed in the glove boxes under an air rarefaction of not less than 20 mm H₂O. Intake air and exhaust air are purified in passage through V-0.4 type filters using FPP-15 fabric. Luminescent ceiling luminaires giving 1=0 W and illuminating the work position with 300 lx at tabletop level are installed at each work position. The work can be observed and monitored through OPM-100 type shielded viewing windows.

Process piping and collectors are installed beneath the glove box tabletop: cold and hot running water, a special detergent, compressed air, domestic gas, vacuum, and waste drain lines run to the glove boxes. All these lines are provided with valves and shutoff cocks controlled in the service room.

The transfer box has two working compartments. The right-hand compartment acts as a transfer chamber and air lock, and is designed to receive clean glassware and hardware from the service room, as well as tools, reagents, and so forth. The compartment has a loading handhole and a glove set. The left-hand compartment allows radioactive materials entry and exit. On the maintenance zone side there is a receiving unit with a carrier accommodating containers, sample removers, and a lift mechanism. The compartments are separated by a removable baffle with pressure-tight doors. A Kaktus type micro-roentgenmeter is used in combination with a DIG-5 chamber to measure the γ emission level of original and finished products; this arrangement is also used to measure γ emission from samples placed in the receiving compartment. The receiving compartment is equipped with through-wall manipulators and a hoist mechanism capable of lifting 10 kg.

The packing and crating glove box is equipped with a liquid metering device of 20 cm³ volume, a can lid opener, and miscellaneous accessories, for sealing and cutting vials, and for crimping containers. The work positions of the glove box use through-wall manipulators.

Solid products are packed in the weighing box. This box is provided with OVM-100 scales and a wire cutter which cuts wire stock into measured lengths. The scales handle 100 g, and measure to within 0.1 mg.

Objects are transferred from one glove box to the next via a horizontal carrier, a pressure-tight box 300 mm \times 300 mm running along the rear faces of the boxes. A dolly with a movable platform with 20 kg load-carrying capacity moves on this box. This vehicle is manually operated, with a cable system which provides mechanical and visual indications of the vehicle position.

CHEMICAL USES OF NUCLEAR REACTORS AND PARTICLE ACCELERATORS IN THE USA

B. G. Dzantiev, A. K. Pikaev

The 151st annual meeting of the American Chemical Society took place in March-April, 1966 (Pittsburgh, Pa., Mar. 22-31), and in this period a symposium on hot-atom chemistry was also held in the USA (Purdue University, Lafayette, Ind., April 1-2). Soviet specialists in nuclear chemistry and radiation chemistry were in attendance at these conferences, and had the opportunity to visit research centers, research institutes, and laboratories maintained by private concerns.

Work involving nuclear reactors is being pursued in many chemical laboratories. This includes research in hot-atom chemistry, chemonuclear synthesis, neutron diffraction analysis and activation analysis, and production of radioactive isotopes.

The USA has a rather broad program underway to probe the possible use of fission fragment energy in chemical synthesis. Chemonuclear synthesis research is being carried on at governmental research institutes, laboratories of universities, and at research centers of industrial corporations. The Harteck laboratory at the Rensselaer Polytechnic Institute, where Harteck and Dondes performed the first experiments on chemonuclear synthesis of nitrogen oxides a decade ago, can be considered the central point of this research trend. The laboratory is presently continuing in research on radiation synthesis and on decomposition of nitrogen oxides, on the kinetics and underlying mechanisms of reactions involving nitrogen and oxygen atoms. Photochemical techniques are widely exploited in theoretical research. Serious attention is being given to radiolysis of carbon monoxide, carbon dioxide, and mixtures of these oxides and nitrogen. Radiolysis of CO_2 to $\text{CO} + \text{O}_2$ is fairly efficient ($G \approx 10$) when fission fragments can be relied upon to increase pressures and when slight amounts of NO_2 are present. Catalytic combustion of carbon monoxide ($Q = 68 \text{ kcal/mole}$) opens up some basically new and interesting possibilities in devising an energy cycle. Radiolysis of CO leads to the formation of a suboxide, and eventually to a water-soluble polymer which on dissolution yields valuable oxygenous products, malonic acid for one. The effect of fission fragments on a mixture of carbon monoxide and nitrogen is effective binding of the latter with the formation of a nitrogenous polymer product ($\sim 20\%$ nitrogen). Harteck and Dondes are continuing to develop recipes and improvements for a glass fiber matrix disperse nuclear fuel; they have produced heat-resistant (to 1000°C) and radiation-stable specimens (capable of withstanding pile irradiation over a year) with high U^{235} content (to $50\% \text{ U}_3\text{O}_8$). The laboratory has also succeeded in developing methods for purification of chemonuclear vapor-phase synthesis products to get rid of fission-fragment activity.

Steenberg and Sutherland have been engaged in research at BNL on chemonuclear synthesis of hydrazine in the vapor phase from ammonia, and are developing special equipment for the purpose and metal foil chemonuclear fuel. Kusack, Jaffey, Carpenter, Miller, and Kahn on the staff of the Aerojet-General Nucleonics research center in California have devised a vapor-phase chemonuclear pilot loop (15 kW), and a series of experiments on production of hydrazine from liquid ammonia through the use of dust fuel has been set up at the Idaho materials testing reactor. This team is studying the possible production of bound nitrogen in fission-fragment radiolysis of N_2 - CO mixtures, as well as some other processes. Process efficiencies are being calculated and tests are being run on disperse chemonuclear fuel. The dose dependence of G and other factors in vapor-phase radiation synthesis of hydrazine exposed to fission fragments are being studied by White at Illinois Polytechnic Institute.

Chemonuclear synthesis of prussic acid from methane and nitrogen is being studied (Stier, King, Osterholtz, Morse, others) at the research center of one of the USA's leading chemical companies, Union Carbide (UC), at Tuxedo, New York. Radiolysis of CO_2 and some theoretical problems (the role of LET, the radiolytic mechanism in nitrogenous mixtures) are also under study there. The work of scientific centers of such companies as UC and AGN in chemonuclear synthesis follows a unified plan and includes theoretical, technological, and cost studies. The center near Tuxedo has a specially equipped pool-type

Translated from *Atomnaya Énergiya*, Vol. 22, No. 2, pp. 147-149, February, 1967.

nuclear reactor (5 MW), a Van de Graaff accelerator (for theoretical research projects), a hot laboratory. The laboratory accounts for about 50% of all the radioisotopes produced in the USA for medical purposes. The reactor is the site for activation analysis research and some interesting experiments involving cold neutrons (determination of low-lying molecular levels, determination of the structure of water and ice). A continuous facility (5 MW) operating at pressures to 30 atoms and at temperatures in the 200-450° C range has been built at the reactor site for research on chemonuclear synthesis of HCN and nitrides. The yield of the HCN radiation synthesis process depends on the LET. Under optimum conditions, G(HCN) amounts to three. Radiochemical techniques have revealed that radioactive carbon C^{14} formed in the system via the reaction $N^{14}(n,p)C^{14}$ is practically completely stabilized in the form $HC^{14}N$. The basic results achieved by the UC staff have been reported out at the 151th annual meeting of the American Chemical Society in Pittsburgh.

Accelerators are employed primarily in theoretical research in nuclear chemistry and radiation chemistry. Most of this work is done with heavy-particle accelerators, tandem generators, and accelerators for multiple charged ions, in nuclear chemistry, while the favorite machines for radiation chemistry research are linear electron accelerators and pressurized Van de Graaff electron generators. There are about ten pulse radiolysis plants functioning in radiation-chemical laboratories throughout the USA, and these have been valuable tools in solving such basic problems as identification of short-lived radiolytic products, the kinetics of fast free-radical radiation reactions.

Findings of purely kinetic studies of free-radical reactions (shock tubes, photochemistry, electrical discharges) such as those conducted at Harvard University (Kistiakowsky), at the University of Chicago (Ingram, Berry), at Rensselaer Polytechnic (Hartek, Dondes), and at the University of California (Bayes), have been vital to an understanding of the mechanism underlying radiation-chemical processes. Up-to-date equipment has been an important factor in successful radiation-chemical and kinetic research; this equipment includes fast time-of-flight mass spectrometers, high-sensitivity recording gas chromatographers, optical kinetic spectroscopes, monochromators with interchangeable sources, and operational links to computer centers.

Serious attention is being given in the USA, as in many other countries, to investigations of the chemical consequences of nuclear transmutations. These studies center on nuclear reactor installations. Twenty or so laboratories and scientific groups are currently studying the peculiarities of chemical reactions between fast radioactive atoms formed in nuclear reactions (hot-atom chemistry). These research projects are concentrated at the national science centers: at BNL (Wolf, Harbottle), ORNL (Carlson, White), ANL (Wexler), and in many university laboratories, notable among which are Yale (Wolfgang) Wisconsin (Willard), California (Rowland, Libbey, El-Sayed, Root), Michigan (Gordus), John Hopkins (Koski), Iowa (Voigt). These groups are of moderate size (5 to 10 men), but usually benefit from highly trained personnel, excellent up-to-date equipment, and are very productive.

The peculiar and regular features of chemical reactions involving hot radioactive hydrogen atoms (tritium), carbon atoms, halogens, phosphorus, iron, chromium, manganese, and other elements formed in a variety of nuclear processes, are being studied to probe the chemical aftereffects of nuclear transmutations in the vapor phase and in condensed phases. There is particular interest in reactions placing atoms and atomic groups in interstitial positions or substitution reactions, of types not observed in thermal chemistry, as well as the generation of excited radicals through the interaction of hot atoms and molecules. The relationship between chemical forms of stabilization of recoil atoms and thermal anneal or radiation anneal of crystals is being studied in many solid-state experiments. Attention is being given to the chemical behavior of fission fragments immediately following fission events. The enhanced chemical activity of the primary fission fragments, as compared to isotopes of the same element formed through a β -decay chain, has been noted (Gordus, Denschlag, etc.).

Accelerators have proved better tools than nuclear reactors for exciting hot atoms in some cases where hot atoms are generated through nuclear reactions. As an example, in the study of reactions involving fast carbon atoms, a recent suggestion has been to work with the isotope C^{11} (half-life 20 min) formed in the $C^{12}(\gamma,n)C^{11}$ process rather than with the long-lived isotope C^{14} formed from nitrogen in a reactor through the $N^{14}(n,p)C^{14}$ process (Wolfgang, Yale). In this instance, hard monochromatic γ emission is obtained by means of a 40 MeV electron accelerator by the scheme: $e^- (40 \text{ MeV}) \rightarrow \text{x-ray bremsstrahlung} \rightarrow \text{generation of } e^+e^- \text{ pairs} \rightarrow \text{magnetic separation of } e^+ \text{ from } e^- \text{ and energy separation of } e^+ \rightarrow \text{annihilation of monoenergetic positrons in flight}$. The dose $< 0.01 \text{ eV/molecule}$ received by the system and the radiation damage in these experiments are inconsequential.

Radiation and photochemical techniques are also utilized to generate hot atoms. For example, Moser and Shores (U. of Kansas) have observed the formation of fast tritium atoms ($E = 2.2$ to 5.2 eV) in the decay of excited $T_2(^3\Sigma_u)$ molecules appearing as a result of electron ($E = 30 - 50$ eV) bombardment of molecular tritium. Carlson and White (ORNL) demonstrated an explosion of multiple charged ions with the formation of fast fragments. Kuppermann (California Institute of Technology), in a study of photolysis of $DI + H_2$ mixtures, first established the threshold of $0.033 - 0.02$ eV in the reaction $D + H_2 \rightarrow HD + H$.

Increasing attention is being given to the development of techniques for generating beams of monoenergetic atoms and molecules (Wolfgang, Menzinger-Blacksell at Yale; Kuppermann at Caltech; Wharton at U. of Chicago, Herschbach at Harvard, etc.).

The Wharton linear molecule accelerator, now being assembled, is also of interest. This machine is expected to produce a beam of polarized (LiF) molecules at 10^{10} sec^{-1} intensity and energies to 4 eV, with a record precision of ± 0.002 eV. The use of monochromatic atomic and molecular beams is a highly promising trend in chemical kinetics, which opens up fundamentally new possibilities in the study of chemical reaction mechanisms, and which will be important both in the chemistry of high-energy particles and in conventional thermal chemistry.

DELEGATION OF SOVIET MEDICAL SCIENTISTS VISITS USA

E. I. Vorob'ev

A delegation of Soviet medical scientists visiting the USA in the period from June 20 through July 3, 1966, was acquainted at first hand with the uses made there of accelerators in the therapy of malignancies.

Investigations using heavy charged particles have been in progress in the USA since 1935. The radiobiological effects of heavy charged particles are now being studied, as well as the possible therapeutic use of these particles in oncological practice. This work is being conducted at various nuclear research centers equipped with high-energy particle accelerators and accelerators for multiple charged ions (The Lawrence Radiation Laboratory, the Carnegie Institute, Brookhaven National Laboratory, Harvard University, the University of Chicago, and elsewhere).

In 1964, R. Wilson mentioned the possible use of protons and α -particles accelerated to 100 MeV for radiation therapy of deep-seated malignant tumors.

A large group of investigators is currently engaged in studying the medico-biological characteristics of heavy charged particles. A considerable volume of information has been accumulated on the topic, and about 200 articles and reviews have been published.

The basic advantage sought in the use of beams of heavy charged particles in oncological theory is the extremely favorable depth-dose distribution, and (to be specific) the negligible scattering of particles beyond the geometrical confines of the beam, the presence of the Bragg peak at the end of the range, and the concomitant possibility of irradiating a small focal lesion located at a considerable depth with a rather high dose, while eliminating severe radiation injury to the surrounding tissues. Multipole irradiation and rotation techniques contributed to a tumor dose/surface dose ratio of ~ 150 . Single doses five to ten times greater than those used in x-ray and γ -ray therapy can be used in treatment with heavy charged particle beams.

Attempts at radiosurgical intervention to modify the structural or functional properties of tissues in some organs have led to a method known as stereotaxic radiosurgery. The assumption that mass radiation effects on the hypophysis can be brought about with a proton beam or a beam of other particles has been confirmed in the work of G. Lawrence, C. Tobias, and others (1954-1966). Earlier experiments by Tobias showed that heavy charged particle beams can cause 65% of the integrated radiation dose absorbed by head tissues to be localized in the target structure (the hypophysis in this case). Complete and very rapid hypophyseal destruction ensued when the dose was not less than 19 krad. Beams of α -particles, protons, and deuterons of 910 MeV, 340 MeV, and 190 MeV, respectively, were employed. A specially shaped plastic mask was slipped over the patient's head, so that the hypophysis was located at the center of a sphere. In this way the patient was positioned to within ± 0.5 mm precision. A table of special design equipped with electron-optical beam pointing devices was built at Berkeley for this purpose.

Results of hypophysis irradiation were discussed by Lawrence, Tobias, and other authors in several papers. 397 patients were irradiated in the program. Hypophysectomies were performed on 176 patients as a palliative for breast cancer. Data on complex investigations of the state of many patients implied that hypophysectomy by means of heavy charged particles is more efficient than the use of radio-gold and radioyttrium preparations for the purpose.

The hypophysectomy dose was 24 krad over a 11-19 day period. The response of the patients was observed for periods from 6 months to 6 years. Data on the effective use of beams of heavy charged particles in therapy are given in the Table below.

Translated from Atomnaya Énergiya, Vol. 22, No. 2, pp. 149-151, February, 1967.

Effectiveness of Treatment with Beams of Heavy Charged Particles

Nature of illness	No. of patients	Percentage of cases in which improvement observed
Radiation hypophysectomy, or suppression of hypophyseal function		
Breast cancer	176	34
Diabetic retinopathy	139	55
Acromegaly	47	94
Cushing's syndrome	8	80
Malignant exophthalmia	3	67
Chromophobic hypophyseal adenoma	6	—
Cancer of the prostate gland	3	—
Miscellaneous	4	—
Irradiation of deep-seated malignancies		
Brain tumors, tumors in internal organs, Parkinson's disease	7	—

Irradiation of the hypophysis with 910 MeV α -particles in the treatment of breast cancer yields almost the same results as surgical operations do. But irradiation with α -particles can be performed on ambulatory patients, and the operation is painless.

139 diabetics suffering from retinopathic syndrome were treated. Improvements were recorded in 55% of the patients. At first doses for complete or partial destruction of the hypophysis ran from 8 to 24 krad in 11-19 days. A dose of 12.5 krad is now accepted.

Eosinophilic adenoma of the hypophysis, manifested in the acromegaly syndrome, was the object of irradiation by 910 MeV alphas in 47 cases. The tumor was first bombarded with doses in the 3 to 10 krad range for periods of 11 to 21 days. The optimum dose level has now been found: 7.5 krad for 12 days. Radiation therapy is 94% effective in acromegaly cases. Patients have no trouble in standing the treatment.

A similar radiotherapeutic procedure has been developed for basophilic hypophyseal adenoma (Cushing's disease) and for chromophobic hypophyseal adenoma.

Investigations have shown that hypophyseal exposure to beams of heavy charged particles is accompanied by minimal radiation damage to the nervous tissue in which the hypophysis is embedded.

Utilization of heavy charged particles for direct irradiation of malignancies is still in the initial phase of study. Swedish specialists are pioneers in this field (Gustav Werner Institute, Uppsala), radiotherapy of brain tumors, breast cancer (Donner laboratory, Berkeley), uterine cancer (Harvard) is also being pushed in the USA. Tumor dosage runs from 4 to 10 krad. Certain features of the tissue dose distribution of heavy charged particles and the minimum total and cutaneous radiation effects on the patients make it possible to complete the entire treatment in three to five sessions.

The principal difficulty in radiation teletherapy using heavy charged particles is how to map the exact boundaries of the tumor. Despite all the advantages inherent in the use of heavy charged particles, nonuniform irradiation of the target tumors is still a drawback vitiating the results of the therapy.

The study of clinical applications of heavy charged particles in the USA is marked by a certain onesidedness. Clinical-radiological aspects of radiation effects exerted on the hypophysis by exposure to 910 MeV alphas have been studied to some extent, and investigations have been initiated on radiotherapy of some localized malignancies. But these are still isolated cases with limited observation periods on record. Radiotherapy of lung tumors, or tumors of the gastrointestinal tract, remain outside the scope of practical and scientific activities of the medico-biological centers mentioned. In any case, the literature offers no data on clinical observations in this area.

The unique physical properties of heavy charged particles recommend these particles for use as "atomic scalpels" in the treatment of such common malfunctions of the central nervous system as Parkinson's disease, epilepsy, and unalleviable morbid syndromes. How urgent this problem is can be appreciated from the fact that there are about a million patients in these categories in the USA. Some of them receive purely surgical treatment. But the idea of using beams of heavy charged particles for bloodless brain operations is an intriguing one.

Swedish scientists are vigorously active in this area, and have found that nervous tissue has a high radioresistance to 185 MeV protons. B. Larsson, L. Leksell, et al. have also shown that statistical irradiation is not well suited to stereotaxic radiosurgical interventions: destruction of the cerebral tissue is observed throughout the particle range. Rotational stereotaxic exposure techniques are being developed in both the USA and Sweden to meet this challenge.

R. Kjellberg at Harvard and Leksell at Uppsala have completed their first clinical experiences in bringing about local destruction of tissue in the ventrolateral nucleus of the optic thalamus by means of

protons, using stereotaxic beam targeting and rotational exposure techniques. Electronic computer work played an important part in calculations for the radiosurgical intervention.

The possible use of accelerated multiple charged ions and pions for therapy, as well as protons and α -particles, is also being studied at some USA research centers. Tissue cultures of living cells in vitro and experimental use of ascites cells in animal hosts are the basis of a study of the nature of radiation effects for particles of differing LET. These studies will provide information on proper radio-therapeutic conditions and procedures, and optimized beam variables for direct irradiation of tumors. Calculations by D. Fowler and D. Perkins indicate that about 10^9 pions per gram of tissue will be required to produce a dose of 150 rad. But towering difficulties stand in the way of producing such a beam of monoenergetic pions of any useful intensity at the present state of the art. The utilization of mesons in clinical practice is only of theoretical interest at this writing.

One of the basic directions in the study of radiobiological effects of radiations is seen in experiments probing the role of ionization and excitation.

Some research efforts are directed to obtaining information on the relationship between RBE and ionization density in induced mutations. Yeast is an important research subject here. It has been shown that the RBE-LET relationship is a rather complex one in the light of certain effects (mutations to prototrophism, death of cells). Establishing such a relationship would be of no mean interest, since it would pave the way for some important inferences on the nature of interactions of radiations and genetic material, and on the mechanisms responsible for death of cells.

IAEA DISCUSSION OF RADIOACTIVE WASTES DISPOSAL

G. Apollonov

An IAEA conference of experts on costs aspects of radioactive wastes disposal was held in Vienna, October 17-21, 1966. Specialists from the USSR, USA, Britain, France, India, Belgium, Italy, Norway, West Germany, Czechoslovakia, Sweden, and Japan were in attendance, as well as observers from the World Health Organization, Euratom, and some other international agencies. Many member-nations of IAEA are interested in obtaining data on the costs of rival methods for processing radioactive wastes.

The conference was called for the purpose of studying factors affecting processing and disposal costs, and choice of appropriate methods of cost calculations.

On the basis of information made available by IAEA member nations, the conference prepared a report proposing a reasonably simple procedure for calculating costs, and a sample calculation table which, with small changes to meet the concrete conditions of a particular country, can be used to calculate radioactive wastes disposal costs.

The total costs incurred in processing radioactive wastes are made up of expenses for: 1) collecting the hot wastes, 2) transporting the wastes, 3) measuring the activity of the wastes prior to treatment, 4) treatment of the wastes, 5) measuring the activity of processed wastes prior to disposal, 6) disposal of treated wastes, 7) treatment of radioactive concentrate prior to storage or disposal, 8) storage or final disposal of radioactive concentrate, 9) dosimetric inspection of the surrounding environment.

Translated from Atomnaya Énergiya, Vol. 22, No. 2, p. 151, February, 1967.

BOOKS REVIEWS

L. P. Zalukaev and V. I. Pivnev. NUCLEAR MAGNETIC
RESONANCE IN ELASTOMERS*

This book contains five chapters. The first chapter presents the fundamentals of NMR theory. The second discusses NMR in oriented polymers. NMR observation techniques are discussed in Chap. 3. Here the reader will find information on single-coil and two-coil NMR spectrometers and on techniques for measuring relaxation times. Different applications of NMR to elastomers are described in Chap. 4. Information on heat aging of rubber grades (both crude and processed rubbers) is found in Chap. 5. The appendices give recipes of mixtures tested by NMR. The book contains a list of 153 references.

I. V. Grinberg and M. E. Petrikovskaya. INVESTIGATION
OF THE ISOTOPE COMPOSITION OF FOSSIL FUELS†

This book describes methods for studying the content of stable isotopes in different types of fossil fuels. The equipment and techniques employed in isotope analysis of the basic elements of organogens in gas, liquid, and solid fossil fuels are detailed. Several theoretical problems in research on chemical and genetic separations and on separation of isotopes in fossil fuels are considered. Concrete examples are used to illustrate how changes occur in isotope ratios (H/D, C¹²/C¹³, etc.) with the depth of occurrence, oil-water contacts, and other variables. Data are presented on chemical and genetic relationships of the isotope makeup of elements of the group of organogens and organic minerals found on the earth and elsewhere. The list of pertinent literature contains 174 titles, over half of which are of Soviet papers.

* Published by Voronezh Univ. Press, 184 pp., 1965.

† Published by Naukova Dumka Press, Kiev, 148 pp., 1965.

Translated from Atomnaya Énergiya, Vol. 22, No. 2, pp. 152-160, February, 1967.

This is a basic monograph in two parts: 1) Physical and geological fundamentals of radioactive techniques, equipment, laboratory techniques; and 2) Field methods. Part One presents information on the laws of radioactive transmutations (Chap. 1), on interactions between ionizing radiations and matter (Chap. 2), radiometric equipment and methods used to measure ionizing radiations (Chap. 3), abundance of the radioactive elements in nature (Chap. 4), and radiometric assay of ore samples (Chap. 5). Part Two describes methods employed in prospecting for radioactive ores: a) using γ -radiation (Chaps. 6-10), b) using radioactive and nonradioactive gases (Chaps. 11-13), c) based on the study of lithochemical, biochemical, and geochemical samples (Chaps. 14-15), and radiation-based techniques for assay of radioactive ores (Chaps. 16-17). There is a detailed literature list consisting mostly of Russian-language book and periodical references. The book is intended for students in mining and economic geology schools.

E. D. Dubovyi. RADIATION THERAPY IN OTOLARYNGOLOGY†

This book draws on data and studies in the literature to elucidate various radiotherapy methods in the treatment of non-tumor ailments and malignant neoplasms in otolaryngological practice. Immediate and remote consequences of treatment, and the equipment used, are discussed and described in detailed fashion. The book ends with an extensive list of literature (14 pages full), mostly referring to Russian-language sources.

N. A. Kraevskii, N. M. Nemenova, and M. P. Khokhlova. PATHOLOGICAL ANATOMY AND PATHOGENESIS OF LEUCOSES‡

This is a basic monograph by leading Soviet Scientists on one of the most frequently encountered malfunctions of the blood system. The monograph consists of an introduction, 15 chaps., a summary,

* Published by Nedra Press, Moscow, 760 pp., 1965.

† Published by Zdorov'e [Health] Press, Kiev, 180 pp., 1965.

‡ Published by Meditsina Press, Moscow, 420 pp., 1965.

and a list of literature. Chapter 1 gives information on the history of the development of theories on leucoses and on embryogenesis of hematopoietic tissue, and Chap. 2 presents data on the etiology and pathogenesis of this illness. Chapter 3 is devoted to statistical material indicating an increasing incidence of leucoses over recent decades. Discussion topics on classification of leucoses are found in Chap. 4.

Chapters 5 and 6 deal with the pathological and anatomical characteristics of acute, subacute, and chronic leucoses. Information on leucoses with pronounced destructive growth is reserved for a separate chapter (Chap. 8). Chapter 9 on illnesses accompanying leucoses is followed by a detailed description of pathological-anatomical features of leucoses under modern conditions of treatment (Chap. 10), which drastically alter the course of the illness. Leukemoid reactions particularly difficult to diagnose properly are discussed in Chap. 11.

The physiological recovery of hematopoietic tissue and breakdown of this tissue are analyzed in detail in a discussion of preleucosis states (Chap. 12). Chapter 13 deals with what are termed radiation leucoses. Because of the severe difficulty in diagnosing certain forms of leucoses which closely simulate other illnesses, the monograph includes sections devoted to leukemoid states (Chap. 12) and osteomyelodysplasia (Chap. 14). The last chapter, Chap. 15, deals with the pathological anatomy of spontaneous and experimentally induced leucoses in animals. The book offers an expanded bibliography (14 pages long) in Russian and other languages.

M. S. Dul'tsin, I. A. Kassirskii, and M. O. Raushenbakh. LEUCOSES*

This is a basic monograph written by leading Soviet specialists, shedding light on the present level of the etiology and pathogenesis of leucoses—illnesses whose incidence has been increasing in the wake of overexposures of which humans have been subjected. The book makes a critical analysis of various theories on the origin of leucoses, examines the mutation theory and the significance of hereditary factors. A special section discusses classification and clinical handling of various forms of acute and chronic leucoses. Close attention is given to diagnostics and to modern methods for treating these diseases. A generous bibliography (15 p.) is keyed to the chapters in the monograph.

*Published by Meditsina Press, Moscow, 142 pp. 1965.

HANDBOOK ON LABOR HYGIENE*

Edited by Prof. F. G. Krotkov. Volume 1. Fundamentals of general labor hygiene. Physiology of labor, physical factors of the production environment. Edited by Prof. A. A. Letavet

The first volume of this three-volume work on general labor hygiene and safety presents a consistent and detailed analysis of various physical factors which affect the human organism. Chapter 1 presents the fundamentals of the physiology of labor, and the book goes on to discuss such factors as the microclimate (Chap. 2), infrared radiation (Chap. 3), noise (Chap. 4), vibrations (Chap. 5), electromagnetic fields at radio frequencies (Chap. 6), enhanced and depressed atmospheric pressure (Chap. 7 and 8). The book ends in the extended Chap. 9 (about 150 pp.) on labor hygiene in the handling of radioactive materials and sources of ionizing radiations. Appendices offer a detailed subject index and authors' index.

NUCLEAR STRUCTURE AND ELECTROMAGNETIC INTERACTIONS. †

Edited by N. MacDonald.

This book contains the prepared texts of a lecture course given by leading specialists in the summer of 1964 at the University of Edinburgh. The monograph contains 10 sections: 1) Nuclear models and the electromagnetic properties of nuclei, 2) basic aspects of nuclear models, 3) radiative transitions accompanying nuclear reactions, 4) photonuclear reactions, 5) scattering of electrons, 6) coulomb excitation, 7) structure of the transitional state of nuclei undergoing fission, 8) recent improvements in nuclear radiation detectors, 9) nanosecond pulse electronics, 10) processing of observational data. Each section is supplied, as a rule, with a bibliography containing several dozen titles.

SYMMETRIES IN ELEMENTARY PARTICLE PHYSICS ‡

Edited by A. Zichichi

This book contains the texts of papers delivered by a group of prominent physicists in the summer 1964 at the international Ettore Majorana school of physics, and the stenograms of the discussions. The

* Published by Meditsina Press, Moscow, 652 pp., 1965

† Published by Plenum Press, New York, XVI+510 pp., 1965.

‡ Published by Academic Press, New York, 430 pp., 1965.

book ends with a review paper by R. Feynmann, "The present state of the theory of strong and weak electromagnetic interactions." A list of participants in the seminar is included in an appendix.

R. H. Dalitz. NUCLEAR INTERACTIONS OF THE HYPERONS *

This monograph, authored by a professor of physics at the University of Chicago, contains eight sections: 1) Introduction, 2) review of data on hypernuclei, 3) phenomenological analysis of data on hypernuclei binding energies, 4) spin dependence of hypernucleon interactions, 5) theoretical analysis of the nature of hyperon nuclear forces, 6) hyperon-nucleon scattering and nuclear reactions, 7) models of the decay of light hypernuclei, 8) some problems in the study of hypernuclei. The book ends in a list of 97 titles from the literature (mostly from the periodical literature).

W. Kunz and J. Schintlmeister. TABELLEN DER ATOMKERNE. TEIL II.
TABLES OF ATOMIC NUCLEI. PART II. NUCLEAR REACTIONS. VOLUME I.
ELEMENTS, FROM THE NEUTRON TO MAGNESIUM †

The book contains all available data on nuclear reactions and schemes of nuclear levels of most nuclides, compiled in convenient and compact tables arranged in the order of increasing atomic number of the nuclides. A slight preface and explanations of the use of the tables are published in German, English, and Russian. An exhaustive bibliography of contributions to the periodical literature (covering the period up to and including 1962) on the nuclides of each element runs in many instances to hundreds of titles on each.

* Published by Oxford University Press, 106 pp., 1965.

† Published by Akademie Verlag, Berlin, 700 pp., 1965.

C. M. Smith. A TEXTBOOK OF NUCLEAR PHYSICS*

This book is an introduction to modern nuclear physics, written for students in engineering colleges or for persons with no specialized training in this field. The author's preface leads into 33 chaps. which discuss many topics from the kinetic theory of matter and elements of quantum theory and relativity theory to the modern theory of elementary particles and thermonuclear reactions. The appendices present tables of physical constants, information on spins of nuclei, and a supplement on new elementary particles: the antiproton-hyperon and the two types of neutrino and antineutrino. Each chapter ends in exercises (detailed subject index and authors' index end the book.)

D. N. Chesney and M. O. Chesney. RADIOGRAPHIC PHOTOGRAPHY†

This is a fundamental handbook on applications of photographic emulsions in recording x-radiation. The handbook consists of 17 chaps. The first few chapters describe the basic gist of the photographic process (Chap. 1), photographic emulsions (Chap. 2) and sensitometry (Chap. 3). Chapter 4 is a compendium of recommendations on proper storage of x-ray film, and Chap. 5 discusses ways and means of intensifying, and enhancing the contrast of, x-ray images. Information on development of photographic emulsions is found in four chapters: development (Chap. 6), fixing (Chap. 7), washing and drying (Chap. 8), and the equipment used in these steps (Chap. 9). Chapter 10 provides the reader with data on darkroom equipment for x-ray diagnostic laboratories. Chapter 11 analyzes radiographic image contrast. Exposure factors in diagnostic radiography are described in Chap. 12. Methods for inspecting and analyzing x-ray plates are presented in Chap. 13, optical principles of photography and descriptions of the design of photographic cameras in Chaps. 14 and 15. The last two chapters contain information on fluorography. The list of pertinent literature is surprisingly brief, 19 titles in all, mostly from the American periodical literature. The 34-page appendix gives detailed coverage of names and subjects in the book's text.

P. A. Lykourezos. PRECISION MEASUREMENT OF H^3 AND C^{14}
IN GAS-FLOW PROPORTIONAL COUNTERS‡

This monograph consists of a short introduction and three sections: 1) calibration of proportional gas-discharge counters for measuring radioactive gases, 2) simultaneous recording of H^3 and C^{14}

* Published by Pergamon Press, Oxford-London, XVI+822 pp., 1965.

† Published by Blackwell Scientific Pub., Oxford, 460 pp., 1965.

‡ Published by Juris-Verlag, Zurich, 164 pp., 1965.

emissions by means of proportional counters, and 3) methods for converting labeled organic compounds to gaseous products. 10 articles from the periodical literature are listed as references.

B. Rossi. COSMIC RAYS*

This popular-science style book by a prominent cosmic-ray research scientist consists of 15 chaps. and two appendices. It offers a consistent, simple, and attractive presentation of the history of the discovery and study of cosmic rays, from the first airborne balloon experiments by V. Hess (1912) to the discovery of the radiation belts encircling the earth. The book ends with sections on the relationship between cosmic rays and solar phenomena, and modern hypotheses on the origin of cosmic rays. Almost every chapter contains some data from work done by the author. Appendices by Rossi present the necessary information on the structure of the nucleus, elementary particles, and other topics, while introducing the simplest mathematical relationships into the text. The last pages of the book are taken up with an authors' index and a subject index.

PROBLEMS OF ATMOSPHERIC AND SPACE ELECTRICITY.† Proc.

Third Intern. Conf.

Edited by S. C. Coroniti

This book publishes the proceedings of the III International Conference on Atmospheric and Space Electricity, which was held at Montre (Switzerland) in May, 1963. The reports are all printed in English, irrespective of the original language, and appear grouped in seven sections: 1) reviews of the present state of the art (4 papers); 2) basic problems in atmospheric electricity in an undisturbed atmosphere (2 papers, 10 brief communications); 3) basic aspects of atmospheric electricity in a disturbed atmosphere (4 papers); 4) theory of charge generation in thunderheads (5 papers, 4 brief communications); 5) physics of lightning (5 papers), 6) relationship between lightning and geophysical or physical phenomena (6 papers, 8 brief communications); 7) space electricity (7 papers, 2 brief communications). Each section comes with a corrected stenogram of the discussion. The book ends in liberal author's and subject indexes.

* Published by George Allen and Unwin, Ltd., London, 268 pp., 1966.

† Published by Elsevier Publ. Co., Amsterdam, XVI + 616 pp., 1965.

W. R. Corliss. SPACE PROBES AND PLANETARY EXPLORATION*

This book consists of three parts of unequal length. The brief first part (40 pages) contains a brief historical rundown of interplanetary space research. The voluminous second part (240 pages) deals with the fundamentals of related theory and reviews experience in control and maneuvering of spaceships and monitoring of space flight. Close attention is given to the design and engineering details of the Mariner-1 and Mariner-2 space vehicles, as well as to methods for measuring outer space variables and gathering data on the surfaces of other bodies in the solar system. The third part presents information on instruments used on space vehicles for measuring characteristics of the interplanetary medium, atmospheres and soils of planets, and instruments for detecting the existence of life. An extensive bibliography (515 references) is keyed to relevant chapters. A detailed subject index (10 pages in length) closes the book.

S. Glasstone. SOURCEBOOK ON THE SPACE SCIENCE†

This book, based on NASA materials arranged in handbook form, contains the 13 chaps: 1) introduction to space research (goals, historical review), 2) orbits and trajectories in space, 3) space propulsion engines, 4) control and communications systems, 5) use of satellites in meteorology, navigation, and communications, 6) the sun, 7) the solar system, 8) the earth and space in the vicinity of the earth, 9) the moon, 10) the inner planets: Mercury, Venus, Mars, 11) the major planets and Pluto, 12) the universe, 13) man in space. The handbook ends in a very detailed authors' index and subject index.

W. F. Hilton. MANNED SATELLITES‡

This is a slight book containing a wealth of interesting material on the preparation and execution of manned satellite launches in the Mercury Project. The book begins with a presentation of elementary information on astronautics and ends in an analysis of data on ion propulsion engines and photon propulsion engines. The presentation is in fairly popular style, although elements of higher mathematics are resorted to in some sections. The book offers a short list of recommended literature (mostly NASA publications), plus an authors' index and a subject index.

* Published by Van Nostrand Co., Inc., Princeton, N. J., X+542 pp., 1965.

† Published by Van Nostrand Co., Inc., Princeton, N. J., XVII+938 pp., 1965.

‡ Published by Hutchinson and Co., London, 140 pp., 1965.

C. E. Roth. RELIABILITY IN SPACE VEHICLES *

Proceedings of an NASA seminar on the reliability of electronic equipment used on board space vehicles for either experimental purposes or for control in flight are contained in this book. A list of participants at the seminar and the titles of all 60 papers presented appear in the introduction. The texts of the nine succeeding chapters were prepared by leading NASA specialists on the basis of those papers.

M. Ash. NUCLEAR REACTOR KINETICS †

This nine-chapter book appears in the well-known series of monographs on nucleonics published by this firm. The first chapter describes the properties of delayed neutrons and derives the basic equations of reactor kinetics. Solutions of these equations are the subject of Chap. 2. In the next chapter, the author discusses reactor transients and reactor stability. A broader understanding of reactor stability is formulated in Chap. 5, which also deals with the application of basic principles to a broad range of feedback phenomena pertinent to reactors of different types. Chapter 5 deals with Monte Carlo calculations in reactor problems. Chapter 6, "Dynamic programming, reactor kinetics, and reactor control," is followed by a chapter on spatial kinetic phenomena in reactors (neutron field oscillations, xenon poisoning, core meltdown, etc.). The last two chapters (8 and 9) discuss analysis of kinetic equations and behavior of concrete nuclear reactor types (fast reactors, rocket propulsion reactors, circulating-fuel reactors, boiling-water reactors, pulsed reactors). Each chapter ends with a few problems and a bibliography of 20-30 titles (mostly from the periodical literature). There is a brief index.

REACTORS. NUCLEAR ENGINEERING, VOL. III.

Institut National des Sciences et Techniques

This is the third volume in the scientific and technical nuclear library, edited by F. Perrin, and devoted to a description of nuclear reactors of different types and purposes. Preference is given to French reactor installations in the presentation of the material, and information on other facilities is meager. The book is in two large sections: 1) research reactors and critical assemblies, 2) nuclear power stations, plus a short third section (36 pages) on shipboard nuclear power plants. The book is primarily of a reference nature: designs of particular reactors and their components are enumerated

* Published by Engineering Publishers, N. J. XXII+118 pp., 1965.

† Published by McGraw-Hill, New York, 416 pp., 1965.

‡ Published by Presses Universitaires de France, 992 pp., 1965. [In French].

briefly and illustrated. The coverage extends from the basic layout of the nuclear plant to the experimental plant facilities. In addition, the first two sections discuss the basic physics and engineering problems in reactor design. Each section is supplemented with a short list of relevant literature (5 to 10 titles). Authors' and subject indexes are detailed. Extensive information on the contents of the preceding two volumes in the series, and on other volumes being prepared for press, appears at the end of the book.

DRAGON-HIGH-TEMPERATURE REACTOR PROJECT* Seventh
Annual Report 1965-1966

The European Nuclear Energy Agency has published its seventeenth annual report on the Dragon reactor. This 20 MW(th) high-temperature reactor was built at Winfrith (England), with construction and operation through the joint efforts of member nations of the Agency. The reactor was brought up to power in the period from April 1965 through March 1966, whereupon (in April 1966) it was brought to full design power. The positive experience accumulated in the operation of Dragon has made it possible to plan development of 540 MW economically competitive power stations based on Dragon type power reactors.

Three basic trends are noted in the year covered in the report: 1) research and experiments geared to improvements in the reactor and its components, 2) ironing out bugs in reactor performance, 3) feasibility studies and cost evaluations of large-scale power generating stations based on the Dragon type reactor. Radiation tests of Dragon reactor fuel are part of an intensive program. The tests have yielded encouraging results on the use of finely dispersed fuel with pyrolytically coated particles for high-temperature reactors. The behavior of graphite at high irradiation temperatures and in a gas atmosphere, corrosive attack on core materials, vibration, removal of fission fragments from helium (coolant helium), were investigated.

Extensive measurements, mostly involving control rod calibration, reactivity, and the use of fuel elements with different fuels, were performed in the period prior to bringing the reactor up to 2.5 MW and 10 MW power levels. Coolant activity and helium leakage from the loop (0.75 kg/week) were determined. A lot of work has been done to eliminate some kinds of defects. Close attention was also given to studying the possible construction of a large-scale power station with a 1250 MW (th) and 540 MW (e) Dragon type reactor (41 atmos helium coolant pressure, 750° C operating temperature). On-power refueling is being attempted. Components, assemblies, and parts of power stations are being planned. It has been found that building a large reactor presents serious problems not encountered in building the prototype Dragon reactor.

Cost evaluations showed that the cost of electric power generated by a nuclear power station can be completely competitive with "conventional" electric power. The report also discussed certain administrative questions (a proposed reorganization of the structure of the Dragon project, cutback in personnel, etc.).

*Published by O. E. C. D. European Nuclear Energy Agency, 1966.

V. A. Kuznetsov. REACTOR LAYOUT AND CALCULATIONS
FOR MARITIME NUCLEAR POWER PLANTS*

The book consists of three chapters of unequal length. The first two chapters take up the basic parameters of maritime nuclear power plants (Chap. 1, 32 pages) and reactor design principles plus basic heat transfer calculations (Chap. 2, 53 pages). Chapter 3, the main chapter, handles neutron physics calculations for water-moderated water-cooled pressurized reactors, boiling-water reactors, organic-cooled and gas-cooled reactors. The appendices contain the reference material needed for the calculations (conversion factors, basic heat transfer properties of nuclear fuel, fuel element cladding materials, etc.). The list of literature, covering 130 titles, covers mainly Russian sources.

L. T. Chadderton. RADIATION DAMAGE IN CRYSTALS †

This is an eight - chapter monograph. The first deals with various types of crystal imperfections: point defects and defects with spatial extent. Displacement of atoms from lattice sites is discussed in Chap. 2. Chapter 3 analyzes cascades of displacements and the thermal spikes. An analytic description of radiation damage in crystals and other ordered structures is given in Chap. 4. Simulation of complicated radiation damage processes is described in Chap. 5. This is followed by a chapter on the interatomic interaction potential, and then Chap. 7 analyzing energy loss rates by ionizing particles traversing a medium. The book ends with Chap. 8 on equipment and techniques for monitoring radiation defects. A short appendix reviews calculations of the number of displaced atoms. There is a brief subject index.

G. Friedlander, J. Kennedy, and J. Miller. NUCLEAR AND
RADIOCHEMISTRY ‡ 2nd ed.

This is an expanded and greatly revised edition of the now famous textbook on radiochemistry written by prominent American scientists. The authors describe the discovery of radioactivity (Chap. 1), make a thorough review of the structure of atomic nuclei (Chap. 2), equations of radioactive decay (Chap. 3), interaction of radiations with matter (Chap. 4). Radiation detection and measurement techniques

* Published by Transport Press, Moscow, 220 pp., 1966.

† Published by Methuen and Co. Ltd., London, 202 pp., 1965.

‡ Published by Wiley, New York, 586 pp., 1965.

are discussed in Chap. 5, and statistical treatment of radioactive decay in Chap. 6. Radiotracers and their applications are discussed in Chap. 7, which is followed by Chap. 8 on radioactive decay processes. The various models of the atomic nucleus and some theories on nuclear forces are summarized in Chap. 9. Nuclear reactions and radiation sources are described in Chaps. 10 and 11. Information on special radiochemical research techniques is relegated in Chap. 12. Chapter 13 handles applications of certain specific nuclear processes (the Mössbauer effect, positron annihilation, meson production, etc.). Nuclear reactor operating principles are the subject of Chap. 14. Chapter 15 closes the monograph with a discussion of nuclear processes in geological and astrophysical phenomena.

The five appendices present conversion factors, relativistic equations, thermal neutron activation cross sections, a list of literature on cross sections of nuclear reactions, and tables of the nuclides. The book ends with generous indexes of authors and subject matter. Each chapter has its own bibliography (10-15 titles) plus some exercises (10 to 20).

E. Schwarz. INVESTIGATION OF RADIOACTIVITY IN SEDIMENTARY ROCKS OF THE AACHEN COAL RANGE *

This brochure covers results of natural radioactivity measurements performed on minerals from the Aachen coal basin. A brief introduction leads into chapters on radiations emitted by naturally radioactive elements and methods for measuring these emissions. Chapter 4 cites and analyzes the results of a study of γ emission intensity, while Chap. 5 summarizes measurements of natural γ emission through the use of scintillation spectrometers, and Chap. 6 does the same for nuclear photographic emulsion measurements. The reader is offered some brief conclusions in the last chapter. The monograph has a short list of pertinent literature (35 titles) appended.

C. C. Washtell and S. G. Hewitt. NUCLEONIC INSTRUMENTATION †

This book consists of a brief introduction, 11 chaps., and a short subject index. The first chapter presents the reader with information of the operating principles and basic component designs of electronic circuits: resistors, capacitors, vacuum tubes, semiconductor detectors. The second chapter deals with passive and active, linear and nonlinear circuit elements. A brief chapter describes the design principles of nucleonic instruments. Pulse amplifiers of different types are discussed in Chap. 4, scalers and pulse counters in Chap. 5, dekatrons, indicating lamps, and voltage-stabilizing tubes in Chap. 6.

* Published by Köln and Opladen, Westdeutscher Verlag, 188 pp., 1965.

† Published by George Newnes Ltd., London, VII + 144 pp., 1965.

Operating principles of pulse height discriminators are dealt with briefly in Chap. 7 (both single-channel and multichannel discriminators are discussed). Count rate meters are the subject of Chap. 8, which also deals with rudiments of count rate recording statistics. Information on power supplies may be found in Chap. 9, and electronic circuits for automating certain radiometric operations in Chap. 10. The book ends in a brief section devoted to maintenance of equipment and to equipment reliability.

NUCLEAR ELECTRONICS*

This compendium of materials presented at the IAEA Bombay conference on nuclear electronics (November 22-26, 1965) comes in eight sections: 1) reactor power and neutron energy measurements; 2) thermodynamic measurements; 3) coolant variable monitoring; 4) detection of fuel cladding failures; 5) reactor performance; 6) review of reactor operating safety; 7) data processing and optimization; 8) servomechanisms and miscellaneous electronic circuitry. The first section discusses ionization chambers for reactor work (multicompartiment ion chambers with each compartment sensitive to specific modes of radiation; low-voltage ionization chamber operated in recombination, etc.), automated arrangements for measuring basic variables of energy-sensitive detectors; resolution, stability, noise; some instruments designed to measure or monitor reactor variables; techniques for minimizing electrical noise affecting the performance of reactor monitoring instrumentation.

The second section presents a report on a capacitance two-phase in-pile flow meter, and the third section discusses carbon dioxide as a coolant. Some papers deal with equipment used to test leaks in fuel element cladding: fission fragment meters, γ -ray spectrometers, and others (section 4). Equipment for measuring reactivity, for rapid analysis of reactor runaway data on analog computers, for automatic monitoring of specific reactors, is described in section five. Nuclear reactor safety instrumentation is discussed in section 6. Section 7 discusses processing of measurement data and determinations of the optimum number of variables measured simultaneously.

B. J. Williams. A SELECT BIBLIOGRAPHY ON SEMICONDUCTOR RELIABILITY†

This brochure runs down bibliographic references in alphabetical order, with contents of each annotated briefly. The references are grouped in sections: general information, bibliography and reviews, applications, costs, special devices, environmental factors, microminiaturization. Brief subject and author indexes are appended.

* Published by IAEA, Vienna, 662 pp., 1966.

† Published by Hertis Publ., Hatfield, 156 pp., 1965.

PRACTICAL INSTRUMENTAL ANALYSIS *

Edited by J. Krugers and A. I. M. Keulemans

This is a textbook on the utilization of modern instrumental technique in analytical chemistry. 20 chapters and numerous appendices written by different authors are aimed at readers with no experience in utilizing the methods discussed. The contents of the book are quite varied, ranging from photometry in the visible spectrum (plus ultraviolet and infrared ranges) to applications of liquid scintillation counters and activation analysis. There is a detailed subject index.

W. B. Mann and S. B. Garfinkel. RADIOACTIVITY AND ITS MEASUREMENT †

This book is in popular science style, and accessible to students on the engineering school freshman level, and is written by leading American physicists. Its eight chapters are followed by a brief list of literature and authors and subject indexes. The contents of the book are obvious from the chapter headings: 1) discovery of radioactivity and earlier experiments on the nature of radioactivity; 2) radioactive series and theory of nuclear transmutations; 3) interaction of α -, β -, γ -radiations with matter; 4) the neutrino and the neutron, 5) energy of nuclear transmutations, 6) radiation detectors; 7) instruments; 8) methods for standardizing radioactive preparations.

RADIOACTIVE FALLOUT ON THE TERRITORY OF WEST GERMANY.
REPORT NUMBER THREE COVERING PERIOD THROUGH MAY 1963 †

This constitutes the third publication in a series of reports summarizing observations of radioactive fallout on the territory of West Germany (covering the period ending with May 1963). A brief introduction (Chap. 1) is followed by the basic text, running through three chapters: artificially radioactive substances in the biosphere (Chap. 2), population exposure levels due to natural and artificial radiation sources (Chap. 3), and biological and medical sequelae of exposure to radiation (Chap. 4). A brief closing chapter (Chap. 5) is followed by the text of a program of further research on natural and artificial radioactivity in the biosphere. There is some reference material on conversion factors useful in radiometry, and a glossary of terms used.

* Published by Elsevier Publ. Co., Amsterdam, X+264 pp., 1965.

† Published by Van Nostrand Co., Inc., Princeton, N. J. 168 pp., 1966.

‡ Published by Verlag Thieme, Stuttgart, 132 pp. 1965, [in German].

THE BASIC REQUIREMENTS FOR PERSONNEL MONITORING*

[IAEA Safety Series, No. 14].

This brochure publishes a code of practice elaborated by the IAEA as an aid in organizing dosimetric monitoring of personnel in facilities handling radioactive materials and sources of ionizing radiations. The compendium is an expanded and revised text restating the "basic radiation shielding safety rules" (Safety Series No. 9, 1962). The safety rules are discussed along with the purpose of personnel monitoring and the volume involved (in the introduction), basic concepts and organization of the monitoring services (sect. 2), techniques of measurements (sect. 3), extent of monitoring work (sect. 4), the equipment used (sect. 5), dose assessment techniques (sect. 6), recording of data (sect. 7). Special sections take up instruction and training of monitoring service personnel and publicity in reporting monitoring results. A first appendix lists 19 titles of relevant literature (mostly IAEA publications), and a second appendix gives a glossary of terms used in the field.

MONITORING RADIOACTIVITY IN FOOD PRODUCTS†

Complete texts of papers and notes on communications presented at two West German seminars in 1963 on radioactive pollution of the biosphere, nutrients and food materials included, as a result of nuclear weapons testing, are contained in this publication. The book's title does not do justice to the scope of the contents. The reader will find not only papers on the content of radioactive materials in various foodstuffs (both in terms of total β -activity or total γ -activity and in terms of content of specific isotopes, Cs^{137} and Sr^{90} to be specific), but also results of investigations of radioactivity in humans (by means of a whole body counter). The book ends with the resolutions of the seminars (consisting chiefly of new research programs) and a list of participants.

COMPUTER CALCULATION OF DOSE DISTRIBUTIONS IN RADIOTHERAPY ‡

Proceedings of a conference of specialists convened in October 1965 by IAEA are included here. Part One (24 pages) consists of the official report on the work of the conference, plus recommendations worked out by the experts. Attention is centered on dose field calculations in radiotherapy in

* Published by IAEA, Vienna, 44 pp., 1966. [in English, Russian, French, or Spanish].

† Published by Gersbach und Sohne Verlag, Munich, 218 pp., 1965. [in German].

‡ Published by IAEA, Vienna, 216 pp., 1966.

single-beam or multiple-beam work, or using rotating radiation sources. Body shape factor corrections, corrections for tissue inhomogeneity, etc., are discussed. The book consists mainly of tests of papers delivered at the conference of experts (20 reports). This is accompanied by an extensive bibliography (9 pages long), a glossary, a questionnaire on the utilization of computers for dose field calculations in radiation therapy, a list of institutes engaged in work of this sort, and a list of participants.

S. C. Pearce. BIOLOGICAL STATISTICS: AN INTRODUCTION*

This is a text on the application of statistical techniques to biological experiments. It is written expressly for readers with no background in higher mathematics. Each of 12 chaps. contains numerous examples illustrating the use of the formulas. All the necessary reference data appear either in the body of the text or in the appendices. The literature list contains 32 titles of books in English. Brief indexes of subjects and authors end the book.

PROCEEDINGS OF THE FIRST INTERNATIONAL SYMPOSIUM ON BASIC ENVIRONMENTAL PROBLEMS OF MAN IN SPACE †

Edited by H. Bjurstedt

This book contains the texts of reports and stenograms of discussions at the I international symposium of problems on the external environment in space (held in Paris, October-November, 1962). Thirty-one reports were presented at this symposium (8 from the USSR, 8 from the USA, 15 from other countries). The topics covered range far afield, from physical conditions of space flight to medical criteria in the selection of astronauts. Papers are published in their original languages (mostly English), and reports by Soviet scientists appear in both English and Russian. Each report carries brief abstracts in English, French, and Russian. Stenograms are given only in English.

* Published by McGraw-Hill, New York, XVI+212 pp., 1965.

† Published by Springer-Verlag, Vienna, VIII+506 pp., 1965.

This first part of the proceedings of the 1964 Roentgen congress on x-rays contains work on nuclear medicine (functional diagnostics utilizing radiotracer isotopes), x-ray research on tumors, the physics and techniques of radiation exposures and measurements, and x-ray diagnostic techniques and practice. The texts of papers presented are accompanied by stenograms of the discussion (all in German).

ISOTOPES IN WEED RESEARCH †

A symposium on the use of isotopes in scientific research geared to coping with weeds was held in Vienna, October 25-29, 1965, under joint auspices of IAEA and FAO. 67 specialists from 18 countries were in attendance. Reports presented demonstrated the exceptional importance of tracer applications in developing weed control techniques, and particularly in the study of uptake of herbicides by different parts of plants, as well as migration and distribution of herbicides in different parts of plants. These topics were discussed in papers submitted by A. Krafts, D. Pate, O. Leonard (USA), G. Costa et al. (Brazil), H. Peterson (Denmark), and R. Creekwood et al. (UK).

Five papers on different aspects of metabolism between soil and plants in the presence of herbicides were discussed. The symposium also focused attention on techniques in tracer studies and tracer research equipment. Papers on these topics were submitted by R. Boll and D. Hooper (USA), A. Klock and K. Reiberg (West Germany), and E. Levi (Euratom). E. Grossbeard (Britain) discussed the potential use of tracers and autoradiography in the study of biological relations between herbicides and soils. Two seminars were held during the symposium, one to discuss the latest progress in weed control methods, the other to deal with basic research trends in that field and to assess the possible applications of nucleonics to solve extant problems.

THE PROVISION OF RADIOLOGICAL PROTECTION SERVICES ‡

[IAEA Safety Series, No. 13].

Part One of the brochure publishes a code of practice on the organization of radiological protection safety services in research centers using radioactive materials and ionizing radiation sources.

* Published by Georg Thieme Verlag, Stuttgart, 350 pp., 1965.

† Published by IAEA, Vienna, 227 pp., 1966.

‡ Published by IAEA, Vienna, 80 pp., 1966. [Available in English, Russian, French and Spanish].

This code has been recommended on the basis of rules or recommendations adopted by member nations of IAEA. Part One deals with: 1) introduction, 2) purposes of radiation protection, 3) responsibility and delegation of responsibilities in radiation protection work, 4) functions of radiological protection supervision, 6) organizational measures.

Part Two cites examples of the organization of radiation safety services: a) in nuclear research centers (Finland, West Germany, Turkey, Britain, the Uzbek SSR, at the Kiev VVR-M reactor); b) at universities and engineering schools (Birmingham and London, Britain); and c) in medical institutes and hospitals (USA and Mexico). The last section publishes data on national radiological protection services in Czechoslovakia and Mexico.

D. D. Glower. EXPERIMENTAL REACTOR ANALYSIS AND RADIATION MEASUREMENTS*

This textbook opens with a chapter on exposure tolerance levels for humans, concerning ionizing radiations and biological consequences of overexposures. Chapter 2 deals with the principal techniques employed to record ionizing radiations. The characteristics of subcritical facilities are dealt with in Chap. 3. Chapter 4 presents information on experiments with pulsed neutron sources. Chapter 5 analyzes experimental research on shielding against penetrating radiations. Radiation damage in solids is discussed in Chap. 6. The author gives special attention to description of experiments conducted at reactors of different types (Chap. 7). This chapter also relates experiments on determination of reactor period and supercriticality, and presents information on calibration of control rods, supercriticality approximations, etc. Chapter 9 contains a concise presentation of basic data on reactor kinetics and reactor transients. The monograph ends with brief indexes of subjects and authors.

EFFECTS OF IONIZING RADIATIONS ON PLANT AND ANIMAL ORGANISMS (Trudy inst. genetiki AN SSSR, Vol. 32)†

Edited by Corresponding Member of the USSR Academy of Sciences
N. I. Nuzhdin

This is a collection of 19 experimental papers on the study of different aspects of the biological effects of ionizing radiations. Some of the investigations unearthed new material analyzing the effect of

* Published by McGraw-Hill, New York, 348 pp., 1965.

† Published by Nauka Press, Moscow, 268 pp., 1966.

radiation intensity on the frequency of occurrence of chromosomal aberrations in cells. Fractional and single exposures of plants were performed against a background of effects caused by agents activating or inhibiting cell metabolism. Some of the papers dealt with studies of mutations induced by γ -ray or neutron bombardment. The effect of ecological conditions during growth of plants, and the effect of the degree of ripening of seeds on radiosensitivity, on the frequency and nature of hereditary changes induced by exposure to radiation, were investigated. The relative biological effectiveness of different modes of ionizing radiations is treated in terms of effect on the frequency of dominant lethal genes in animals. Some of the papers deal with radiosensitivity and the modifying effect of radioprotectant chemicals. Each paper comes with a substantial bibliography, in most cases (the reference articles are mostly from specialized Soviet and foreign journals).

IONIZING RADIATIONS IN BIOLOGY*

The proceedings of a coordinated conference on radiobiology topics, convened by the Institute of Biology of the Academy of Sciences of the Latvian SSR in the spring of 1963, appear here.

Most of the papers deal with the effects of ionizing radiations on plants—the use of low-dose γ radiation for radiostimulation and other effects (4 papers) and the study of radiation-induced mutagenesis (10 papers). Two reports discuss radiosterilization of trichinella and insects. Two papers discuss general aspects of radiobiology. A paper by B. I. Styro et al. deviates somewhat from the overall trend in its treatment of detection of aerosol α -active hot particulates in the atmosphere.

E. R. Popescu. LEUKEMIA†

This monograph by a leading Rumanian scientist consists of preface, 11 chaps., summaries, a list of reference literature, and a subject index. General information on neoplasms of the hematopoietic tissue accompanied by leukemia is presented in Chap. 1; data on the incidence of these maladies in Chap. 2. Chapter 3 discusses the etiology of leukemias, and Chap. 4 reviews the features of a leukemic cell. Information on the course of certain types of leukemia and on specific features of those types is found in three chapters: general pathophysiology of leukemias (Chap. 5), acute and chronic forms of the disease (Chaps. 6, 7). Malignant lymphomas and plasmocytomas are discussed in Chaps. 8 and 9. Chapter 10 takes up leukemia therapy and prognoses of the outcome of the disease at different stages of its development. The book ends with Chap. 11 on cytochemical techniques used in the diagnosis and study of leukemias. Each chapter has a generous bibliography (40-50 titles), and a subject index appears as an appendix.

* Published by Zinatne Press, Riga, 165 pp., 1965. [in Russian].

† Published by Medical Press, Bucharest, 356 pp., 1965. [in Russian].

NUCLEAR HEMATOLOGY*

Edited by E. Szirmai

Written by a panel of renowned specialists from several countries, this book approaches the present state of knowledge in the field of nuclear hematology in many countries (USA, Britain, France, Poland, Belgium, India, Hungary, West Germany, Italy, Japan) from different angles. The first part (Chaps. 1-9) presents, in addition to a historical review and a section on electron microscopy, material on the use of tracers for research on the morphology, physiology, and pathology of blood cells and blood-forming organs. The second part (Chaps. 10-17) analyzes the effect of ionizing radiations (including those accompanying nuclear bomb explosions) on blood formation in the organism. Special attention is given to radiation injury to the blood and the hematopoietic system. Experimental research on prophylaxis and therapy of radiation sickness and possible clinical effects (including transplants of brain tissue) are discussed in detail. Each chapter has an exhaustive bibliography attached. Generous authors' and subject indexes end the book.

RADIATION INJURY AND RADIATION HEMATOLOGY†

Edited and Compiled by A. Morczek

The edited texts of reports by East German specialists on radiation hazards associated with isotopes used in hematology are published in this book. Various aspects of the problem are tackled, from the physical fundamentals of the use of radioisotopes in medical research and basic radiobiological laws to the treatment of certain illnesses with P^{32} and a description of the pattern of acute radiation sickness. A report on the organization of a radiological protection service in East Germany appears at the end of the book. A short subject index is appended.

* Published by Academic Press, New York, 590 pp., 1965

† Published by VEB Verlag Volk und Gesundheit, Berlin, 166 pp., 1965.

THE DETECTION AND RECOGNITION OF UNDERGROUND EXPLOSION*

[A Special Report of the United Kingdom Atomic Energy Authority]

This is the full text of a UKAEA report presenting the findings of theoretical and experimental seismographic studies in an effort to detect underground explosions (with emphasis on nuclear tests). The book divides into three main sections: 1) historical introduction, 2) techniques and processing of seismograms, 3) summaries and conclusions. A special fourth section goes into greater detail on techniques, equipment, observational data, and offers some reference data. The book is profusely illustrated with graphs and photographs.

METHODS FOR INVESTIGATING AND MEASURING MARINE
RADIOACTIVITY† [Report by a Panel of Experts] (Safety Series No. 11)

This handbook prepared by a panel of experts from IAEA member nations consists of five chapters: 1) a brief introduction, 2) an extended chapter on choice of representative samples (of sea water, bottom deposits, plankton, benthos, algae and seaweeds, fish); 3) a short section on investigations of sea water and marine products; 4) a brief description of basic dosimetric monitoring techniques; 5) a presentation of radiochemical analysis practices relevant to the most important isotopes of 15 elements (from manganese to plutonium). Each chapter has its list of references. Four appendices make available information on terminology in the field of radioactivity measurements, on the abundance of naturally radioactive elements in sea water and bottom sediments. Also covered in the appendices are sampling methods in relation to the volume of samples, and examples of dosimetric surveys of the sea and seashore regions in Britain (Windscale), Italy, and the USA.

INTERNATIONAL CONVENTIONS ON CIVIL LIABILITY‡ [IAEA Legal Series No. 4]

This is the fourth in a series of IAEA publications on juridical matters, begun in 1959. It deals with major juridical problems in the field of atomic energy, civil responsibility for nuclear damage which can occur in operation of nuclear facilities or a nuclear shipboard power plant, or during transportation of nuclear materials. The book reproduces the official texts of conventions (as well as

* Published by Her Majesty's Stationery Office, London, 118 pp., 1965.

† Published by IAEA, Vienna, 98 pp., 1966. [Available in English, Russian, French, and Spanish].

‡ Published by IAEA, Vienna, 250 pp., 1966.

auxiliary documents) now accepted on an international basis: the Vienna Convention on Civil Liability for Nuclear Damage (Vienna, May 21, 1963); an optional protocol concerning compulsory settlement of disputes (Vienna, May 21, 1963); the resolution of a Board of Governors on maximum limits for exclusion of small amounts of nuclear material from coverage by the Vienna convention (September 11, 1964); convention on third party liability in the field of nuclear energy (Paris, July 29, 1960); decisions by the steering committee of the European Nuclear Energy Agency on elimination of small amounts of nuclear material from coverage by the third party liability convention in the field of nuclear energy (November 26, 1964); convention on the liability of operators of nuclear-powered ships (Brussels, May 25, 1962); conventions amending the July 29, 1960 Paris convention on third party liability in the field of nuclear energy. The texts of the documents are published in the four IAEA working languages: English, French, Russian, Spanish.

WORLD NUCLEAR DIRECTORY*

This is the third revised and augmented edition of a handbook on international and national organizations engaged in the fields of atomic energy, nuclear research, and various aspects of the utilization of either. The handbook contains information on administrative and research organizations in 77 countries, and runs through the list of all periodicals which publish work on nuclear topics. The exact titles of organizations are given in their English version, with the address, name and initials of the official in charge, and brief data on the main avenues of activity of the organization, plus the names of officials in charge of major subdivisions. The handbook is a highly useful reference for any person working in the field of nuclear industry, and also for specialists involved in international collaboration in this field.

*Published by Harrap Research Publications, London, 712 pp., 1966.

ERRATA

Soviet Atomic Energy, 21, 5 (1966)

Where found	Was given as	Should be
p. 1077, Eq. (2)	e^{θ/θ_0}	$e^{-\theta/\theta_0}$
p. 1077, Eq. (3)	e^{θ/θ_0}	$e^{-\theta/\theta_0}$
p. 1077, Eq. (3)	$e^{\pi/2\theta_0}$	$e^{-\pi/2\theta_0}$
p. 1080, Eq. (1)	$e^{-(\sum_t^H + \sum_t^{L1})}$	$e^{-(\sum_t^H + \sum_t^{L1})R}$
p. 1080, Eq. (2)	$e^{-k \sum_t^{L1}(E)}$	$e^{-k \sum_t^{L1}(E) R}$
p. 1083, Eq. (6)	$\left[1 - \exp\left(-\frac{1}{\theta_0} \arctan \frac{R_0}{R}\right) \cdot \frac{R_0/(R\theta_0 + 1)}{\sqrt{1 + (R_0/R)^2}} \right]$	$\left[1 - \exp\left(-\frac{1}{\theta_0} \arctan \frac{R_0}{R}\right) \cdot \frac{\frac{R_0}{R\theta_0} + 1}{\sqrt{1 + (R_0/R)^2}} \right]$

SPECIFIC HEATS AT LOW TEMPERATURES

By E. S. R. Gopal

The Clarendon Laboratory, Oxford University


Surveys the entire field of low-temperature specific heats at a level suitable for graduate courses. After outlining the thermodynamic background, specific heat behavior (lattice, electronic, and magnetic contributions) of solids, liquids, and gases is discussed in detail. This readable and comprehensive account is kept at an elementary physical level, but full references to advanced treatments are given. Students or research workers unfamiliar with the field will find this an excellent supplementary text which functions as a bridge between basic theory and modern research work.

Considerable practical information is included on calorimetric and refrigeration problems; for example, the basic theory, tables, and supplementary information is given to enable the reader to calculate the refrigeration needed to cool any piece of apparatus to a desired point. Of special interest are six-figure tables of Einstein and Debye internal energy and specific heat functions, given in an appendix, and of use to physicists and chemists performing calculations of the thermodynamic properties of gases and solids.

CONTENTS: Elementary concepts of specific heats • Lattice heat capacity of solids • Electronic specific heats • Magnetic contributions to specific heats • Heat capacity of liquids • Specific heats of gases • Anomalies in specific heats • Miscellaneous problems in specific heats • *Appendix:* Six figure tables of Einstein and Debye internal energy and specific heat functions

240 pages

\$11.50

 **PLENUM PRESS** 227 West 17th Street, New York, New York 10011
A DIVISION OF PLENUM PUBLISHING CORPORATION

